THE UNIVERSITY OF OKLAHOMA

GRADUATE COLLEGE

IDENTIFICATION OF SYSTEM FREQUENCY RESPONSE BY STATISTICAL CORRELATION AND SPECTRAL ANALYSIS

A DISSERTATION

SUBMITTED TO THE GRADUATE FACULTY

in partial fulfillment of the requirements for the

degree of

DOCTOR OF PHILOSOPHY

BY

PAUL WILSON GALLIER

Norman, Oklahoma

1962

IDENTIFICATION OF SYSTEM FREQUENCY RESPONSE [illegible]
STATISTICAL CORRELATION AND SPECTRAL ANALYSIS

APPROVED BY

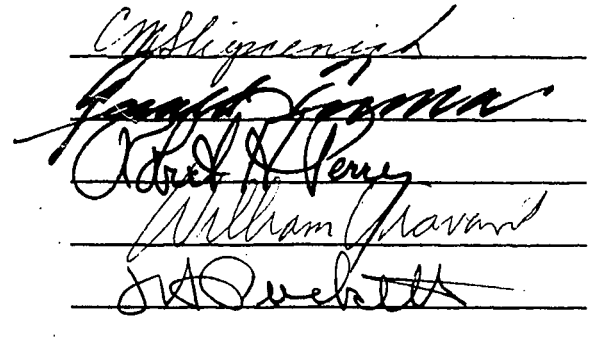

DISSERTATION COMMITTEE

ACKNOWLEDGMENT

The author takes this opportunity to express sincere gratitude to his advisor, Dr. C. M. Sliepcevich, Associate Dean of the College of Engineering, for the advice and invaluable assistance given so readily throughout this work.

Likewise, sincere appreciation is expressed to Dr. T. H. Puckett, Assistant Professor of Electrical Engineering, for the instruction and advice concerning many phases of this work.

Dr. W. J. Viavant of the Computer Laboratory contributed a number of helpful points to the writing of the computer programs.

Mr. K. A. Bishop contributed to this work through frequent discussions. Messrs. Blancett and Wood assisted in operation of the equipment and in transcribing the large amounts of data.

Appreciation is expressed to the National Science Foundation for the financial support making possible this work. A fellowship granted by the Celanese Corporation has also been appreciated.

Paul Wilson Gallier

TABLE OF CONTENTS

		Page
LIST OF TABLES		v
LIST OF ILLUSTRATIONS		vi
Chapter		
I.	INTRODUCTION	1
II.	REVIEW OF THEORY	6
III.	THEORETICAL APPLICATION	19
IV.	REVIEW OF PREVIOUS WORK AND STATEMENT OF THE PROBLEM	38
V.	EXPERIMENTAL APPARATUS	44
VI.	INVESTIGATION	56
VII.	DISCUSSION OF RESULTS	65
VIII.	CONCLUSIONS	106
BIBLIOGRAPHY		111
APPENDICES		
A.	AUTOCORRELATION OF A RANDOM SQUARE WAVE	114
B.	DERIVATION OF THEORETICAL SYSTEM FREQUENCY RESPONSE	116
C.	FOURIER TRANSFORMATION	121
D.	VARIANCE OF CORRELATION ESTIMATES	131
E.	NOMENCLATURE	138

LIST OF TABLES

Table		Page
1.	Input Power Spectral Density Estimates (For Weighting Function of k = 2).....	76
2.	Cross-Powers Spectral Density Estimates - Magnitude (For Weighting Function of k = 2)...	80
3.	Cross-Power Spectral Density Estimates-Phase, Degrees Negative (For Weighting Function of k = 2).....	81
4.	Input Power Spectral Density Estimates - Two Inputs.....	96
5.	Cross-Power Spectral Density Estimates - Two Inputs (Weighting Function k = 2).....	97
6.	Effect of Weighting Function on Cross-Power Spectral Density Estimate ($N - \tau_m = 4200$).....	99
7.	Normalized Process Frequency Response Results- For Two Inputs.....	103
8.	Parameter Values of Experimental Equipment.....	120
9.	Comparison of Theoretical and Computed Fourier Transforms.....	125
10.	Comparison of Computed and Theoretical Process Magnitude Ratios.....	126
11.	Comparison of Computed and Theoretical Process Phase Lags.....	127

LIST OF ILLUSTRATIONS

Figure		Page
1.	Two Input - Single Output System	24
2.	Multiple Inputs - Single Output System	27
3.	System Having Multiple Input and Output Variables	27
4.	Concentric Pipe Heat Exchanger Model	33
5.	Model For Mass Transport In a Conduit	36
6.	Functional Arrangement of Experimental Equipment	45
7.	A Typical Portion of Recorded Data (One Input Function)	51
8.	A Typical Portion of Recorded Data (Two Input Functions)	52
9.	Autocorrelation of Input Random Square Wave	57
10.	Comparison of Theoretical and Experimental Frequency Responses - Magnitude Ratio	66
11.	Comparison of Theoretical and Experimental Frequency Responses - Phase Lag	67
12.	Correlation Functions For 750 Lagged Products- Single Input	71
13.	Correlation Functions For 3000 Lagged Products - Single Input	72
14.	Correlation Functions For 5592 Lagged Products Single Input	73
15.	Input Power Spectral Density Estimates	75

Figure Page

16. Magnitude of Cross-Power Spectral Density Estimates - Single Input..... 78

17. Phase Lag of Cross-Power Spectral Density Estimates - Single Input..... 79

18. Magnitude of Cross-Power Spectral Density Estimates For Different Weighting Functions - Single Input..... 82

19. Phase Lag of Cross-Power Spectral Density Estimates for Different Weighting Functions - Single Input..... 83

20. Normalized Magnitude Ratio Using Estimates of Input Power Spectral Density..... 84

21. Normalized Magnitude Ratio Using Theoretical Power Spectral Density..... 86

22. Phase Lag of Process Frequency Response..... 87

23. Correlation Estimates From A Record Length of $N - \tau_m = 1200$..... 91

24. Correlation Estimates From A Record Length of $N - \tau_m = 3000$..... 92

25. Correlation Estimates From A record Length of $N - \tau_m = 4800$..... 93

26. Magnitude Ratio of Process Frequency Response- Two Inputs..... 101

27. Phase Lag of Process Frequency Response - Two Inputs..... 102

28. A Random Square Wave..... 114

29. A Stirred Tank Reactor Model..... 116

30. Analog Computer Circuit For Simulating Reactor Equations..... 119

31. Straight Line-Segment Representation of f(t).... 121

32. Spectra of Weighting Functions, $w_k(t)$..... 130

33. Theoretical Standard Deviation of the Auto-Correlation Estimate..... 135

IDENTIFICATION OF SYSTEM FREQUENCY RESPONSE BY STATISTICAL CORRELATION AND SPECTRAL ANALYSIS

CHAPTER I

INTRODUCTION

The intelligent design or analysis of any plant control system requires a knowledge of the plant dynamic characteristics. In the area of chemical processes the dynamic characteristics are not readily known except in the more simple cases. Measurement of dynamic relationships thus plays a vital role in the application of automatic control to chemical processes.

As part of a control system the process to be controlled, or regulated, is normally the most significant component of the system. The accuracy of describing its dynamic characteristics therefore contributes to the resulting degree of control attained. If a measurement method is employed to obtain this knowledge of process dynamics, then the reliability of the method should be established to a satisfactory degree.

After the knowledge of dynamics is gained, the design or analysis problem can be met. A host of textbooks

and papers in the literature are devoted to these aspects and they are not to be treated herein. In the case of linear, time-invariant systems, the entire control system and its parameters can be specified through the use of analytical techniques. For many systems, both non-linear and time-varying, analog computer simulation provides a useful means of studying the control problem.

Furthermore, advanced concepts of control are made possible through the knowledge of dynamics. Computer control utilizing feedforward principles combined with those of feedback can be established. Computer control systems, termed "adaptive," can be programmed to employ a periodic measurement of process dynamics in order to follow their time varying characteristics and thus can be programmed to provide continual optimal control action. Another attack encompassing both of the above concepts is static and dynamic optimization by computer control using the "dynamic programming" techniques of Bellman (2).

Knowledge of process dynamics may be determined possibly in two manners. First, a theoretical model may often give satisfactory results. Mathematical models in the form of differential equations can be obtained through the application of the appropriate mass, energy, and momentum balances. Parameters of these equations can be obtained from equilibrium relations, rate constants, physical properties, and dimensions of the systems to complete the

mathematical model. However, unless considerable experience of representing similar processes in this manner has been accumulated, the model may not represent the process satisfactorily. The second determination, that of an actual measurement method, remains as the only positive check.

Several different types of methods for measuring process dynamics are possible. Certainly an investigator might employ variations of any one method he has found to be advantageous. Yet the measurement methods might be basically classified as (1) the original, direct sinusoidal response, (2) empirical time response fitting techniques, (3) the pulsing Fourier transform method, and (4) the statistical correlation and spectral analysis method. Critical factors affecting the selection of a method are the disturbances imparted to process operation and the desired accuracy and form of the results. Other factors may be the available measuring and recording equipment and the available computing facilities.

Each of the above has its particular advantages and disadvantages. The sinusoidal method, although simple and accurate when noise signals can be minimized, involves relatively long periods of testing which are upsets to normal operation. The empirical time response fitting methods can be made quickly and with little testing equipment required, but these results serve only as approximations. Pulse testing (13) requires a relatively short testing

period and yields accurate results when noise signals are not present. All of these methods require specific input functions and are applicable only to linear systems. However, frequency response description itself, as one form of expressing process dynamics, is significant only for linear systems.

The fourth method, statistical correlation and spectral analysis, makes use of random input variables and places requirements only on the statistical nature of the input variables. Attractive features are that special test signals may not be needed to disturb the process operation and that the effect of the unwanted process "noise" may be made negligible. Therefore, the method provides the potential of measuring dynamic characteristics from the process variables recorded during normal plant operation.

These are decided advantages where large, complex processing equipment are concerned. Dynamic testing which leads to off-specification products can be rather expensive when there are large throughputs. Even when such tests are allowable, the experimenter normally finds few single input--single output relationships but rather processes having a host of interrelated variables.

One example out of many existing in the chemical and petroleum industries is the distillation column. If, for instance, the dynamic relationship between reboiler steam flow rate and analysis of a light key component in the bottom

product were desired, a number of other process variables could simultaneously affect the response. Such variables might be column pressure, feed rate, feed composition, reflux ratio, steam pressure and quality, and several others.

Another advantage of the correlation method is that when applied to non-linear systems the results are those of a linear fit which is the best in a least squares sense.

In theory the correlation method shows excellent potential, but some problems exist yet in its practical application. Experience with the method has been reported in a few previous papers, but the results have been somewhat inconclusive. The present work has been undertaken in order to contribute to adaptation of this method as one of dynamic analysis of chemical, petroleum, and other processes where testing under normal operating conditions is desirable.

CHAPTER II

REVIEW OF THEORY

History

Methods of harmonic, or frequency analysis of periodic and aperiodic functions have been employed as far back as Fourier's original work in 1882. A frequency response approach to feedback control systems probably started with a paper in 1932 by H. Nyquist concerning the stability of feedback amplifiers. The real impetus for using these techniques came during World War II. Contributions were centered upon gun fire-control problems with their electronic, hydraulic, and mechanical servomechanism components. Following the war, applications were made rapidly to other areas. However, not until about 1953 did the literature begin to show many contributions to the dynamics and frequency response of chemical processing equipment for the design of feedback controls. At the present time, many significant contributions are being made.

Theoretical developments concerning random time functions have come somewhat later than with the deterministic variables. A large part of the theory of frequency analysis

of random time functions can be attributed to N. Weiner. In 1930 his papers concerning Brownian motion titled "Generalized Harmonic Analysis" and published in Acta Mathematica provided a mathematical basis for the frequency analysis of random processes. An important paper was published by Kolmogorov (16) in Russia in 1941, but it is Weiner's later work (29) in 1949 which is given broad credit (at least in the United States) for influencing most of the modern developments in both communication theory and information theory. Statistical filtering and prediction theory was a part of this work. As an important implementation of Weiner's work, Lee (20, 21) showed, in 1950, a treatment of random functions especially for the determination of system dynamics. Since that time interest and literature contributions on this subject have continually grown and are given account of in Chapter IV.

Dynamic Systems

Time Relationships

The purpose in presenting the following discussion is to point out to the reader the theory concerning the experimental work described in later parts herein. A number of excellent texts (7, 14, 25, 28) deal with these points in detail. This discussion will summarize applicable relationships and definitions. Many of the following relationships were originally conceived by electrical engineers in conjunction with electrical filters and later

to servomechanisms. The language of methematics, however, is a common one and these relations can be applied to many different systems. Such systems might be construed to be anything from simple mechanical devices to complex chemical processing plants.

A most conveniently handled system is one which can be represented by a constant coefficient, ordinary differential equation as

$$c_n \frac{d^n y(t)}{dt^n} + c_{n-1} \frac{d^{n-1} y(t)}{dt^{n-1}} + \text{---} + c_o y(t) = x(t) \tag{1}$$

where $x(t)$ is an input, or driving, function and $y(t)$ is the output, or response. When the coefficients, c_i, above are constants, the system is said to be linear, time-invariant. The system has the property that for every pair of inputs, $x_1(t)$, $x_2(t)$ and corresponding outputs $y_1(t)$, $y_2(t)$, the input a $\left[x_1(t)\right] + b\left[x_2(t)\right]$ produces an output a $\left[y_1(t)\right] + b\left[y_2(t)\right]$. Or, the effects produced by a number of inputs can be superimposed. Because of this property of superposition, the convolution relationship

$$y(t) = \int_{-\infty}^{\infty} h(t - \tau)\, x(\tau)\, d\tau \tag{2}$$

also holds. After a change of variable, the convolution integral can also be written as

$$y(t) = \int_{-\infty}^{\infty} h(\tau)\, x(t - \tau) d\tau \tag{3}$$

The weighting function, $h(\tau)$, is also the unit impulse response of the system. If, in Equation (1) the input $x(t)$ is Dirac's delta function occurring at $t = 0$, or $\delta(t)$, the solution of Equation (1) is $y(t) = h(t)$. Thus, $h(t)$ is a characteristic of the system which uniquely describes the system behavior for any input through the use of Equation (2) or (3). For all physically realizable systems, $h(t)$ has the property that it is zero for all negative values of its argument; otherwise, the system would produce an effect before the corresponding cause. Also, the system is stable if

$$\int_{-\infty}^{\infty} \left| h(t) \right| dt < \text{constant} < \infty \qquad (4)$$

A system can be termed as "linear" by the definition of superposition above.

Frequency Response

The Fourier transform of the impulse response,

$$H(\omega) = \int_{-\infty}^{\infty} h(t) e^{-j\omega t} dt \qquad (5)$$

exists for stable systems and it is called the frequency response function. This function is the response of the system to a sinusoidal input of frequency, ω. The linear time-invariant system is uniquely characterized by the frequency response function since its response to a sinusoid is a pure sinusoid of the same frequency. One of the simplest ways to catalog the system dynamics is to test

and record the process frequency response by direct sinusoidal testing.

If the input function, x(t), fulfils the condition of Equation (4), its Fourier transform, $X(\omega)$, exists and Equation (2) or (3) can be transformed to yield

$$Y(\omega) = H(\omega) \cdot X(\omega) \tag{6}$$

or

$$H(\omega) = \frac{Y(\omega)}{X(\omega)} \tag{7}$$

This relationship is the basis on which pulse testing (13) is carried out. A pulse yielding an appropriate transform is used as the input and transforms are conputed numerically from the recorded input and output functions to yield $H(\omega)$.

The Laplace transform of the impulse response is, of course,

$$H(s) = \int_0^\infty e^{-st} h(t)dt \tag{8}$$

This function is usually called the process transfer function. In the same procedure as above, it can be shown that it is the ratio of transforms of output to input variable, as

$$H(s) = \frac{Y(s)}{X(s)} \tag{9}$$

It is often convenient to determine this function approximately from the frequency response testing results by comparison with various assumed functions of $\lim_{s \to j\omega} [H(s)]$.

Statistical Theory

Dynamic systems are often under the influence of variables which are non-deterministic, or random, in nature. That is, future values cannot be entirely predicted in light of the past. In the chemical industry an abundance of such functions occurs as load disturbances to control systems. These can occur in the form of feed compositions or flow rates, as "noise" generated within the process (from turbulence, for example), or even as ambient weather changes. These random functions are often best described by their statistical, or averaged, characteristics. For comprehensive treatments on statistical theory, the reader is referred to the work of Cramer (4) and Lanning and Battin (18).

Properties of Random Processes

A random process can be considered as an ensemble or collection comprised of functions of time. For this ensemble, there exist probability distribution functions, although it may be difficult to compute many of these probabilities. The probability that in the set of functions $[x(t)]$ that the variable $X_1 = x(t_1)$ has a value equal to or less than x_1 at time t_1 is expressed as

$$F_1(x_1, t_1) = \Pr (X_1 \leq x_1) \tag{10}$$

and is called the first probability distribution function. It has the properties that

$$F_1(-\infty, t_1) = 0 \tag{11}$$

$$F_1(+\infty, t_1) = 1 \tag{12}$$

A probability density function is also defined as

$$f_1(x_1, t_1) = \frac{\partial F_1(x_1, t_1)}{\partial x_1} \tag{13}$$

if $F_1(x_1, t_1)$ is differentiable. The probability density function is the probability that $x(t_1)$ is greater than x_1, and less than or equal to $x_1 + dx_1$, or

$$\Pr\left[x_1 < x(t_1) \leq x_1 + dx_1\right] = f_1(x_1, t_1)dx_1 \tag{14}$$

The probability density has the property of

$$\int_a^b f_1(x_1, t_1)\, dx_1 = F(b, t_1) - F_1(a, t_1) \tag{15}$$

and similarly,

$$\int_{-\infty}^{\infty} f_1(x_1, t_1)dx_1 = 1 \tag{16}$$

The n-th moment of set $\left[x(t)\right]$ is

$$\overline{x(t)^n} = \int_{-\infty}^{\infty} x^n f(x,t)dx = E\left[x(t)^n\right] \tag{17}$$

$E\left[x(t)^n\right]$ is the mean value, or expectation over all functions of the set $\left[x(t)\right]$. The first moment, $\overline{x(t)}$, is the mean value or expectation of $x(t)$ as

$$\overline{x(t)} = \int_{-\infty}^{\infty} x\, f(x,t)dx \tag{18}$$

The second moment is the mean square value

$$\overline{x^2(t)} = \int_{-\infty}^{\infty} x^2 f(x,t)dx \tag{19}$$

and is the variance, if the mean value is zero.

A second probability distribution function may also be used in the description of the random process. This function is a joint probability for two random variables, say $X_1 = x(t_1)$ and $X_2 = x(t_2)$, where t_1 and t_2 are arbitrary fixed values of t, as

$$F_2(x_1,t_1:x_2,t_2) = \Pr(X_1 \leq x_1 : X_2 \leq x_2)$$
$$= \Pr(x(t_1) \leq x_1 : x(t_2) \leq x_2) \qquad (20)$$

A corresponding probability density function is

$$f_2(x_1,t_1:x_2,t_2) = \frac{\partial^2}{\partial x_1 \partial x_2} F_2(x_1,t_1:x_2,t_2) \qquad (21)$$

when this derivative exists. The joint distribution function has properties that in pairs of variables (x_1,t_1) and (x_2, t_2).

$$F_2(x_2,t_2:x_1,t_1) = F_2(x_1,t_1:x_2,t_2) \qquad (22)$$

and also that

$$F_2(x_1,t_1: +\infty,t_2) = F_1(x_1,t_1) \qquad (23)$$

The general moments may now be defined as

$$\alpha_{ik} = E\left[x_1^i(t_1)\, x_2^k(t_2)\right]$$
$$= \int_{-\infty}^{\infty}\int_{-\infty}^{\infty} x_1^i\, x_2^k\, f_2(x_1,t_1:x_2,t_2)\,dx_2 dx_1 \qquad (24)$$

The function α_{11} will be of special interest and is defined as the correlation function. It is usually given the symbol $\phi_{xx}(t_1,t_2)$ for the ensemble average of the random process $\left[x(t)\right]$ and from Equation (24) is

$$\phi_{xx}(t_1,t_2) = E\left[x_1(t_1)\ x_2(t_2)\right] = \int_{-\infty}^{\infty}\int_{-\infty}^{\infty} x_1x_2f_2\ (x_1,t_1:x_2,t_2)\ dx_2\ dx_1 \quad (25)$$

Likewise, a "cross-correlation" function between two random processes, x(t) and y(t) may be defined as

$$\phi_{xy}(t_1,t_2) = E\left[x(t_1)\ \ y(t_2)\right] = \int_{-\infty}^{\infty}\int_{-\infty}^{\infty} xy\ f_{11}^{(x,y)}(x,t_1:y,t_2)dy\ dx \quad (26)$$

where $f_{11}^{(x,y)}\ (x,t_1:y,t_2)$ is the most elementary joint probability density function between x(t) and y(t). Correlation functions have the property that for random functions where the time difference $(t_2 - t_1)$ is large the correlation function of x(t), or "autocorrelation," becomes

$$\phi_{xx}(t_2,t_1) = E\left[x(t_1)\ x(t_2)\right] = E\left[x(t_1)\right]\ E\left[x(t_2)\right] \quad (27)$$

because the two become statistically independent. If the mean values are zero, then the correlation function becomes zero. Cross correlations have this identical property.

In a manner similar to the joint, or second, probability distribution function, third and higher order distribution functions may be defined. Obviously, as the higher order distributions are known, more is known about the statistical characteristics of the random process. For the case where two or more different random processes are considered together, joint probability distribution of a higher arbitrary order may also be considered.

Stationary Random Processes. In many practical situations, the statistical characteristics do not change

with time. If this criteria is met, the random process is said to be "stationary." There are a number of important properties of such stationary processes. The mean, or expected, value does not change under a translation in the time axis, or

$$E\left[x(t)\right] = E\left[x(t+\tau)\right] \tag{28}$$

The joint probability distribution functions then depend only upon time differences in the events specified, as

$$F_2(x_1,t_1,\ x_2,t_2) = F_2(x_1,0;\ x_2,t_2-t_1) \tag{29}$$

and, similarly, this relation holds for the higher order joint distributions of a stationary random process. For correlation functions, the stationary property allows

$$\phi_{xx}(t_1,t_2) = \phi_{xx}(0,t_2-t_1) = \phi_{xx}(t_2-t_1) = \phi_{xx}(\tau) \tag{30}$$

when $t_2 - t_1 = \tau$.

Ergodic Property. For a stationary random process, an assumption is frequently made that averages made over an ensemble of functions are equivalent to the time averages of one representative function of the ensemble. This condition is known as the "ergodic" property. When this property is valid, some valuable relationships can be made as in the following.

$$E\left[x(t)\right] = \int_{-\infty}^{\infty} x\, f_1(x,t)\, dx = \lim_{T\to\infty} \frac{1}{2T} \int_{-T}^{T} x(t+\tau)d\tau \tag{31}$$

$$E\left[x^2(t)\right] = \int_{-\infty}^{\infty} x\ \ f(x,t)\, dx = \lim_{T\to\infty} \frac{1}{2T} \int_{-T}^{T} x^2(t+\tau)d\tau \tag{32}$$

$$E\left[x(t)x(t+\tau)\right] = \phi_{xx}(\tau) = \lim_{T\to\infty} \frac{1}{2T} \int_{-T}^{T} x(t)x(t+\tau)dt \tag{33}$$

Correlation Functions. The autocorrelation function, $\phi_{xx}(\tau)$, of an ergodic random process as defined in Equation (33) has some interesting and useful properties. When the delay time, τ, is zero,

$$\phi_{xx}(0) = \overline{x(t)}^2 \tag{34}$$

the correlation function is the mean-square value. This value also has the property that

$$\phi_{xx}(0) \geq \phi_{xx}(\tau) \tag{35}$$

The autocorrelation function is an even function and when it has a sharp peak at the origin the view may be taken that $x(t)$ is not correlated with itself well at the time, $t \pm \tau$. The converse may be visualized also.

The cross-correlation function between two ergodic random processes can be expressed as

$$\phi_{xy}(\tau) = \lim_{T\to\infty} \frac{1}{2T} \int_{-T}^{T} x(t)\, y(t+\tau)dt \tag{36}$$

and is not normally an even function. From this equation it can be seen also that

$$\phi_{xy}(\tau) = \phi_{yx}(-\tau) \tag{37}$$

Power Spectral Density. It is often useful to treat signals in the frequency domain by means of a Fourier analysis. For periodic signals a discrete set of coefficients representing harmonic amplitudes in a Fourier series can be obtained. For non-periodic (and non-stochastic) signals, a

continuous spectrum representation may be found if the Fourier transform exists.

Fourier analysis can also be usefully applied to stationary random processes. For this purpose the term power spectral density is convenient. Let us consider the random function x(t) to be represented by

$$x_T(t) = x(t) \qquad \text{for } -T \leq t \leq T \tag{38}$$
$$= 0 \qquad \text{elsewhere}$$

and let us define

$$A_T(\omega) = \int_{-\infty}^{\infty} x_T(t)\, e^{-j\omega t}\, dt = \int_{-T}^{T} x(t)\, e^{-j\omega t}\, dt \tag{39}$$

With this notation, we can define the power spectral density, $\overline{S(\omega, x)}$, of the function x(t) to be

$$\overline{S(\omega, x)} = \lim_{T \to \infty} \left[\frac{A_T(\omega)}{2T} \right]^2 \tag{40}$$

Now an expected value of the above relation can be found for the case when x(t) is a stationary random process. We find the result that the power spectral density of a stationary random process, written as $\Phi_{xx}(\omega)$, is related to the autocorrelation function as its Fourier transform, or

$$\overline{S(\omega, x)} = \Phi_{xx}(\omega) = \int_{-\infty}^{\infty} \phi_{xx}(\tau)\, e^{-j\omega\tau} d\tau \tag{41}$$

Because the autocorrelation function is even, $\Phi_{xx}(\omega)$ is real and can also be expressed as

$$\Phi_{xx}(\omega) = 2 \int_{0}^{\infty} \phi_{xx}(\tau) \cos \omega\tau \, d\tau \tag{42}$$

From Equation (40), it can be seen that $\overline{\Phi}_{xx}(\omega)$ is also non-negative.

A cross-power spectral density, $\overline{S(\omega,x,y)}$, between two random processes, x(t) and y(t), can be derived in the same manner. When both x(t) and y(t) are stationary, their cross-power spectral density can be expressed as

$$\overline{S(\omega,x,y)} = \overline{\Phi}_{xy}(\omega) = \int^{\infty} \phi_{xy}(\tau) e^{-j\omega\tau} d\tau \qquad (43)$$

Because the cross-correlation is normally not even, the cross-power spectral density contains real and imaginary parts.

CHAPTER III

THEORETICAL APPLICATIONS

Now that some fundamental definitions, their properties, and relationships of statistical communication theory have been reviewed, we can investigate methods of analysis involving these functions. The interest in this analysis will be concerning applications to dynamic systems.

Input and Output Autocorrelations and Spectral Densities

Let us consider a linear system with input x(t) and output y(t) and investigate the relation between input and output autocorrelations and their spectral densities. An assumption is made for the derivation that the input is a member function of an ergodic random process. Therefore, the output autocorrelation function is

$$\phi_{yy}(\tau) = \lim_{T\to\infty} \frac{1}{2T} \int_{-T}^{T} y(t)\, y(t+\tau)\, dt \tag{44}$$

The output variables can be expressed as

$$y(t) = \int_{-\infty}^{\infty} h(\lambda)\, x(t-\lambda)\, d\lambda \tag{45}$$

and

$$y(t+\tau) = \int_{-\infty}^{\infty} h(\eta)\, x(t+\tau-\eta)\, d\eta \tag{46}$$

since $h(\lambda)$ represents a physically realizable system. That is, $h(\lambda)$ for λ negative is zero. Then

$$\phi_{yy}(\tau) = \lim_{T\to\infty} \frac{1}{2T} \int_{-T}^{T} \int_{-\infty}^{\infty} h(\lambda)\, x(t-\lambda)\, d\lambda \int_{-\infty}^{\infty} h(\eta)\, x(t+\tau-\eta)\, d\eta dt \tag{47}$$

By combining the integration, inverting the order of integration and recognizing the correlation function inside the integrals we find

$$\phi_{yy}(\tau) = \int_{-\infty}^{\infty} \int_{-\infty}^{\infty} h(\lambda)\, h(\eta)\, \phi_{xx}(\tau + -\eta)\, d\eta d\lambda \tag{48}$$

$$= \int_{-\infty}^{\infty} h(\lambda) \int_{-\infty}^{\infty} h(\eta) \phi\, (\tau + -\eta)\, d\eta d\lambda$$

It is found that a double integral relation between input and output autocorrelations exists. If the above relationship is transformed by multiplying by $e^{-j\omega\tau} d\tau$ and integrating between $\pm\infty$, the result can be obtained that

$$\Phi_{yy}(\omega) = H(\omega) \cdot H(-\omega) \cdot \Phi_{xx}(\omega)$$

$$= \left|H(\omega)\right|^2 \cdot \Phi_{xx}(\omega) \tag{49}$$

where $H(\omega)$ is the Fourier transform of the impulse response, $h(\tau)$. It is apparent that this relationship does not contain phase information; it has only magnitude information for the frequency plot.

Input-Output Crosscorrelation. A relationship of prime importance, and on which much of the work herein is based, is that between the input autocorrelation and input-output crosscorrelation involving the impulse response. For a brief derivation, consider the crosscorrelation function

between the input, x(t), and output, y(t), of a linear system which has an input, a member function of an ergodic random process. The crosscorrelation function is

$$\phi_{xy}(\tau) = \lim_{T\to\infty} \frac{1}{2T} \int_{-T}^{T} x(t)\ y(t+\tau)\ dt \qquad (50)$$

A convolution integral with infinite limits can be substituted for $y(t+\tau)$ as

$$\phi_{xy}(\tau) = \lim_{T\to\infty} \frac{1}{2T} \int_{-T}^{T} x(t) \int_{-\infty}^{\infty} h(\lambda)\ x(t+\tau-\lambda)d\lambda dt \qquad (51)$$

By inverting the order of integration and employing the definition of ϕ_{xx} it can be seen that the expression reduces to

$$\phi_{xy}(\tau) = \int_{-\infty}^{\infty} h(\lambda)\ \phi_{xx}(\tau-\lambda)\ d\lambda \qquad (52)$$

Stable, physical systems have the properties that

$$h(\lambda) = 0 \quad \text{for } -\infty < \lambda < 0$$

$$h(\lambda) = 0 \quad \text{for } B < \lambda < \infty$$

where B is some large value, perhaps 10 times the highest time constant of the system. Therefore, the above may sometimes be expressed as

$$\phi_{xy}(\tau) = \int_{0}^{B} h(\lambda)\ \phi_{xx}(\tau-\lambda)\ d\lambda \qquad (53)$$

The impulse response $h(\lambda)$ might be solved for by a process of deconvolution of Equation (53) when the correlation functions are known.

An equivalent relationship for these "input-output" statistical variables is in terms of frequency. Through a

Fourier transformation of the above equation, assuming the system is stable, it can be shown that the power spectral densities are related by

$$\Phi_{xy}(\omega) = H(\omega)\, \Phi_{xx}(\omega) \tag{54}$$

or

$$H(\omega) = \frac{\Phi_{xy}(\omega)}{\Phi_{xx}(\omega)} \tag{55}$$

This relationship is somewhat simpler than the convolution operation, and the process frequency response can be found when the spectral densities are known.

It should be noticed that no special restrictions are placed upon the input variable, $x(t)$, except that it is to be a member of an ergodic random process. Its autocorrelation function form or power spectral density form are arbitrary. It may even contain periodic components as a constituent of the random variable.

A convenient situation occurs when the input is a pure "white" noise, or one which contains equal power for all frequencies. The autocorrelation function for such noise is an impulse at the origin. The crosscorrelation thus becomes the system impulse response, by Equation (52), and the frequency response $H(\omega)$ becomes proportional to the cross power spectral density by Equation (54).

Prior to the realization of Equation (52), Weiner (29) had derived a very similar relationship. His problem concerned the optimum linear (time invariant) filter for

separating a desired random function from one also containing a disturbance. The criteria used for an optimum was a least mean-square type defined to minimize

$$\overline{\varepsilon^2} = \lim_{T\to\infty} \frac{1}{2T} \int_{-T}^{T} \left[f_o(t) - f_d(t)\right]^2 dt \qquad (56)$$

where $f_o(t)$ is the function obtained and $f_d(t)$ is the desired function. By applying a calculus of variations a criterion for this optimum was derived to be of the form,

$$\phi_{xy}(\tau) = \int_{-\infty}^{\infty} k(\lambda)\ \phi_{xx}(\tau-\lambda)\ d\lambda \text{ for } \tau \geq 0 \qquad (57)$$

This result is called the Weiner-Hopf equation and it differs from Equation (52) only in the restriction on τ above. There is no requirement of this relationship made for $\tau < 0$. Actually, the condition of Equation (57) is met in Equation (52); therefore, the weighting function $h(\lambda)$ of Equation (52) is an optimum (as defined above) linear representation of the system. For the linear, time-invariant system Equation (52) identically defines the weighting function; for the non-linear time-invariant system, the relationship fits a best linear representation (in a least mean square sense) to the system.

Multidimensional Systems. In practice many systems have two or more input variables which affect an observed "output." This condition is certainly true for chemical processing equipment. Consider as a simple example a mixing tank which is diluting a solution with a solvent to some desired concentration. Suppose that the total flow of

the two streams is held constant and that perfect mixing occurs. Either of two variables might simultaneously cause the effluent concentration to change---the concentration of the inlet solution or the ratio of the two inlet flow rates. Many such examples occur; often they are more complex. Goodman (8, 9), among others, has shown how the statistical functions of linear systems may be related using the convenient properties of linearity. The developments of these relationships are outlined below.

Two Inputs. Figure 1 shows a system having two inputs which add together through separate linear responses, g(t) and h(t), to produce an output y(t). The inputs are ergodic random variables, x(t) and n(t). The variable n(t) might be, in some cases, an undesirable but ever-present noise signal that is interfering. The output can be written as

$$y(t) = \int_{-\infty}^{\infty} g(b)n(t-b)db + \int_{-\infty}^{\infty} h(\lambda)x(t-\lambda)d\lambda \qquad (58)$$

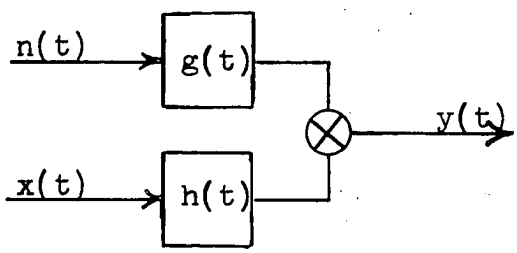

Figure 1.

Two Input - Single Output System

If the equation is shifted in time from (t) to (t + τ), multiplied by x(t) dt, and integrated between -T and +T, there results

$$\int_{-T}^{T} x(t)\, y(t+\tau)\, dt = \int_{-T}^{T}\int_{-\infty}^{\infty} g(\sigma)\, x(t) n(t+\tau-\sigma)\, d\sigma dt + \int_{-T}^{T}\int_{-\infty}^{\infty} h(\lambda)\, x(t)\, x(t+\tau-\lambda)\, d\lambda dt \qquad (59)$$

After multiplying the equation by $\frac{1}{2T}$, obtaining the limit as $T \to \infty$, and inverting the order of integration the result is

$$\lim_{T\to\infty} \frac{1}{2T}\int_{-T}^{T} x(t)\, y(t+\tau)dt = \int_{-\infty}^{\infty} g(\sigma) \lim_{T\to\infty}\frac{1}{2T}\int_{-T}^{T} x(t)n(t+\tau-\sigma)\, dt d\sigma + \int_{-\infty}^{\infty} h(\lambda) \lim_{T\to\infty}\frac{1}{2T}\int_{-T}^{T} x(t)x(t+\tau-\lambda)d\lambda dt \qquad (60)$$

Since the variables are of an ergodic random process,

$$\phi_{xy}(\tau) = \int_{-\infty}^{\infty} g(\sigma)\, \phi_{xn}(\tau-\sigma)d\sigma + \int_{-\infty}^{\infty} h(\lambda)\phi_{xx}(\tau-\lambda)d\lambda \qquad (61)$$

A similar procedure can produce the relationship

$$\phi_{ny}(\tau) = \int_{-\infty}^{\infty} g(\sigma)\, \phi_{nn}(\tau-\sigma)d\sigma + \int_{-\infty}^{\infty} h(\lambda)\phi_{nx}(\tau-\lambda)d\lambda \qquad (62)$$

The time responses, g(σ) and h(λ), could be obtained by a process of simultaneous deconvolution when the correlation functions are known.

It is not uncommon that the noise, n(t) and x(t) are statistically independent of each other. Under these circumstances,

$$\phi_{xn}(\tau) = \phi_{nx}(\tau) = \phi_{nx}(0) = \phi_{nx}(\infty) = \overline{n(t)} \cdot \overline{x(t)} \qquad (63)$$

and if either n(t) or x(t) have a zero mean value, Equation (61) and (62) become independent of each other for the solution for the impulse responses, as

$$\phi_{xy}(\tau) = \int_{-\infty}^{\infty} h(\lambda)\ \phi_{xx}(\tau-\lambda)\ d\lambda \qquad (64)$$

$$\phi_{ny}(\tau) = \int_{-\infty}^{\infty} g(\lambda)\ \phi_{nn}(\tau-\lambda)\ d\lambda \qquad (65)$$

For stable systems, Fourier transforms of Equation (61) and (62) yield

$$\Phi_{xy}(\omega) = G(\omega)\ \Phi_{xn}(\omega) + H(\omega)\ \Phi_{xx}(\omega) \qquad (66)$$

$$\Phi_{ny}(\omega) = G(\omega)\ \Phi_{nn}(\omega) + H(\omega)\ \Phi_{nx}(\omega) \qquad (67)$$

With independent inputs (and if either has a zero mean), the cross spectral densities are zero, and the above relationships would simplify to the form for a single input system.

Multiple Inputs, Single Output Linear System

The previous analysis can readily be extended to a system having, in general, n inputs affecting a single output. With reference to Figure 2 consider a linear system with inputs, $x_1(t)$, $x_2(t)$,,, $x_i(t)$,,, $x_n(t)$. In this model each input, $x_i(t)$, has associated with it a unique function $h_i(t)$ --the impulse response of the output. Considering that the inputs are each members of ergodic random processes, a derivation similar to that for Equations (61) and (62) yields

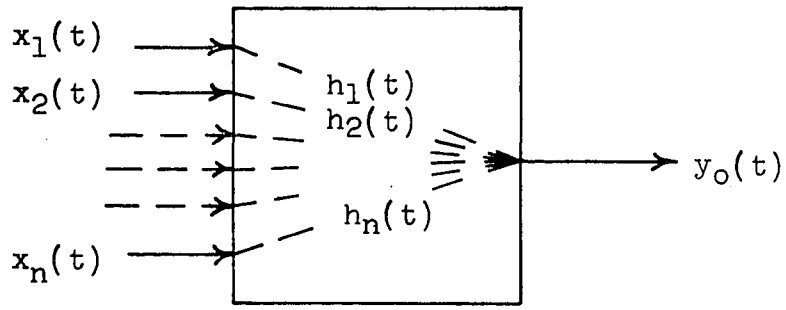

Figure 2

Multiple Inputs - Single Outlet System

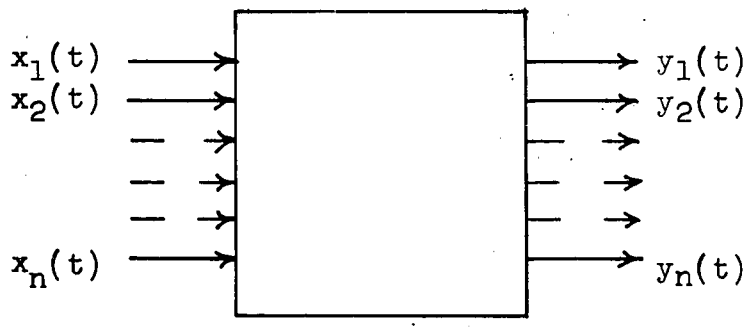

Figure 3

System Having Multiple Inputs and Outputs

$$\begin{aligned}
\phi_{1o} &= \phi_{11} * h_1 + \phi_{12} * h_2 + \cdots + \phi_{1n} * h_n \\
\phi_{2o} &= \phi_{21} * h_1 + \phi_{22} * h_2 + \cdots + \phi_{2n} * h_n \\
&\vdots \qquad\quad \vdots \qquad\quad \vdots \qquad\quad \vdots \\
\phi_{no} &= \phi_{n1} * h_1 + \phi_{n2} * h_2 + \cdots + \phi_{nn} * h_n
\end{aligned} \tag{68}$$

where:

ϕ_{io} = crosscorrelation function and the output $y_o(t)$ between input $x_i(t)$

h_i = impulse response of $y_o(t)$ from input $x_i(t)$

ϕ_{ij} = auto or cross correlation function between inputs $x_i(t)$ and $x_j(t)$

and the symbol, *, indicates the process of convolution. The above may also be expressed in matrix notation as

$$\underline{y} = A * \underline{h} \tag{69}$$

where:

$\underline{y} = [\phi_{io}]$ a column vector of n components

$A = [\phi_{ij}]$ a square matrix of order n

$\underline{h} = [\phi_{jo}]$ a column vector of n components

Each of the above is a function of a time variable.

The equivalent information in the frequency domain can be obtained by a Fourier transformation, assuming that each transfer relation is stable. There results

$$\underline{Y} = \beta \cdot \underline{H} \tag{70}$$

where

$$\underline{Y} = \left[\Phi_{io}\right]$$
$$\beta = \left[\Phi_{ij}\right]$$
$$\underline{H} = \left[H_{io}\right]$$

Either of the column vectors $\underline{h}(t)$ or $\underline{H}(\omega)$ represent the dynamics of the multiple input system.

Multiple Inputs and Outputs. The multiple input, multiple output linear system may be treated by a further extension of the previous analysis. Consider the system as shown in Figure 3 having m inputs and n outputs. For each output, say $y_j(t)$, there exists some impulse response $h_{ij}(t)$ associated with every input $x_i(t)$. Therefore, a system of m equations identical in form to Equation (68) exist for every output. A matrix of m x n impulse responses, or equivalently frequency response functions, can be used to describe the system.

Chemical Processing Equipment

Linearity

The statistical, dynamic relationships considered in the preceding sections have concerned systems which are time-invariant and linear. Linearity, as defined previously, implies that the system responds to a collection of functions in an input just as though the individual responses were superimposed.

The dynamics of chemical engineering equipment inherently seem to defy description as linear systems. However, in a number of cases a few reasonably simplying

assumptions will allow derivation of equations that represent a linear system. The chemical engineering literature is rapidly growing with such linear dynamic representations.

Under the classification of "linear," two divisions may be made --- time-invariant, or stationary, and time-variant.

Time-Invariant System. A time-invariant system can be represented by a constant coefficient equation of the form of Equation (1) as

$$\sum_i a_i \frac{d^i y}{dt^i} = x(t) \tag{71}$$

The impulse response of this type of system is a function of one time variable, the delay τ from the occurrence time of the impulse, such as $h(\tau)$.

Time-Variant Systems. The linear, time-variant system can be represented by an equation of the type

$$\sum_i a_i(t) \frac{d^i y}{dt^i} = x(t) \tag{72}$$

where the coefficients may be functions of time. However, the coefficients can not be functions of the independent variable $x(t)$ and still retain the property of superposition --as Stewart (27) has shown for a flow-forced chemical reactor. The impulse response for the system of Equation (72) is a function of time t and the delay τ from the occurrence of the impulse, and is written as $h(t, \tau)$. The

treatment of time variant, linear systems is beyond the scope of this present work.

Lumped and Distributed Parameter Systems. In addition to the classification of linearity, chemical process dynamics can also be divided into "lumped parameter" or "distributed parameter" systems. A glance at past and even present textbooks concerning control of dynamic physical processes will show attention directed predominantly to the lumped parameter treatment. In spite of the complexity of analyzing dynamic systems having distributed parameters, these systems can possess the property of linearity.

Lumped Parameter Systems.

Equations (71) and (72) are ordinary differential equations and, as such, represent lumped parameter systems. Properties of these systems can be designated at various points or over portions of the systems. Examples of this type are most common. For mechanical systems these might describe the mass---spring---dashpot combination. For electrical circuits they might describe resistance---inductance---capacitance combinations.

Some chemical processes also can be considered as lumped parameter systems. Generally, these are chemical processes for which the assumption of perfect mixing is quite nearly valid, at least in the frequencies of interest. The literature shows numerous examples which cannot be

covered here. Such lumped parameter processes include continuous stirred tank reactors, finite stage liquid-vapor mass transfer operations such as bubble-tray distillation, absorption, stripping, etc. and finite stage liquid-liquid operations such as extraction.

Distributed Parameter Systems

Systems whose variables are continuous functions of two or more independent variables, such as position and time, are classified as having distributed parameters. Their dynamic descriptions, or mathematical models, are in the form of partial differential equations. Chemical processes are predominantly of this type because they normally involve transfer of heat, mass, or momentum (or combinations of these) through the dimensions the equipment and as a function of time. Nevertheless, some distributed parameter systems can have the property of linearity as discussed previously. To illustrate this point, two examples will be considered.

The equipment shown in Figure 4 is a concentric pipe heat exchanger in which a hot fluid, for instance, is transfering heat to the outer, cooler fluid. Flow may be either concurrent or counter-current. An energy balance over a differential length of fluid in the inner tube yields

$$\frac{\partial T}{\partial t} = \frac{F_t}{A_t \rho_t} \frac{\partial T}{\partial x} \quad \frac{U \pi d}{A_t \rho_t C_{pt}} \qquad \text{(S-T)} \tag{73}$$

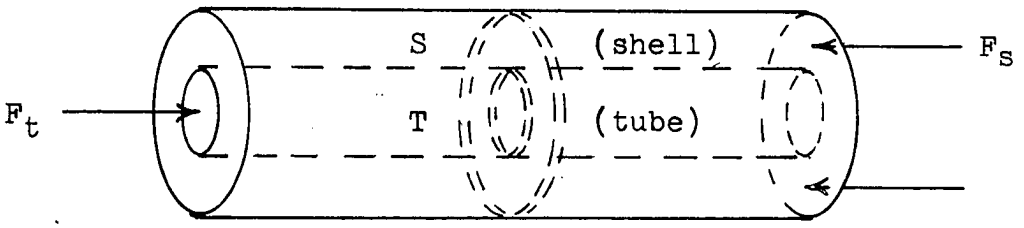

Figure 4

Concentric Pipe Heat Exchanger Model

and similarly for the shell fluid,

$$\frac{\partial S}{\partial t} = \pm \frac{F_s}{A_s \rho_s} \frac{\partial S}{\partial x} + \frac{U \pi d}{A_s \rho_s C_{p_s}} (T-S) \qquad (74)$$

where

T = temperature of fluid in tube

S = temperature of fluid in shell

F = mass flow rate

A = cross sectional area

U = overall heat transfer coefficient (based on d)

d = outside diameter of inner tube

ρ = density

c_p = heat capacity

t = time

x = longitudinal distance

subscripts refer to

s = shell fluid

t = tube fluid

The coefficient of $\frac{\partial S}{\partial t}$ is negative for concurrent flow and

conversly for counter-current flow. Assumptions which permit the use of the above equations for a mathematical model are:

(1.) Properties of the fluids are constant with temperature.

(2.) The inner and outer tube wall thermal capacities are negligible compared to the flowing fluids.

(3.) Plug flow exists in both the shell and tube.

(4.) The fluid thermal conductivities are infinite.

(5.) No heat is transferred across the outer shell wall.

For convenience, the constant coefficients above can be grouped and written as

$$\frac{\partial T}{\partial t} = -k_1 \frac{\partial T}{\partial x} + k_2 (S-T) \tag{75}$$

and

$$\frac{\partial S}{\partial t} = \pm k_3 \frac{\partial S}{\partial x} + k_4 (T-S) \tag{76}$$

Without solving the above equations for the impulse response, or frequency response, in order to identify its linearity, rather let us observe some properties of the equations themselves. Suppose that the inlet tube fluid temperature is the only input variable to the system and the outlet tube temperature response is observed. For a given change in inlet tube temperature the response can be called $\left[T_1(t,x)\right]$ $x = L$, (outlet) as a solution of

$$\frac{\partial T_1}{\partial t} = -k \quad \frac{\partial T_1}{\partial x} + k_2 (S_1 - T_1) \tag{77}$$

$$\frac{\partial S_1}{\partial t} = \pm k_3 \quad \frac{\partial S_1}{\partial x} + k_4 (T_1 - S_1) \tag{78}$$

and certain known boundary conditions, and for a different input the response can be called $\left[T_2(t,x)\right]$ $x = L$, (outlet) as a solution of

$$\frac{\partial T_2}{\partial t} = -k_1 \frac{\partial T_2}{\partial x} + k_2 (S_2 - T_2) \tag{79}$$

$$\frac{\partial S_2}{\partial t} = \pm k_3 \frac{\partial S_2}{\partial x} + k_4 (T_2 - S_2) \tag{80}$$

and known boundary conditions. By adding (77) and (79) it is found that

$$\frac{\partial (T_1+T_2)}{\partial t} = -k_1 \frac{\partial (T_1+T_2)}{\partial x} + k_2 \left[(S_1+S_2) - (T_1+T_2)\right] \tag{81}$$

and by adding (78) and (80) that

$$\frac{\partial (S_1 + S_2)}{\partial t} = \pm k_3 \frac{\partial (S_1 + S_2)}{\partial x} + k_4 \left[(T_1 + T_2) - (S_1 + S_2)\right] \tag{82}$$

The last results show that the system has the property of superposition and is therefore linear. Nearly the same requirements hold for the distributed parameter system to be linear as for the lumped parameter systems. Note that if the flow of one system, say F_t, were changed as an input variable, the system would not remain linear.

Another example of a distributed parameter system is diffusion in a flowing conduit, as represented in Figure 5. If the inlet concentration of a solution (or mixture) to the conduit is $C_i(t)$, concentration becomes a function of

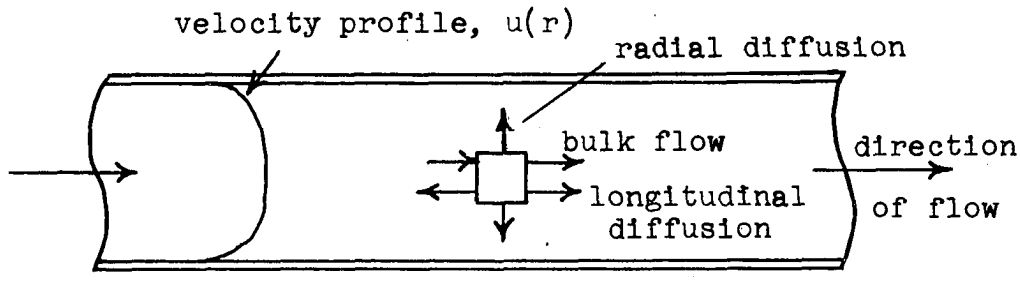

Figure 5

Model for Mass Transport in a Conduit

distance, radius, and time according to the equation

$$\frac{\partial C}{\partial t} = D\left[\frac{\partial^2 C}{\partial r^2} + \frac{1}{r}\frac{\partial C}{\partial r} + \frac{\partial^2 C}{\partial x^2}\right] - u(r)\frac{\partial C}{\partial x} \qquad (83)$$

and the given boundary conditions, where

C = concentration of solute, mass per unit volume

r = radial distance

x = longitudinal distance

t = time

u(r) = velocity profile throughout the radius

D = diffusion coefficient

The assumptions are made that:

(1.) The diffusion coefficient, D, is equal in the directions of r and x and it includes both molecular and eddy diffusion if the flow is turbulent.

(2.) The velocity profile u(r) is constant throughout x and t.

By the same procedure it can be seen that for two different inputs, $\left[C_i(t)\right]_1$ and $\left[C_i(t)\right]_2$ the solutions can be superimposed as

$$\frac{\partial(C_1+C_2)}{\partial t} = D\left[\frac{\partial^2(C_1+C_2)}{\partial r^2} + \frac{1}{r}\frac{\partial(C_1+C_2)}{\partial r} + \frac{\partial^2(C_1+C_2)}{\partial x^2}\right] - u(r)\frac{\partial(C_1+C_2)}{\partial x} \tag{84}$$

when all the boundary conditions except $C_i(t)$ remain the same. Therefore, this distributed parameter system is also linear.

CHAPTER IV

REVIEW OF PREVIOUS WORK AND STATEMENT OF THE PROBLEM

Problems in Practical Determination

The actual practice of determining system dynamics by correlation involves several basic difficulties. Some of these can be realized by observing the assumptions and requirements made in the definitions and the theoretical relationships of the previous chapter. Reference is made here chiefly to Equation (52) involving correlation functions and the impulse response and to Equation (54) or (55) the equivalent relationship as a function of frequency. Some difficulties can be listed as follows.

Ergodic Random Inputs. Correlation functions are most conveniently calculated as time averages in practice. The requirement that the variables are statistically stationary and also are members of ergodic random processes may not be satisfied.

Correlations from Finite Averaging. The time averaging calculation of correlation functions, as in Equations (33) and (36), requires as infinite averaging period in theory. Regardless of the equipment or method

used in practice, only an estimate of the correlation function, taken from a finite length of record, can be determined.

Fourier Transform Truncation. The preferred method of solving the integral equation, Equation (52), for the system response is in the frequency domain, as in Equation (55). By this method the power spectral density estimates are obtained by transforming the correlation function. Calculated estimates of the correlation functions may not be determined out to values of the delay variable, τ_m, high enough for the functions to disappear essentially. A consequence is that such Fourier transform calculations must be truncated at some finite value. This simplification introduces another error in addition to the error resulting from the use of estimated correlation functions.

Deconvolution of Equation (52) in the time domain for the impulse response h(t) leads to divergent and erroneous results when calculated numerically from the correlation estimates.

Calculations. Difficulties or inaccuracies encountered in calculations depend largely upon the methods or equipment used. However, effect of finite record lengths and the effect of the maximum delay, τ_m, used in the correlation functions are common to all methods of calculation. With the more accurate calculation available through the use of a digital computer, the sampling interval,

Δt, must be properly selected. Digital calculation was used in this study and implementation of other (analog) methods was considered beyond the scope of this work. An excellent survey of various correlation computing methods has been presented by Kaiser and Angell (15).

Input Power Spectral Density. It is desired that the input power spectral densities be constant out to the higher frequencies of interest. Inaccuracies of measurement can be encountered when the input variables, such as those of a normally operating system, do not contain sufficient relative power at some frequencies where the response is desired to be measured. Examples of this kind may exist where slightly nonlinear systems are under control but follow a limit cycle in their variations. Under this kind of operation, the input power spectral density may peak greatly at the control system's "resonant" frequency and have relatively little power at other frequencies.

Previous Investigations

Investigations in determining system dynamics under the influence of random disturbances were initially stimulated on the most part by the work of Lee (19) in 1950. As part of this work Lee showed how the dynamics of a linear system could be determined from the statistical properties of its input and output variables. Goodman (8, 9) in 1955 showed in theory the natural extension of the method to multidimensional linear systems. He also

showed that by this method a non-linear system would be fitted by a linear representation under a minimum least-squares criterion. Using random inputs, Goodman studied a distillation column transfer relationship between the reflux flow rate and the overhead vapor stream temperature. His results gave only qualitative agreement with the standard sinusoidal testing method. Also in 1955, Margolis (22) investigated a laboratory heat exchanger and Chang (3) investigated a flow control process to determine system dynamics using random inputs. Their results were approximate due to relatively short record lengths.

Some books have also been published concerning the broader field of random processes in automatic control. Solodovnikov's book (26), published in 1952 in Russia, was one of the first comprehensive treatments. Lanning and Battin (18), in 1956, presented an excellent text on the subject. Davenport and Root's text (5) of 1958 was similar.

Contributions in the chemical engineering literature on determining system dynamics from random disturbances have been scarce until recently. Aris and Amundson (1), in 1958, considered time responses of a chemical reactor from correlation functions involving input and output variables. This work was a theoretical study of a linearized mathematical model disturbed by random noise having assumed statistical properties. Using an analog computer to simulate first and

second order system behavior and digital computation of the statistical functions, Gore (11), in 1959, determined frequency response by this method. His accuracy was limited by record lengths. Homan and Tierney (12), in 1960, simulated the dynamic behavior of a chemical reactor to a random input by a digital computer. They showed the effects of some time parameters used in the determination of the impulse response and real and imaginary parts of the frequency response.

Scope of this Investigation

Experimental determinations of system dynamics by statistical measurements are necessarily approximate. Experimenters in this field are troubled with the question of accuracy. In actual determinations of this kind it is desirable to know beforehand the requirements of the measurements and calculations to produce a given degree of accuracy. A knowledge of the more advantageous numerical techniques also becomes important. This study was undertaken to qualify some of these requirements.

Specific objectives of this study are the following:

(1.) To carry out determinations of frequency response on an experimental apparatus under simulated operating conditions.

(2.) To evaluate the effect of and to establish requirements on time parameters in the recordings and calculations of the above.

(3.) To evaluate accuracy of determinations using this method, especially as a function of the time parameters above.

(4.) To investigate some numerical techniques needed to improve the calculations.

CHAPTER V

EXPERIMENTAL APPARATUS

Experimental work of this study was for the purpose of simulating the dynamic operation of a continuous stirred tank reactor. The aim was to simulate operation of a reactor representative of an industrial type where a liquid phase exothermic reaction would be carried out. The dynamic or transfer relationship of interest for this case is usually that between the coolant flow rate as the input and reactor temperature as a response. The reactor and its auxiliary equipment used were designed to measure this relationship.

No actual chemical reaction was carried out in the reactor; a heat exchange process was made between a hot inlet fluid to the reactor and the fluid passing through the coolant coils. Both fluids used were water. This arrangement served two purposes. It kept the transfer relationship simplified and avoided the expense involved with a continuous flow of reactants.

A functional arrangement of equipment is shown in Figure 6. Hot water entered the reactor at a constant flow

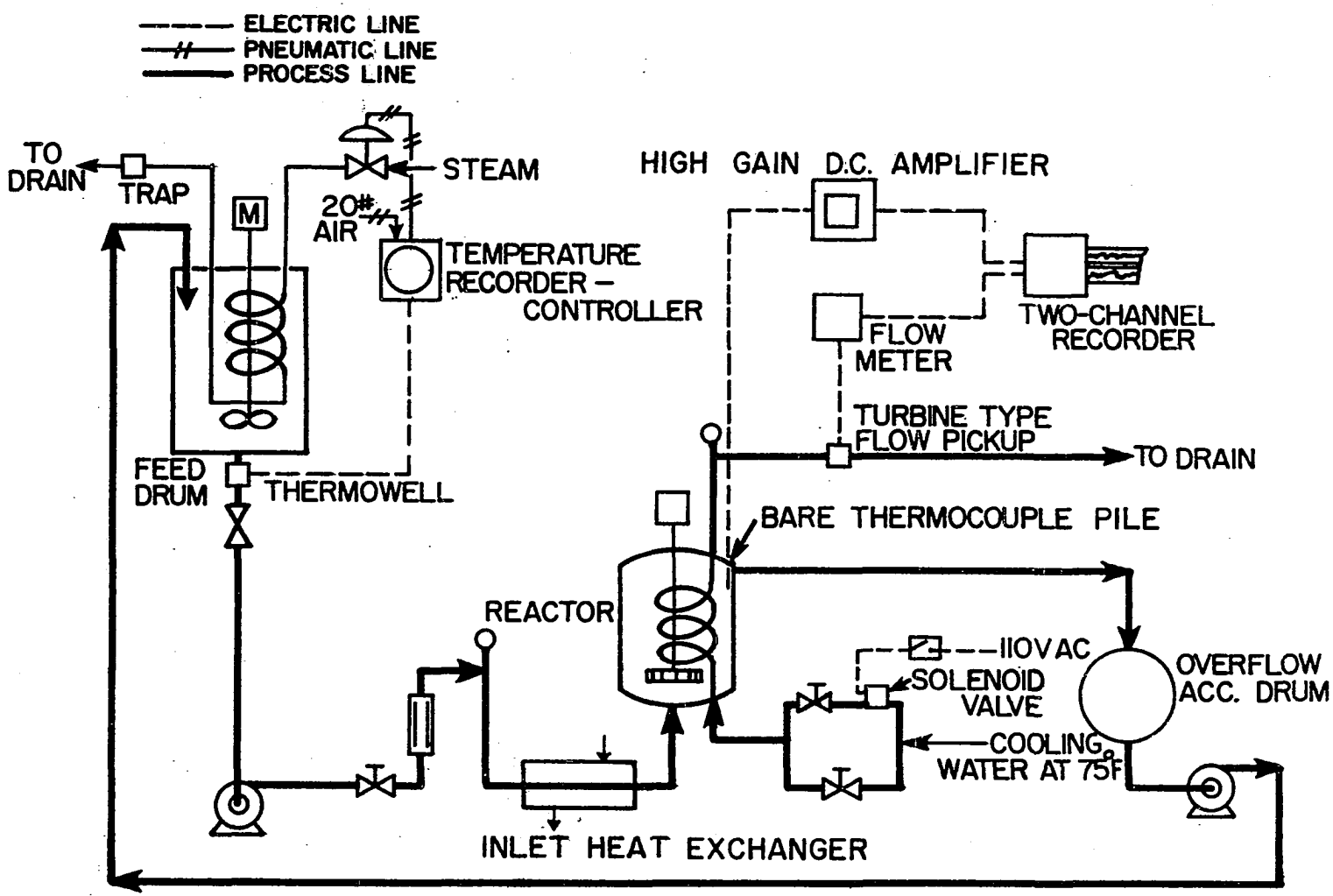

Figure 6

Equipment for Measuring Reactor Coolant Transfer Function by Auto-Crosscorrelation Method

rate. Temperature changes were caused by cooling water flow rate through the reactor coils. The exit reactor fluid recycled back to a feed drum where constant temperature was maintained. The variables, reactor temperature and c lant flow rate, were sensed and recorded as shown.

Two different types of operation were used. The first, employing only one input variable, was made keeping the reactor inlet fluid at a constant temperature. In the second, employing two simultaneous disturbances, the inlet temperature was also varied. This disturbance was accomplished by pulsing steam into the jacket of a small concentric pipe heat exchanger around a section of a inlet pipe.

Reactor

The reactor used in these tests was one for which Fanning (6) has investigated dynamic relationships. A thorough description of the reactor can be found in his thesis. The reactor was basically a tank 12-inches in diameter and 15-inches in height. Throughout the height of the reactor, four vertical baffles extended one inch from the inner wall and were set 90 degrees apart. The walls were #14 gauge type 316 stainless steel. Thermal insulation was provided by a one inch thick covering of glass wool sheathed with aluminum foil.

Operation was carried on at atmospheric pressure. The reactor was open at the top but used with a formed wooden cover over the top to reduce heat and evaporation

losses. Flow entered into the reactor in the bottom at the center and left by a 3/4-inch hole in the side wall near the top. The exit fluid was syphoned through a pipe to an accumulator approximately three feet below the reactor. By maintaining a constant flow through the reactor a constant volume was held in the reactor.

Cooling coils inside the reactor were made from 5/8-inch O.D. copper tubing. Heat exchange area was 1.84 square feet produced by 7.5 turns wound on an approximate 5-inch diameter.

Stirring action was provided by a Model CV-4 "Lightnin" portable mixer with a turbine type impellor. The mixer motor was a 1/4 H.P. variable speed brush shifting type. The 4-inch diameter turbine was run at 360 R.P.M. for all runs.

Fluid entering the reactor was pumped from a feed drum by a centrifugal pump and controlled manually with a 3/8-inch needle value in the line. The pump was a Gould 10 G.P.M. pump (rated at 20 feet of water differential). A Fischer-Porter series 1700 "Flowrator" was used to indicate flow rate. All runs were made at 3.84 G.P.M. Some minute flow rate variations were encountered, but the rate did not drift significantly during any run.

After leaving the reactor, the exit fluid was collected, by siphoning, in a 55 gallon overflow accumulator barrel. A 10 G.P.M. Deming centrifugal pump (rated at 20

feet of water differential) was used to remove this fluid from the barrel. Since the recirculation rate was well below 10 G.P.M., this barrel remained nearly empty during a run.

Temperature-Controlled Feed Tank

Fluid recirculated from the overflow accumulator tank was mixed in a temperature controlled feed drum before reentering the reactor. About 30 gallons of fluid were kept in this 55 gallon open-top barrel. The fluid was kept well stirred by the use of a 1/4 H.P. portable mixer clamped on the top edge of the barrel. The mixer shaft transmitted its power to the fluid by two, 3-inch diameter propellors.

A temperature control system was used to maintain temperature at approximately 150°F. Temperature was sensed in a pipe tee immediately after leaving the feed drum by means of a bare copper-constantan thermocouple. Indicating, recording, and controlling actions of this temperature were carried out by means of a Model 152 Minneapolis-Honeywell Brown "Electronik" Potentiometer. Pneumatic controls were an integral part of the instrument. Used with the type T thermocouple, the range was 50°F to 250°F. Both proportional and reset action were used. The 3-15 psi output signal operated a Research Controls valve Model 75B to produce the required steam flow through the coils immersed in the tank. The control valve had a linear trim, a C_v equal to 1.25,

and air to close action. Steam supply pressure was regulated at approximately 60 psig. and a steam trap was employed at the discharge of the steam coils. The 5/8-inch copper tubing coils provided approximately 2.8 square feet of outside surface. After final adjustments of proportional band and rest, temperatures could be maintained within a range of 1°F at a desired temperature level.

Cooling Water Flow Controls

Cooling water flow rate was the main variable used to cause reactor temperature variations during operation. For the statistical input, it was desired to have a random square wave, which necessitated a means of holding two drift-free levels of flow and swi hing between them rapidly. It was accomplished by providing two parallel paths for flow. In one, a 3/8-inch needle valve was used and in the other path, a 1/4-inch needle valve was used in series with an electric solenoid valve, a Skinner Model LC-2 normally closed valve which uses a 110 volt AC coil. This arrangement allowed rapid flow changes between 0.8 G.P.M. and 1.2 G.P.M., although some rounding of the leading edges of the square wave was produced. To assure a constant upsteam pressure, and thus to practically eliminate the flow rate "drifting," the valve manifold was fed from a standpipe 29 feet above the exit of the reactor coils. With the above aparatus, either of two coolant flow rates could be selected by means of a switch. Steady state reactor temperatures

produced by the two flow rates were 2.9°F in difference. Figure 7 shows a sample of the recording for this single input case.

Reactor Inlet Fluid Heat Exchanger

To produce the second input variable, reactor inlet temperature, the fluid entering was passed through the center tube of a concentric pipe heat exchanger. A thin-walled 5/8-inch outside diameter brass tube was used as the inner pipe and the outer jacket was constructed of a 3-inch diameter steel pipe. The jacket length was 12-inches and thus an effective area for heat exchange was 47.1-square inches. Saturated steam regulated at 60 lb/sq.in. gage was allowed to flow into the jacket volume by means of a solenoid valve---the same type as used in the water line. Switching of the valve on and off did not produce a square wave response in reactor inlet temperature because of the thermal capacity of the inner tube wall and flowing water. The shape of response to random switching can be seen in Figure 8. The heat flux difference imported by this exchanger was enough to produce steady state reactor temperature differences of 1.8°F.

Sensing and Recording the Operating Data

Reactor Temperature. In order to provide the reactor temperature measurement with good sensitivity and a wide bandwidth in frequency response, a pile of five bar

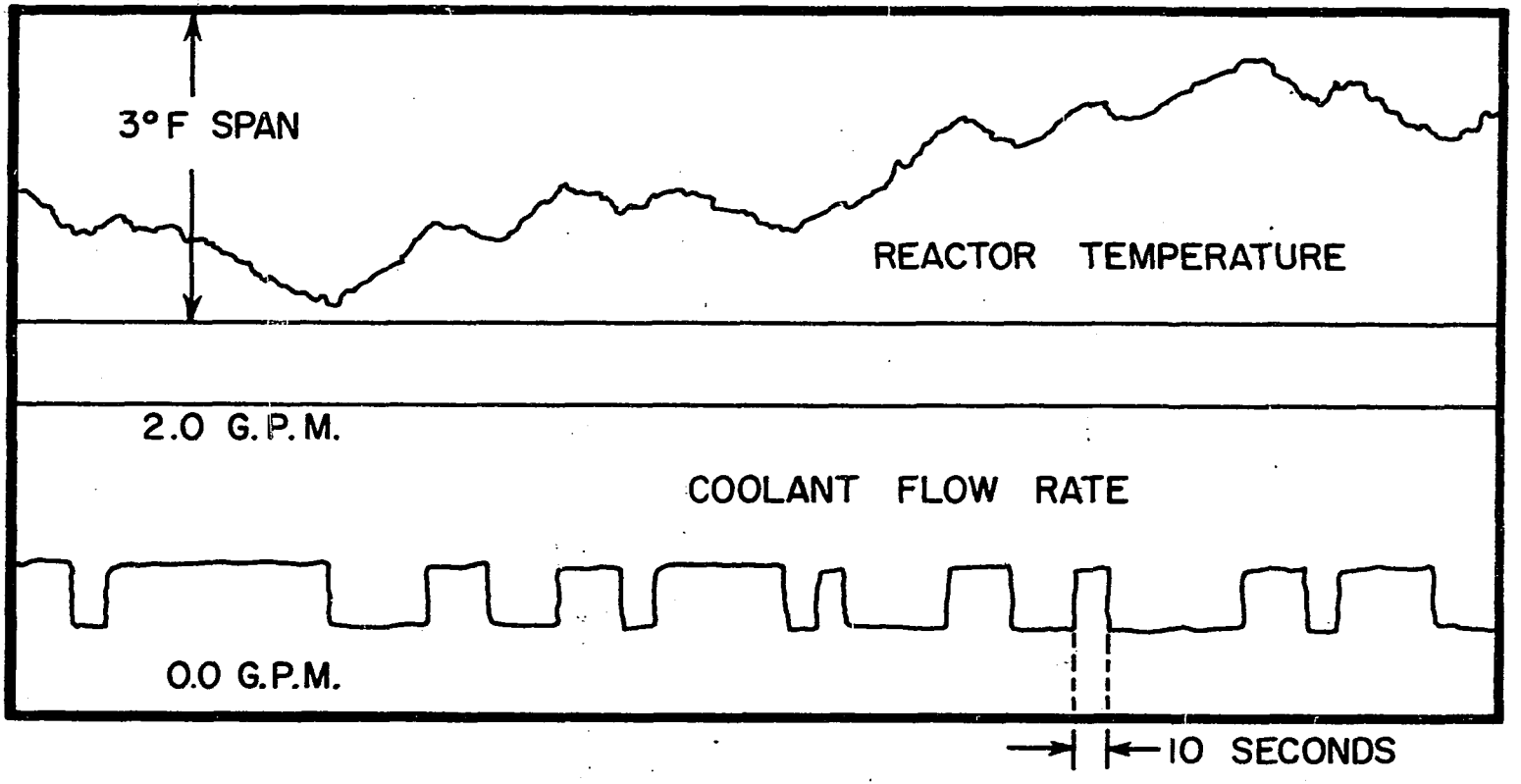

Figure 7

A Typical Portion of Recorded Data
(One Input Function)

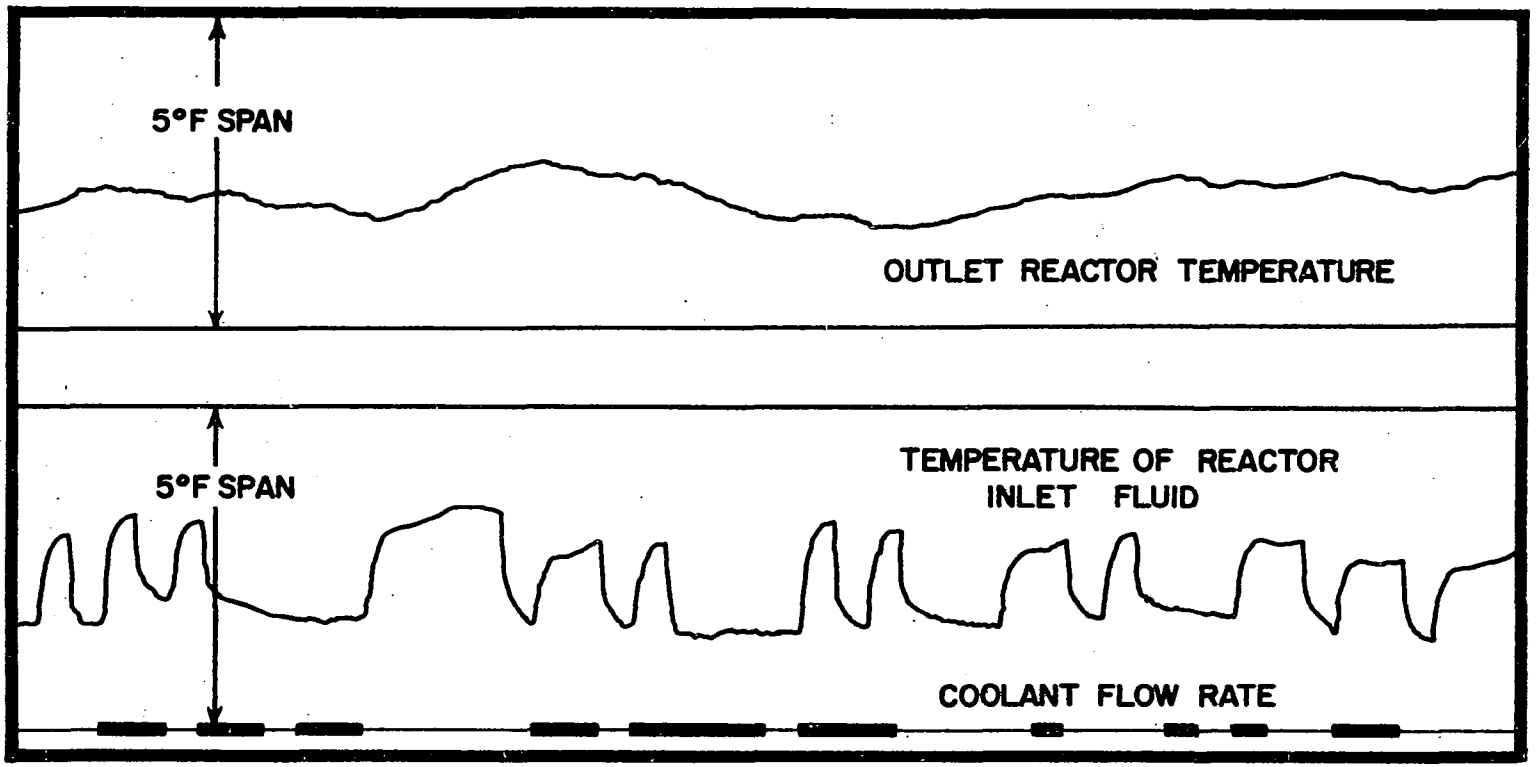

Figure 8

A Typical Portion of Recorded Data For Two Input Functions

copper--constantan thermocouples were used. The thermocouples were mounted on a probe around circle of an approximate $1\frac{1}{4}$-inch diameter. The probe was extended into the reactor so that the thermocouple junctions were approximately $2\frac{1}{2}$-inches from the side exit hole, and approximately $2\frac{1}{2}$-inches below the top surface of fluid. Thermocouple leads were carried out for approximately 3-ft. to an ice bath used as the cold junction for all five thermocouples. From the ice bath, the potential developed by the five couples in series was carried by a two (copper) conductor shielded cable to an amplifier. A potential of approximately 110 microvolts per degree Fahrenheit could be obtained by this arrangement.

In order to record a suitable temperature range, the thermocouple potential was amplified using a Sanborn Model 350-1500 Low-Level D.C. Preamplifier with a Model 350-2 Plug-in Unit. This instrument allowed a continuously adjustable gain factor up to 50,000 and an input suppression of $\pm$ 100 millivolts. Its input impedance was 100,000 ohms and frequency response was 0 to 100 cycles per second.

In the case of two input functions only, between the preamplifier and amplifier of the recorder, the thermocouple signal was passed through a two stage R.C. filter having break frequencies at 82.2 and 541. radians per minute. Its purpose was to filter out unnecessary noise at frequencies far beyond the bandpass of the chemical reactor

being measured. The filter thus served to reduce aliasing while not attenuating greatly at those frequencies of interest.

Recordings were made on a Sanborn Model 60-1300 Two Channel Recorder. The maximum sensitivity available on this recorder and its amplifiers was 0.025 volts for a full scale deflection of 5 centimeters. This sensitivity made it possible for the overall system to record a temperature range as low as .00455°F full scale. For the work herein a range of either 3.2° or 5.9°F full scale was used. The zero level of this range could be changed widely by a potentiometer setting the millivolts of suppression. The recorder bandwidth was 0 to 45 cycles per second so that no "useful" frequencies were attenuated.

Reactor Inlet Temperature. The reactor inlet temperature was sensed and recorded in a duplicate system. At approximately two feet before entering the reactor, five bare copper-constantan thermocouples sensed the temperature of the flowing fluid. The sensing location was in a $\frac{1}{2}$-inch pipe tee where the flow direction was changed 90 degrees. The thermocouples were led through and held in place by a cylindrical Teflon plug fitted snugly in a $\frac{1}{2}$-inch Crawford pipe-to-tubing adapter. Gain settings on the preamplifier and recorder amplifier were made to record a 5°F range and the recorder zero level could be varied to any desired temperature. A typical record of inlet temperature is

shown as a part of Figure 8.

Coolant Flow Rate. Measurement of the coolant flow rate after leaving the reactor coils was provided by a Waugh Model F1-6S turbine type flow pickup. The signal from this device was carried by a shielded two conductor cable to a control, panel-mounted conversion unit. This unit was a Waugh Model FR-111 Pulse Rate Converter which served to convert pulse frequencies to an analog voltage proportional to flow. These two devices combined to give a calibration of 0.3 to 2.0 G.P.M. on a linear scale with less than 0.5 per cent error. The analog voltage, 0 to 50 millivolts, from the pulse rate converter could be recorded on the two channel recorder. A typical recording is shown in Figure 7.

For the runs in which two inputs were used, it was desired to record three variables, inlet reactor temperature, inside reactor temperature, and coolant flow rate. Because the coolant flow rate assumed only two different values, or was binary type information, another arrangement was made to record it. In place of sensing the flow and recording it, information was put on the recording by the marker pen. A relay energized through the coolant solenoid switch was used to actuate the marker pen. When the high flow occured, the marker pen then gave an envelope of 60 cycle variations, and when low flow occurred, the marker pen was still. Three channels of information could thus be recorded as shown in Figure 8.

CHAPTER VI

INVESTIGATIONS

Transfer Relationship

Experimental data of these investigations consisted of operating records of the equipment as described in the previous chapter. Two different recordings were made for the determination of the transfer relationship between cooling water flow rate and reactor temperature. Each recording was made for a period of approximately 3 hours and 10 minutes. In the first, only one random disturbance-cooling water flow rate was imposed upon the reactor. All other input variables were held essentially constant. In the second recording, random disturbances were introduced by both cooling water flow rate and temperature of the reactor inlet fluid.

Data Generation and Processing

Random Input Functions. Coolant flow rate disturbances were introduced into the experimental equipment in the form of a random square wave. This type of random input was a rather simple matter to generate. It was generated by selecting one of two predetermined flow rates at a fixed

interval of time, 10 seconds. The random selection of either flow rate was made by the use of a table of random digits (23) in which each digit appears with equal probability. A high or low flow rate, selected by switching an electric solenoid valve, was determined from sampling an odd or even digit at the beginning of each time interval. Therefore, during any future interval of time, a high or low flow rate could occur with equal probability.

Input Autocorrelation Function. The autocorrelation function of this input function has the simple form of an isosceles triangle centered at the origin as

$$\phi_{xx}(\tau) = \overline{x^2(t)} \left[1 - \frac{|\tau|}{T_s}\right] \quad \text{for } 0 \leq |\tau| \leq T_s$$

$$= 0 \quad \text{for } |\tau| > T_s \tag{85}$$

where T_s is the table sampling, or switching, period. A derivation of this relationship is presented in Appendix A. With reference to Figure 9, it can be seen that this autocorrelation function approaches an impulse function as T_s approaches zero.

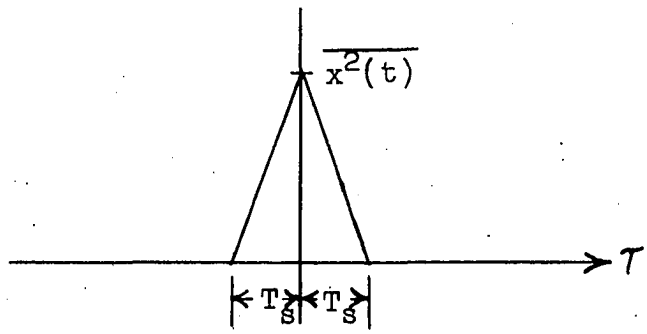

Figure 9

Autocorrelation of Input Random Square Ware

This property becomes convenient, because a crosscorrelation, ϕ_{xz}, between this input x(t) and the output z(t) then approaches an impulse response function.

The power spectral density of this random square wave is, of course, the Fourier transform of Equation (85). The result becomes

$$\Phi_{xx}(\omega) = \overline{x^2(t)}T_s \left(\frac{\sin \frac{\omega T_s}{2}}{\frac{\omega T_s}{2}} \right)^2 \qquad (86)$$

(See Appendix A.) For small values of the parameter T_s this function is broad in frequency and the converse holds. A necessity of this statistical method of measuring a system frequency response is that the input function contains enough power at the frequencies of interest so that a response can be measured at those frequencies. This requirement holds similarly for all types of frequency response measurements, including pulse testing. It is therefore quite helpful to know a priori the approximate frequency response of the system or the frequency range of interest.

Selection of T_s. A mathematical model of the experimental system was first examined to approximate its frequency response. A lumped parameter system and linear constant coefficient equations were assumed to apply. See Appendix B for the derivation. A comparison of the model's frequency response and the input power spectral density

(from Equation (86) for T_s = 10 seconds was made. The power sectral density of this random square wave does extend beyond the system frequency response but it has a slight disadvantage in that it has a repeating zero value at $\frac{\omega T_s}{2} = n\pi$, where n = 1,2,3, etc. Selection of a 10 second basic switching period makes the first zero occur at 37.7 radians where the system response is expected to be attenuated more than 2 decades. The value T_s = 10 seconds was thus suitable for the experimental work.

Preparation of Recorded Data for Digital Computation

Selection of Sampling Interval, Δt. Digital computer calculations made on the continuously recorded data from the experimental equipment must necessarily involve discrete values taken at some definite sampling interval. To minimize the computation, large intervals are desired; but to recover the higher frequency information of the function, the interval must be less than one-half of the period of the highest frequency ω_f, to be recovered, according to the Nyquist sampling theorem. Any information above the frequency ω_f is folded back and added to the true spectrum as the resulting spectrum of the discrete function. Thus, the sampling interval must be chosen to give a folding frequency that will not fold back, or cause aliasing, into the significant range of the frequency response.

The sampling interval used was 1.93 seconds corresponding to one millimeter of record length. This

interval defines the folding frequency to be 97.5 radians per minute. This frequency is well above the significant response of the equipment.

Data Transfer to Digital Computer. The process of transferring recorded data to the digital computer was performed almost entirely by hand. An outline of this procedure was as follows:

(a) Each sampled point of the system variables was read (by eye) to two digits from the 50 division, 5 centimeter wide recordings. Values for the coolant flow rate were read as either plus or minus one for the high and low flow rates respectively.

(b) The series of numbers were punched on IBM cards.

(c) The cards were read into the computer and converted to floating point decimal numbers. The average value for the entire record was computed and subtracted from each number. Coolant flow rate values were kept as plus or minus one.

(d) These series of numbers were stored for computations. In the first phase of the work, for one input variable, storage was in the form of IBM cards. In the second part, storage was made on magnetic tape of an IBM 727 unit.

Because the variables were read from a recording, it

was convenient to use only the recorder units to specify their levels. In so doing, a transformation of the variables was made as the following:

For the one input case,

$$r_i = +1 \quad \text{for } W(i\Delta t) = 1.0 \text{ G.P.M.}$$

$$= -1 \quad \text{for } W(i\Delta t) = 0.6 \text{ G.P.M.} \tag{87}$$

and

$$c_i = a_1 \cdot \left[T_2(i\Delta t) - (T_2)_{LOW}\right] \tag{88}$$

where $T_2(i\Delta t)$ is the reactor temperature (^oF) at time $i\Delta t$, $(T_2)_{LOW}$ is the steady state reactor temperature at the high coolant flow rate and $a = \frac{10 \text{ scale units}}{3.2\ ^oF} = \frac{3.12 \text{ units}}{^oF}$

For the two input case,

$$x_i = +1 \quad \text{for } W(i\Delta t) = 1.0 \text{ G.P.M.} \tag{89}$$

$$= -1 \quad \text{for } W(i\Delta t) = 0.6 \text{ G.P.M.}$$

$$y_i = a_2 \cdot \left[T_1(i\Delta t) - (T_1)_{AVG}\right] \tag{90}$$

where $T(i\Delta t)$ is the reactor inlet temperature (^oF) at time $i\Delta t$, $(T_1)_{LOW}$ is the reactor inlet temperature when no heat is added to the inlet exchanger, and

$$a_2 = \frac{10 \text{ scale units}}{5.9^oF} = 1.695 \frac{\text{units}}{^oF}$$

and

$$z_i = a_3 \left[T_2(i\Delta t) - (T_2)_{LOW}\right] \tag{91}$$

where $a_3 = \frac{10 \text{ scale units}}{5.9^oF} = 1.695 \frac{\text{units}}{^oF}$

Computations

The computations of this work have been programmed and run on an IBM type 650 digital computer at the University of Oklahoma Computer Laboratory. The latter part of this work involving two input functions was run on this computer when augmented with immediate access storage, a #305 disk storage file and two #727 magnetic tape units.

Correlation Estimates. The correlation function estimates were calculated from the discrete data using an expression of the form

$$\phi_{rc}^{*}(\tau) = \frac{1}{N-\tau_m} \sum_{i=1}^{N-\tau_m} r_i \, C_{i+\tau} - \left(\frac{1}{N-\tau_m} \sum_{i=1}^{N-\tau_m} r_i \right) \left(\frac{1}{N-\tau_m} \sum_{i=\tau_m+1}^{N} C_i \right) \quad (92)$$

Equation (92) defines a cross-correlation estimate and an autocorrelation estimate is similar. The factors on the far right were used to subtract any bias of the function that might occur when fractions of the total record were used.

A normalized correlation estimate could also be computed as

$$\rho_{rc}^{*}(\tau) = \frac{\phi_{rc}^{*}(\tau)}{\frac{1}{N-\tau_m} \sum_{i=1}^{N-\tau_m} r_i c_i - \left(\frac{1}{N-\tau_m} \sum_{i=1}^{N-\tau_m} r_i \right) \left(\frac{1}{N-\tau_m} \sum_{i=\tau_m+1} C_i \right)} \quad (93)$$

Time required for computations were approximately proportional to the product -- $(N-\tau_m)$ (τ_m). For an

autocorrelation function the time required was approximately $0.02\ (N-\tau_M)(\tau_M)$ seconds. For a crosscorrelation function the time was approximately $0.03\ (N-\tau_M)\ (\tau_M)$ seconds.

Fourier Transforms. The power spectral density estimates were obtained by calculating Fourier transforms of the correlation function estimates. The computer program for this calculation considered the correlation function, or any time function to be transformed, to be represented by straight line segments between discrete values. A constant increment length between discrete values was used. Sums of terms resulting from analytical integration over each increment were added to yield the transform. The expression programmed was

$$F(\omega) = \sum_{n=N}^{N-1} \int_{n}^{n+1} W_k(t) \left[\alpha_n + \beta_n(t-n\Delta t)\right] e^{-i\omega t}\, dt \qquad (94)$$

where, if $f(n\Delta t)$ is the function to be transformed,

$$\alpha_n = f(n\Delta t)$$

$$\beta_n = \frac{f((n+1)\Delta t - f(n\Delta t)}{\Delta t}$$

and

$$W_k(t) = \left[1-\left(\frac{t}{T}\right)^2\right]^k \qquad (95)$$

This procedure avoids the inaccuracies at high frequencies which result when the product $f(n\Delta t)\ e^{-j\omega n\Delta t}$ is formed and integrated by a trapezoidal or Simpson's rule method.

Two types of errors can occur in calculating Fourier transforms by this method, assuming that there is

no error in the discrete values given the program. One is the representation of the time function to be transformed, $f(\Delta t)$, by straight line segments between the discrete values. Of course, if the function is a straight line, this type error does not occur. Otherwise for a given time function, this error in transforming varies with interval length. However, this error is not serious as can be seen from some actual results presented in Appendix C. The second type of error is due to using a truncated representation of the time function. Only if the time function exists beyond the time limit of integration does this error occur. Fortunately, the correlation functions of random functions diminish for high values of it's time argument so that this error involved in the power spectral density is not serious. To compensate for this truncation effect and yet to preserve the frequency information of the time function, a weighting function $W_K(t)$ has been incorporated into the above program. This function, as defined by Equation (95), has been devised by Ross (24) and is discussed in Appendix C.

CHAPTER VII

DISCUSSION OF RESULTS

Reactor Dynamics

Prior to the correlation determinations, frequency response of the reactor was obtained by two other approaches in order to establish a basis for comparing accuracy of the subsequent correlation results. The first determination was a theoretical analysis as presented in Appendix B, and the other was by an experimental, or siunsoidal, testing. A comparison of these results is shown in Figures 10 and 11.

The theoretical normalized frequency response, as determined from the work of Appendix B, is a linear, second order system determined to be

$$\frac{T_2(j\omega)}{W(j\omega)} = \frac{9.413}{(9.413-\omega^2) + j13.082\omega} \qquad (96)$$

where the frequency, $j\omega$, is in radians per minute. A good agreement exists between these results and sinusoidal testing, although it is not within the limits of experimental accuracy. In general, experimental points lie to the right of the theoretical model indicating that time constants smaller than the theoretical values are in effect. This

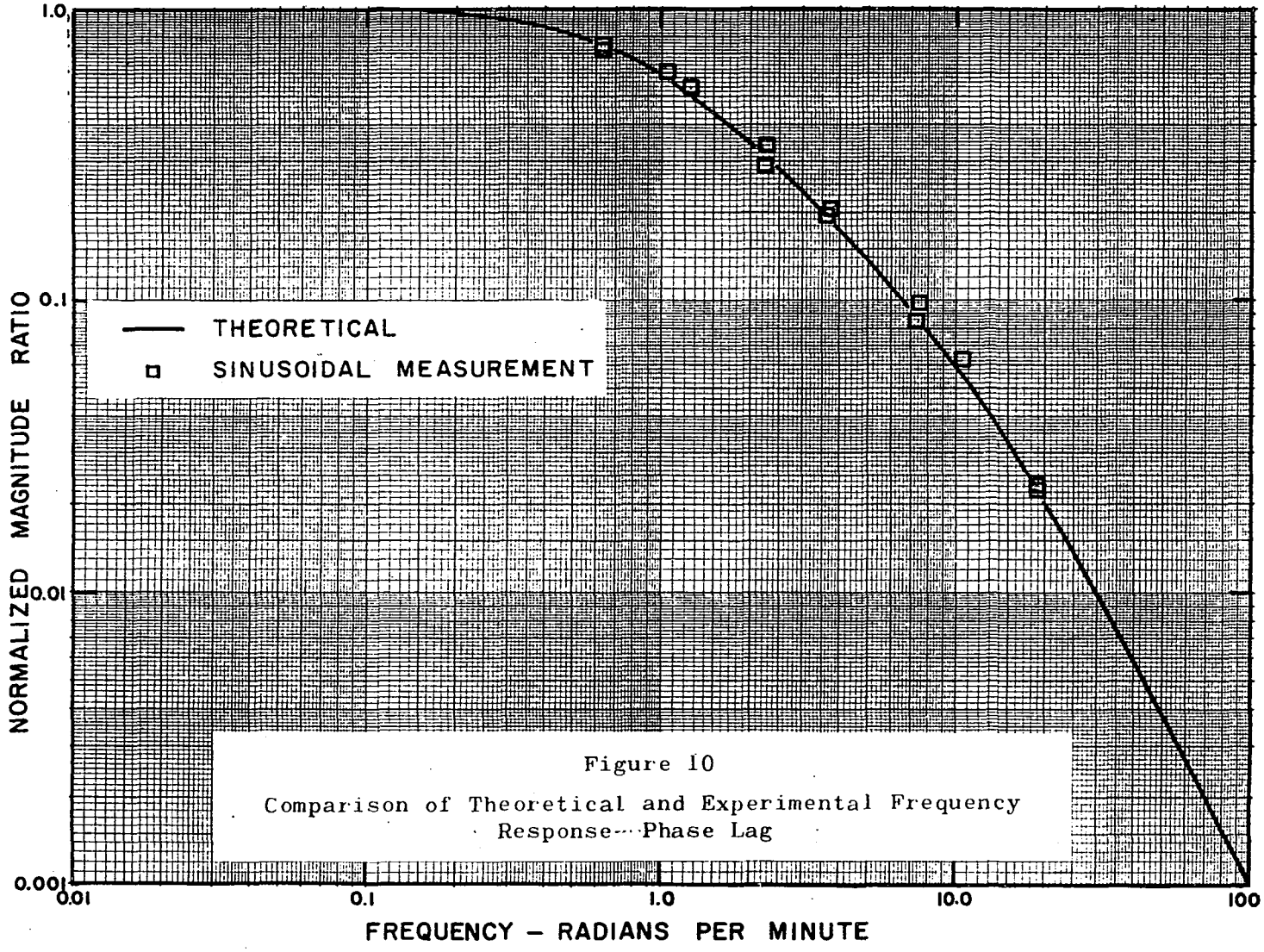

Figure 10

Comparison of Theoretical and Experimental Frequency Response--Phase Lag

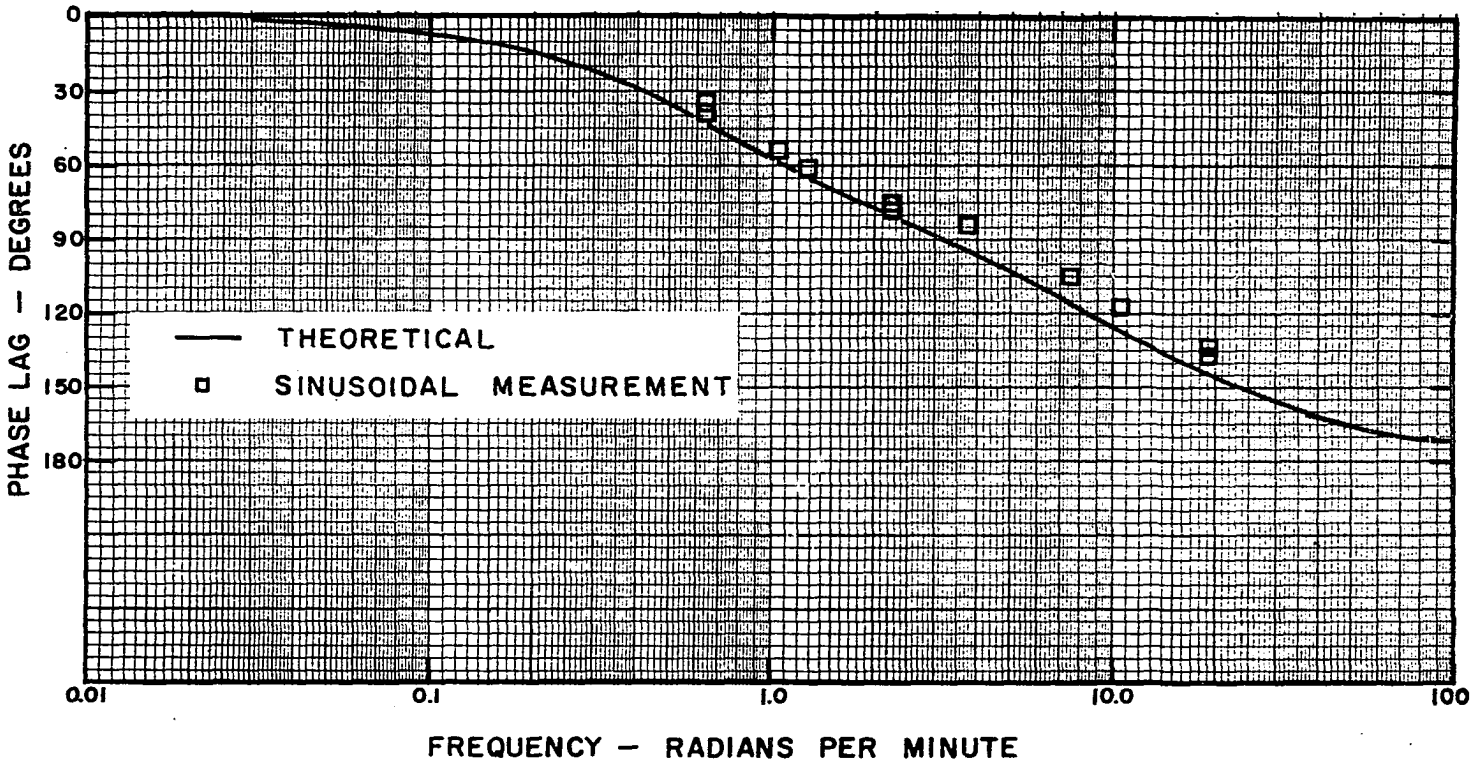

Figure 11

Comparison of Theoretical and Experimental Frequency Response--Phase Lag

deviation is more pronounced in the phase lag diagram of Figure 11. These differences are believed to reveal an interesting point in the dynamic behavior of the reactor and are discussed below.

The second order theoretical model, neglecting thermal capacitances of the cooling coil walls and reactor walls, has been verified by Fanning's earlier work (6) to be the more exact model. This theoretical model assumes perfect stirring within the reactor and constant physical parameters. These parameters were carefully checked for accuracy and the effect of the overall heat transfer coefficient, U, varying with coolant flow rate was found not to change the normalized frequency response more than the width of the line shown in Figure 10 and 11. The discrepancy is therefore believed to lie in the assumption of perfect mixing.

In fact, the flow patterns of the reactor support this viewpoint. The impeller, near the bottom of the reactor, generated fluid flow outward past the lower portion of the coil where most of the heat exchange took place, upward around the outside of the coils, and downward through the center of the reactor. The sensing thermocouples were in the path of this fluid in the outside at the top. Thus, something of a "short circuit" probably existed which could account for an appreciable phase lead and decrease in attenuation.

Although these two determinations do not agree perfectly, continuous values of the theoretical frequency response serve as a good reference and are used in later comparisons with the "correlation" results.

Statistical Determinations for a Single Input

The dynamic behavior of the experimental equipment was first investigated by using records of randomly varying input-outputs when only one forcing function was imposed. The relationship of Equation (55) was used to define the system frequency response. This relationship involves the input and cross-power spectral densities. Calculations were made as described in the previous chapter to determine first the auto- and cross-correlation estimates and then the power spectral density estimates by Fourier transformation. To help evaluate this experimental technique determinations were made for various record lengths and degrees of weighting functions.

Correlation Estimates. Both auto- and cross-correlation function estimates were calculated for the following record lengths:

$$N - \tau_m = 750$$

$$N - \tau_m = 1500$$

$$N - \tau_m = 2250$$

$$N - \tau_m = 3000$$

$$N - \tau_m = 3750$$

$$N - \tau_m = 4500$$

$$N - \tau_m = 5250$$

$$N - \tau_m = 5592$$

The value, $N - \tau_m$, is the number of products averaged to determine the correlation estimate. The maximum value of τ, denoted as τ_m, which was used in the calculations was 180 increments of the basic sampling period, 1.93 seconds. Or, the maximum delay was for a time of approximately 5.8 minutes. Since the largest time constant of the experimental equipment was 1.31 minutes, this delay corresponded to approximately 4.4 time constants, for which any response would settle to approximately one per cent of its initial value.

Correlation estimates for values of $N - \tau_m = 750$, 3000, and 5592 are shown in Figures 12, 13, and 14 respectively. Estimates for the other record lengths were quite similar. (Results of all correlation function estimates are on file in digital form at the School of Chemical Engineering, University of Oklahoma.) Cross-correlation function estimates are normalized as expressed by Equation (93). As related by Equation (53), the cross-correlation function is the response to the input, the autocorrelation function. The expected value of the auto-correlation function estimate is an isosceles triangle at the origin as pictured in Figure 9 previously. The correlation functions appear to approach their expected values as the record length increases. Otherwise, a

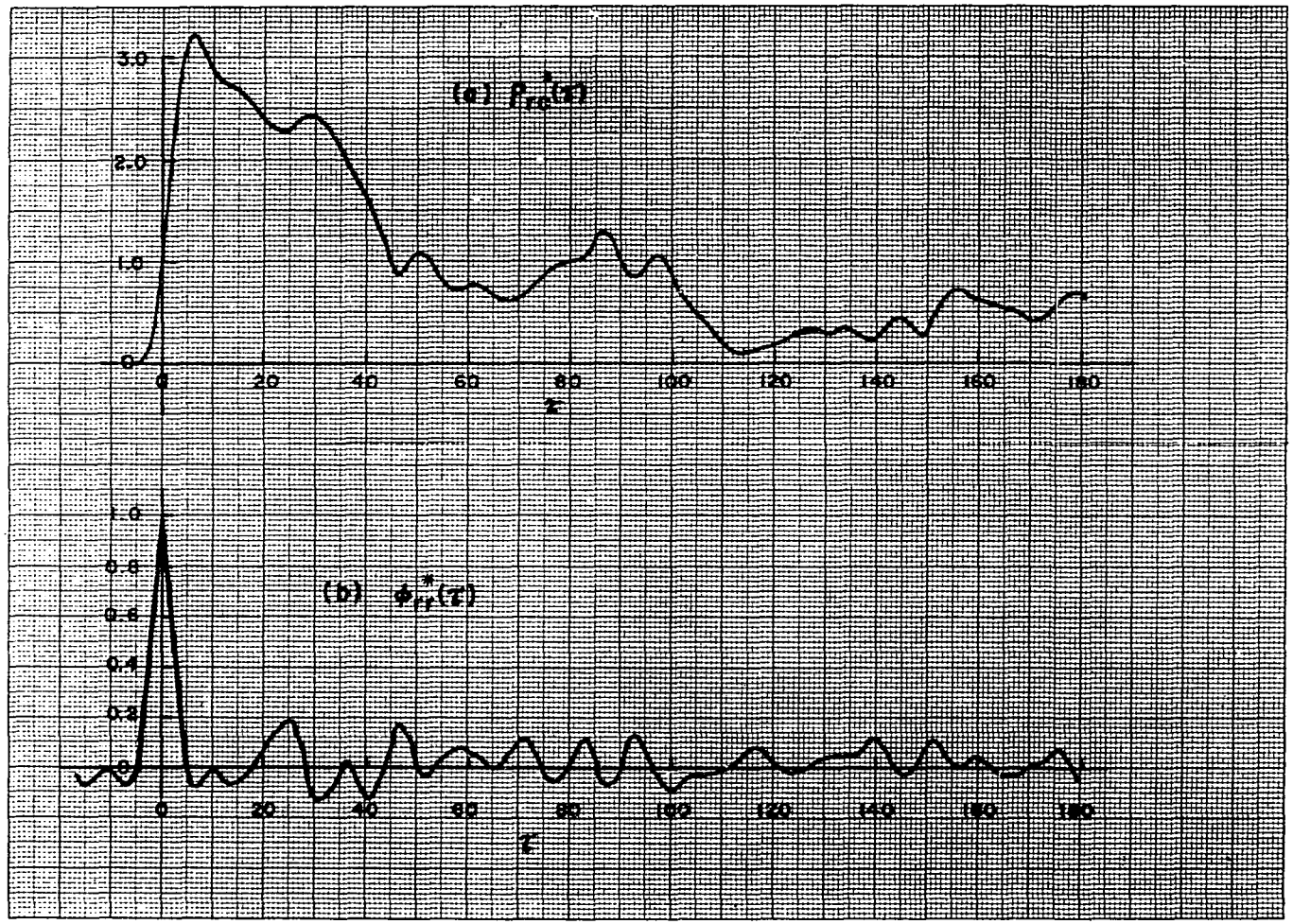

Figure 12

Correlation Estimates for 750 Lagged Products---Single Input

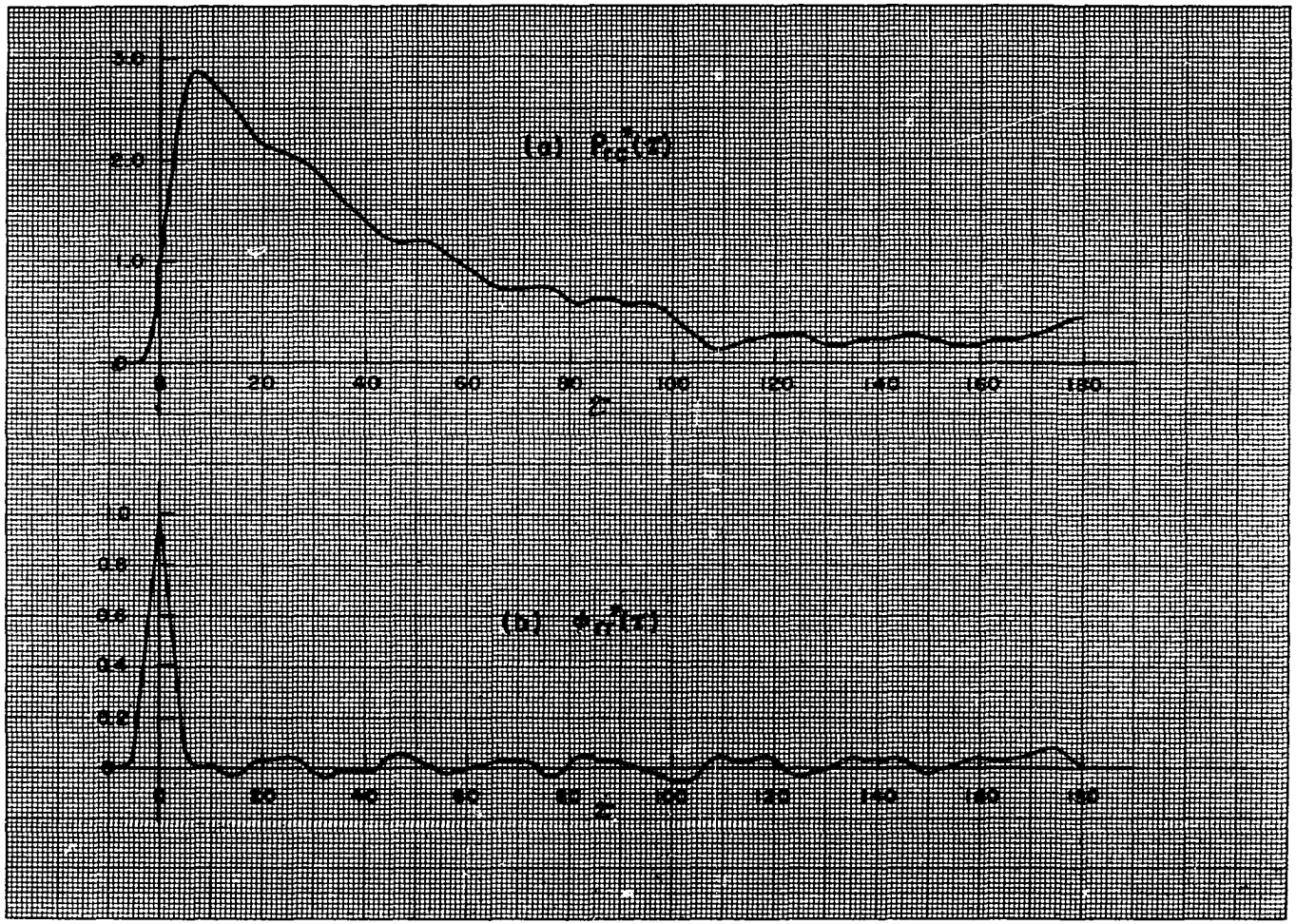

Figure 13
Correlation Estimates for 3000 Lagged Products--Single Input

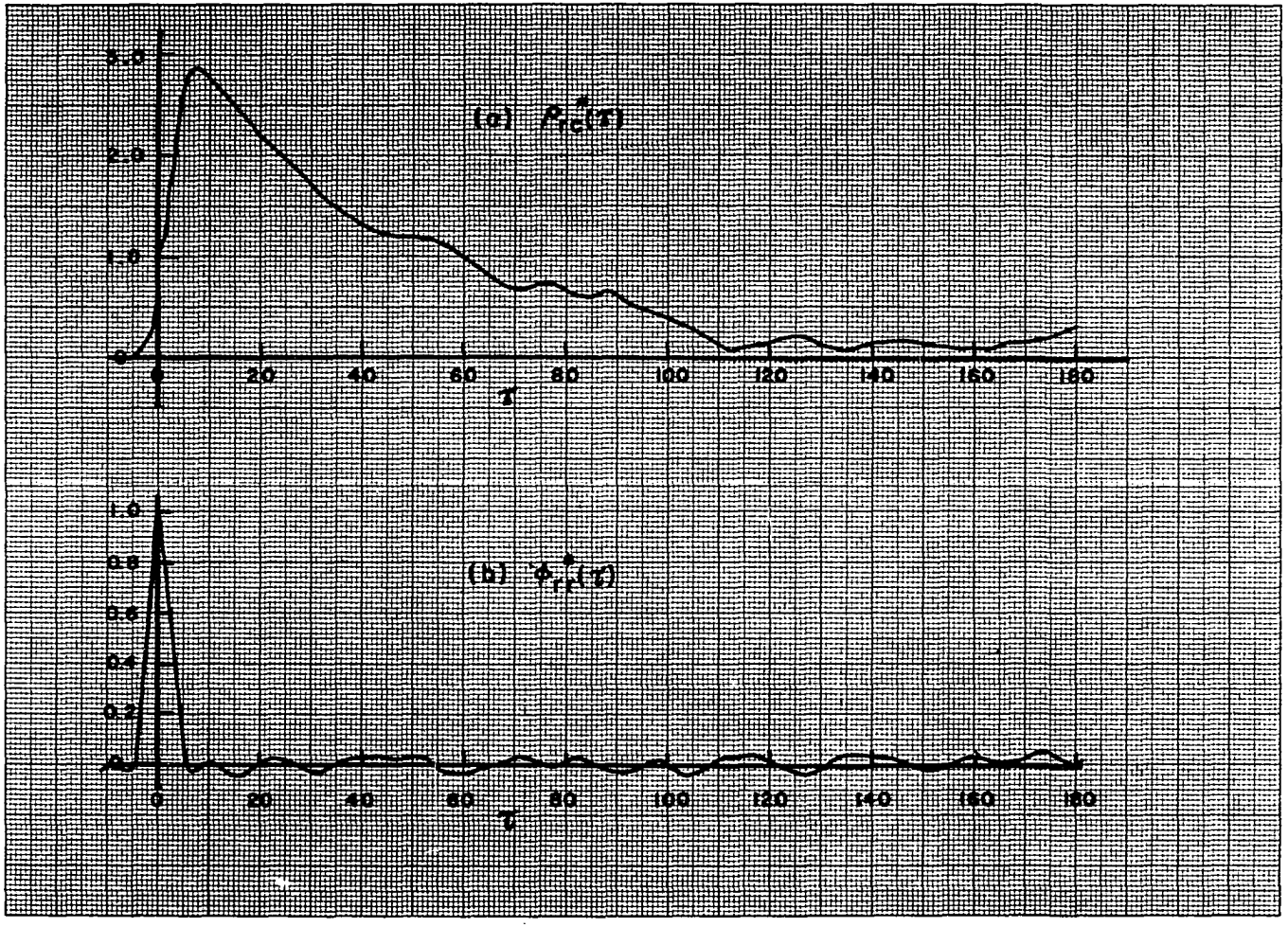

Figure 14

Correlation Estimates for 5592 Lagged Products--Single Input

definite variance, or "noise," seems to exist. Variance of the correlation estimate about its expected value is treated more fully in Appendix D.

An increase of coolant flow caused a decrease in reactor temperature; therefore, the cross-correlation estimate $\phi_{rc}^*(\tau)$ was negative as a response to the auto-correlation function which was a positive, even pulse at the origin. The Figures 12 to 14 show the cross-correlation estimates normalized with respect to their values at $\tau = 0$; the peak values are therefore positive. The maximum value of cross-correlation occurred at a delay of approximately 7 sampling increments, or 13.5 seconds, after the origin of the input. Cross-correlation estimates for τ negative were calculated only out to $\tau = -6$ increments since the expected values were zero for $\tau \leq -5$ increments. Negative arguments for the autocorrelations were not calculated either, since the expected values were known to be even functions.

Spectral Estimates. The input power spectral density estimates are shown in Figure 15 as obtained from 750, 3000, and 5592 products. Calculations in the form of Fourier transformations were made on each of the auto-correlation estimates and are listed in Table 1. The expected value of the input spectrum, derived in Appendix A, is also listed for comparison. In each of these calculations the Fourier transform weighting function for k = 2 was used; therefore these estimates were smoothed considerably over

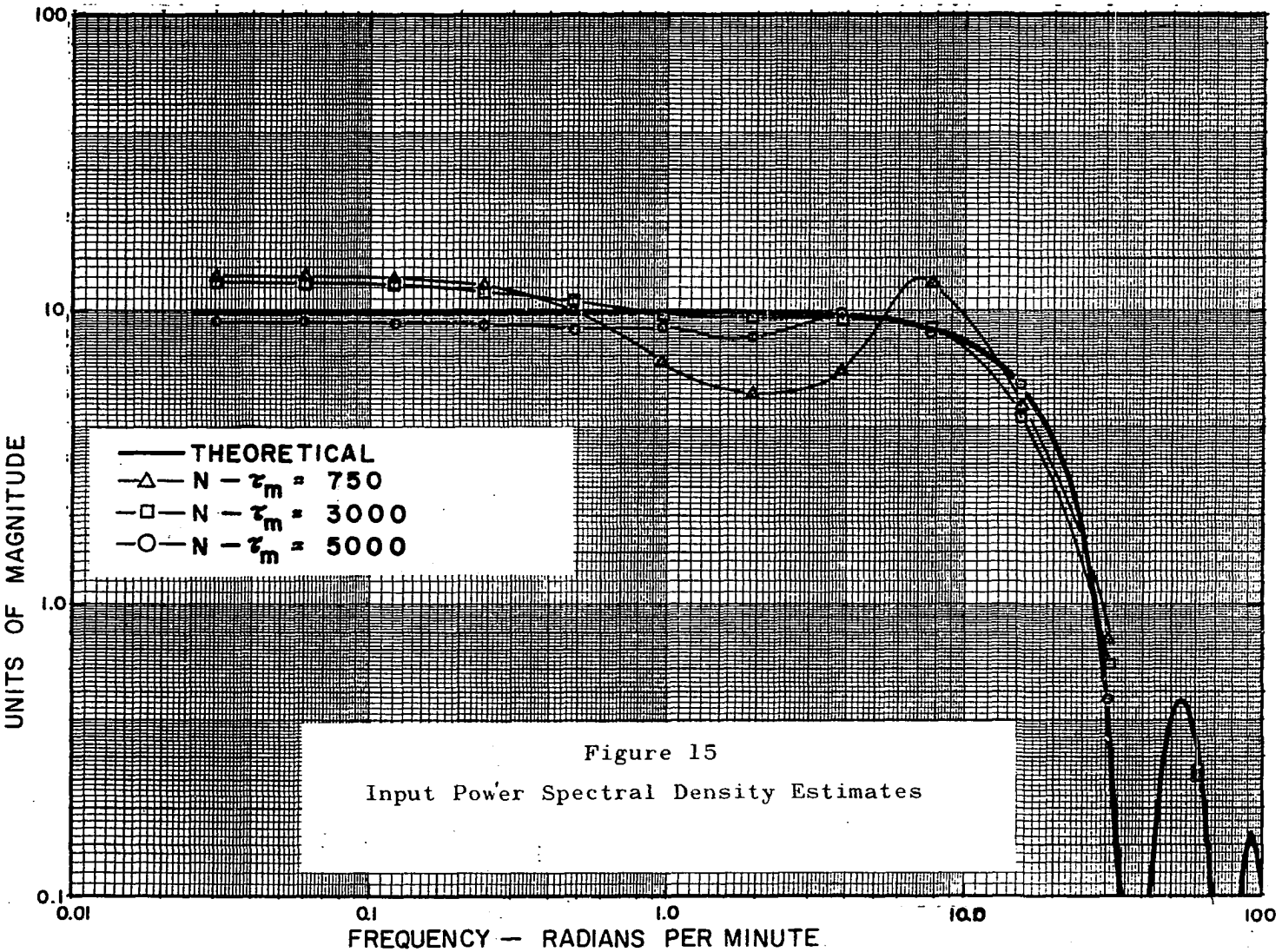

Figure 15

Input Power Spectral Density Estimates

TABLE 1

INPUT POWER SPECTRAL DENSITY ESTIMATES
(FOR WEIGHTING FUNCTION OF k = 2

Frequency Radians Per Minute	N - τ_m = 750	1500	2250	3000	3750	4500	5250	5592	Expected Value
0.03	13.14	13.14	13.88	12.72	11.03	10.57	9.95	9.12	10.0
0.06	13.09	12.82	13.74	12.44	11.07	10.42	9.66	9.22	10.0
0.12	12.86	12.72	13.52	12.30	10.98	10.14	9.49	9.025	10.0
0.24	12.21	12.34	13.20	11.95	10.76	9.94	9.31	8.95	10.0
0.48	10.22	11.38	12.36	10.92	10.19	9.43	8.81	8.72	10.0
0.96	6.66	9.76	11.99	9.66	9.73	8.89	8.46	8.70	9.99
1.92	5.19	6.57	7.29	9.50	9.72	8.16	8.40	8.09	9.92
3.84	6.30	7.28	7.70	9.35	9.42	9.94	9.67	9.85	9.66
7.68	12.54	9.28	9.59	8.80	9.00	9.44	8.68	8.58	8.70
15.36	4.74	3.86	3.75	4.34	5.19	5.03	5.28	5.62	5.60
30.72	0.758	0.532	0.623	0.620	0.549	0.512	0.466	0.469	0.460
61.44	0.257	0.200	0.259	0.258	0.251	0.248	0.287	0.277	0.321
122.88	0.0349	0.0318	0.0245	0.0221	0.0231	0.0277	0.0279	0.0277	0.0504

non-weighted estimates. The transform calculations were truncated at the maximum value of τ_m = 180 sampling increments. Only the theoretical, or expected, value is plotted in the high frequency range because not enough values of the estimates were calculated to give the resolution necessary for defining curves. The estimates at 61.4 radians per minute are within 20 per cent accuracy.

Figures 16 and 17 show the magnitude and phase respectively of the cross-power spectral density estimates. The weighting function for k = 2 and a maximum of 180 time increments were used in the Fourier transform calculations. The complete results of magnitude and phase are presented in Tables 2 and 3 respectively. The differences in magnitudes at low frequencies for each record length is due to the finite averaging times for the correlation estimates.

The effect of smoothing by using higher order weighting functions can be seen in Figures 18 and 19. Magnitude and phase of the cross power spectral density estimate from 5592 products show smoother plots for k = 2. The weighting was found particularly useful to recover phase information at the higher frequencies.

Process Frequency Response. Figure 20 shows the normalized magnitude ratio of the frequency response determined from the spectral density estimates. Normalization was performed by dividing by the highest values of

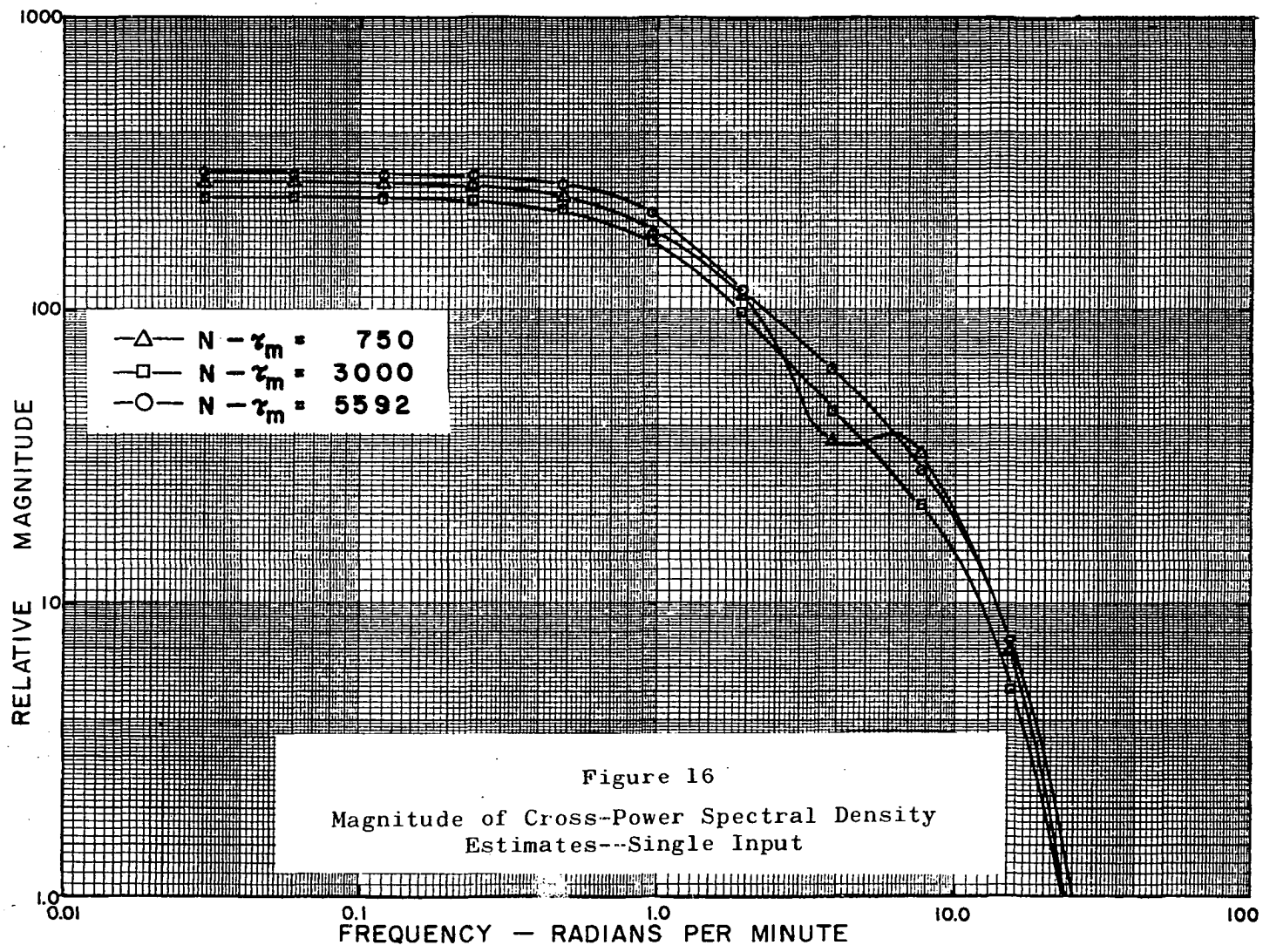

Figure 16

Magnitude of Cross-Power Spectral Density Estimates--Single Input

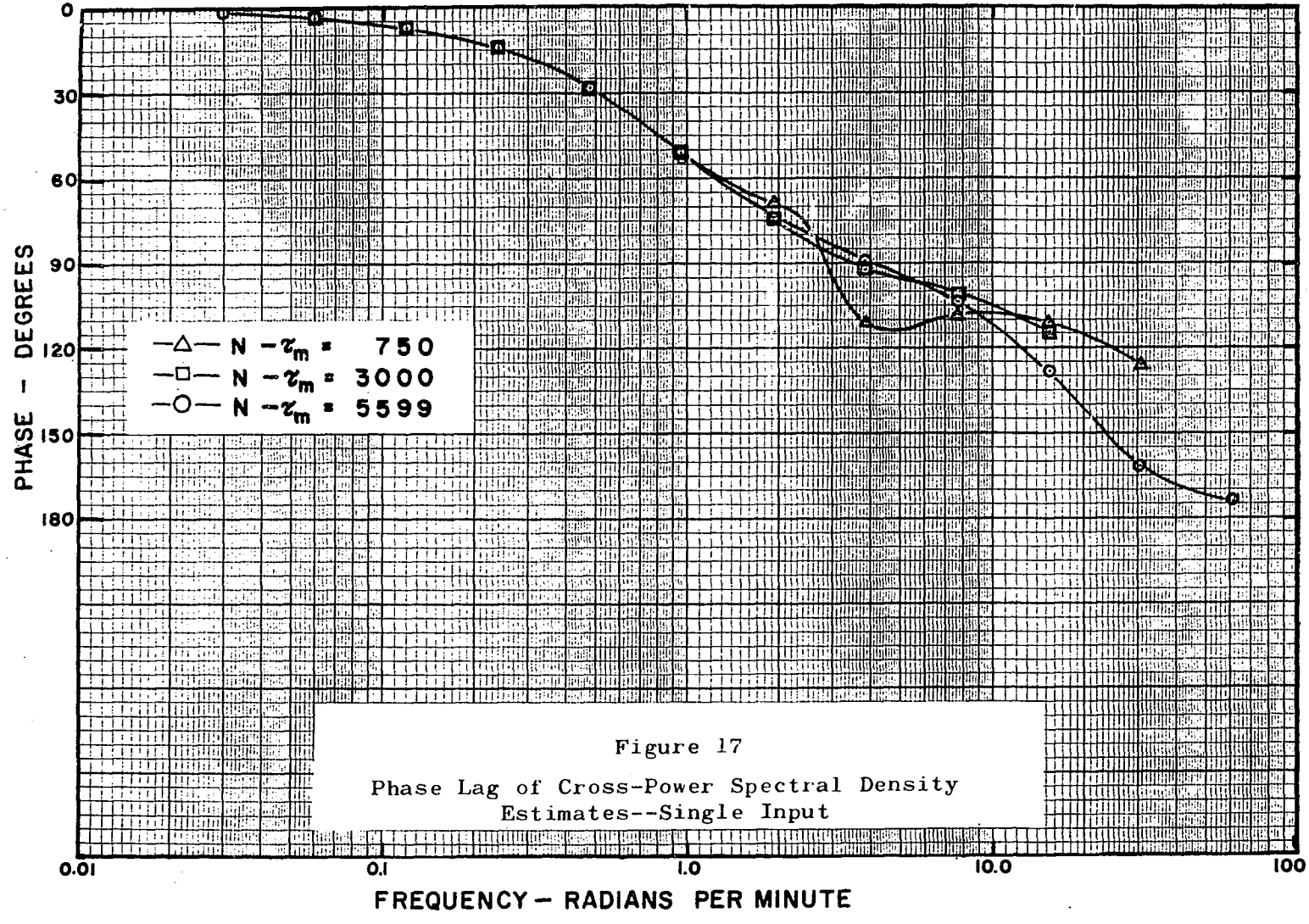

Figure 17

Phase Lag of Cross-Power Spectral Density Estimates--Single Input

TABLE 2

CROSS-POWER SPECTRAL DENSITY ESTIMATES - MAGNITUDE
(FOR WEIGHTING FUNCTION OF k = 2)

Frequency Radians Per Minute	$N-\tau_m$ = 750	1500	2250	3000	3750	4500	5250	5592
0.03	271.	251.	236.	240.	251.	278.	285.	292.
0.06	270.	251.	236.	240.	251.	277.	285.	291.
0.12	269.	249.	236.	239.	250.	276.	284.	290.
0.24	264.	244.	232.	235.	246.	271.	279.	285.
0.48	243.	223.	216.	219.	230.	254.	261.	268.
0.96	183.	160.	170.	172.	181.	199.	207.	213.
1.92	113.	80.3	89.4	97.0	102.	108.	116.	117.
3.84	35.9	36.3	40.7	45.0	49.3	57.6	60.8	62.8
7.68	32.0	19.7	21.9	21.7	23.0	26.9	27.6	28.1
15.36	6.86	4.78	4.61	5.02	5.74	6.22	6.91	7.44
30.72	0.245	0.409	0.380	0.303	0.223	0.0984	0.161	0.202
61.44	0.0608	0.095	0.0606	0.0293	0.0226	0.04847	0.0604	0.0838
122.88	0.0177	0.0282	0.0241	0.0224	0.0202	0.00592	0.00552	0.00836

TABLE 3

CROSS-POWER SPECTRAL DENSITY ESTIMATES -- PHASE (DEGREES NEGATIVE)
(FOR WEIGHTING FUNCTION OF k = 2

Frequency Radians Per Minute	N-τ_m= 750	1500	2250	3000	3750	4500	5250	5592
0.03	1.97	2.20	1.90	1.88	1.85	1.87	1.83	1.83
0.06	3.94	4.4	3.8	3.76	3.71	3.73	3.66	3.64
0.12	7.87	8.8	7.58	7.49	7.40	7.45	7.31	7.25
0.24	15.60	17.50	15.07	14.90	14.70	14.80	14.50	14.40
0.48	30.30	34.00	29.34	29.00	28.70	29.00	28.30	28.30
0.96	53.2	60.50	53.10	52.50	52.10	52.90	51.50	51.80
1.92	67.80	73.70	78.00	74.80	74.30	74.00	73.80	74.10
3.84	110.10	95.90	95.14	92.30	92.00	89.10	87.80	89.50
7.68	107.60	102.00	99.87	100.00	100.00	103.10	103.70	103.40
15.36	111.30	97.50	108.60	114.80	119.00	123.30	129.60	127.70
30.72	126.70	22.40	29.80	35.10	46.30	109.20	153.50	162.10
61.44	258.90	19.8	50.30	36.10	80.40	149.00	183.20	174.00
122.88	228.80	351.90	342.40	350.10	349.20	21.90	-68.10	114.90

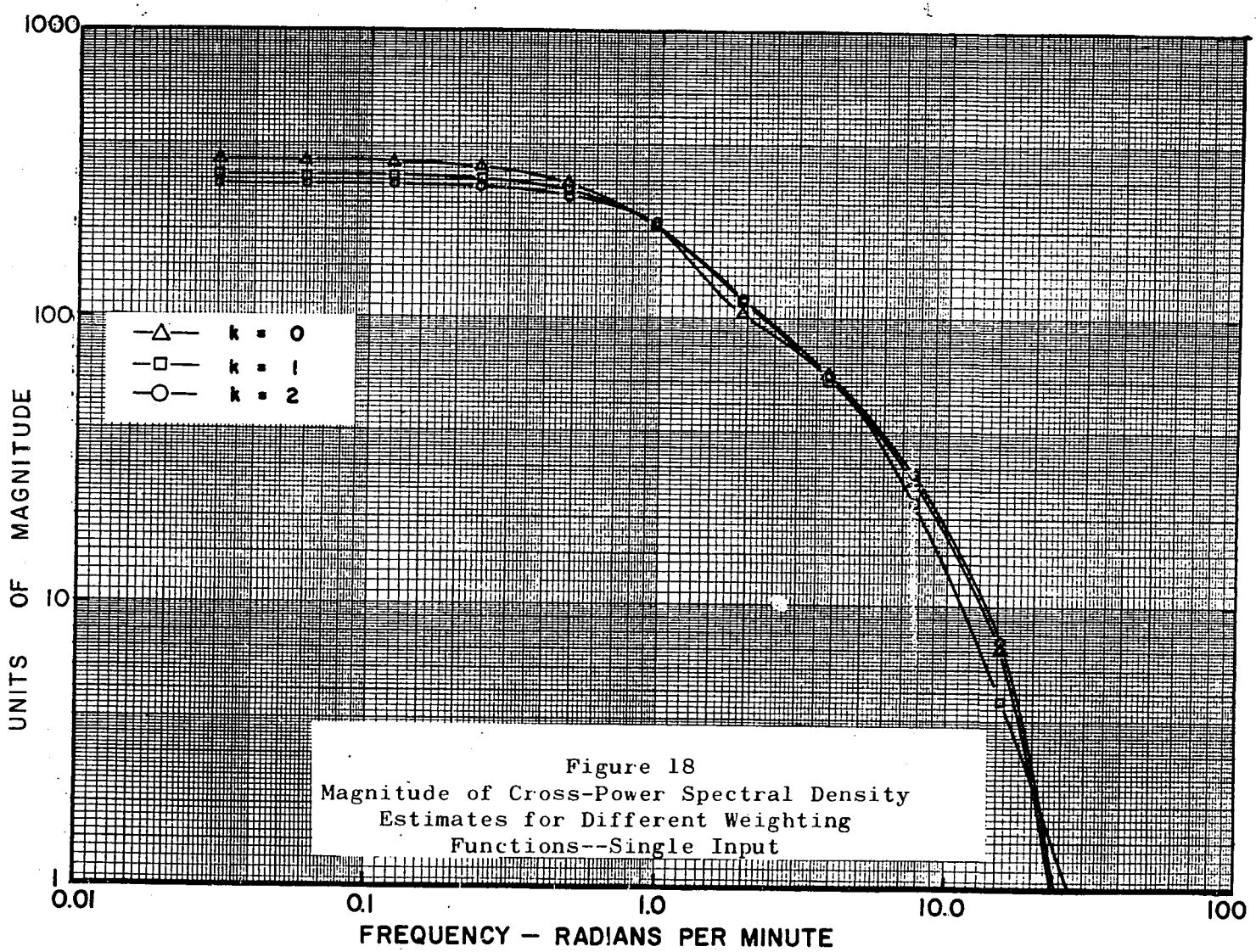

Figure 18
Magnitude of Cross-Power Spectral Density
Estimates for Different Weighting
Functions--Single Input

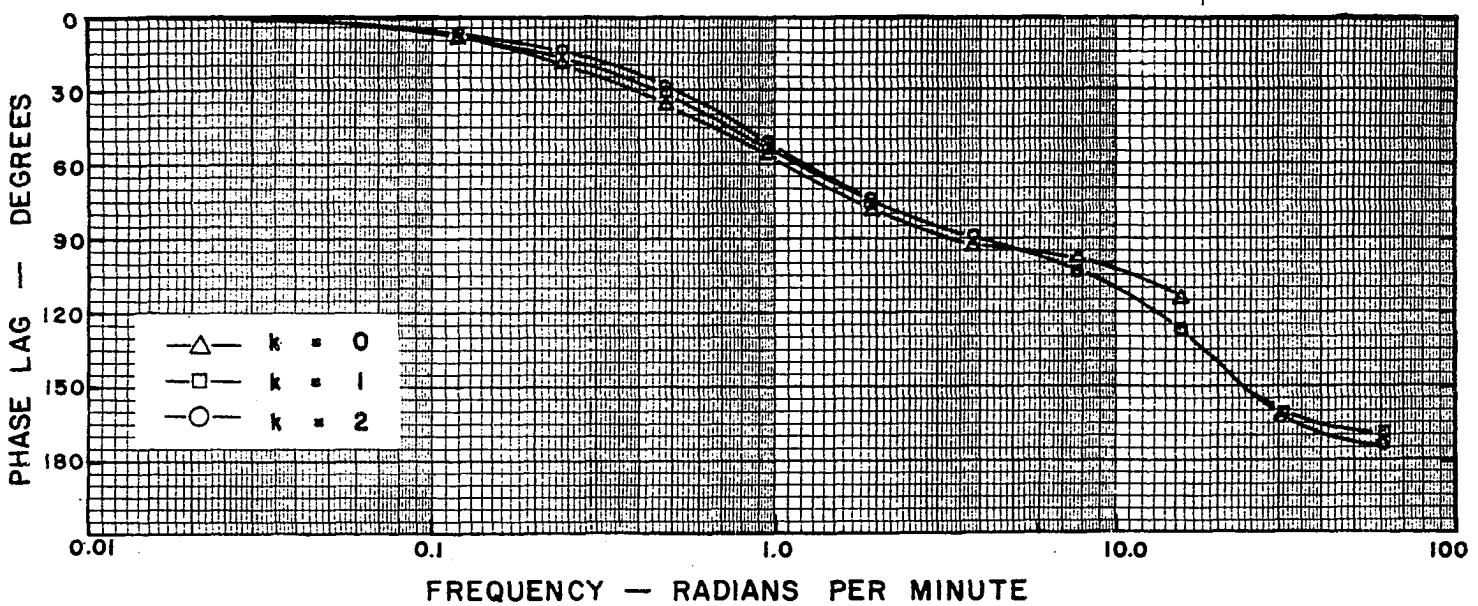

Figure 19

Phase Lag of Cross Power Spectral Density Estimates
for Different Weighting Functions Single Input

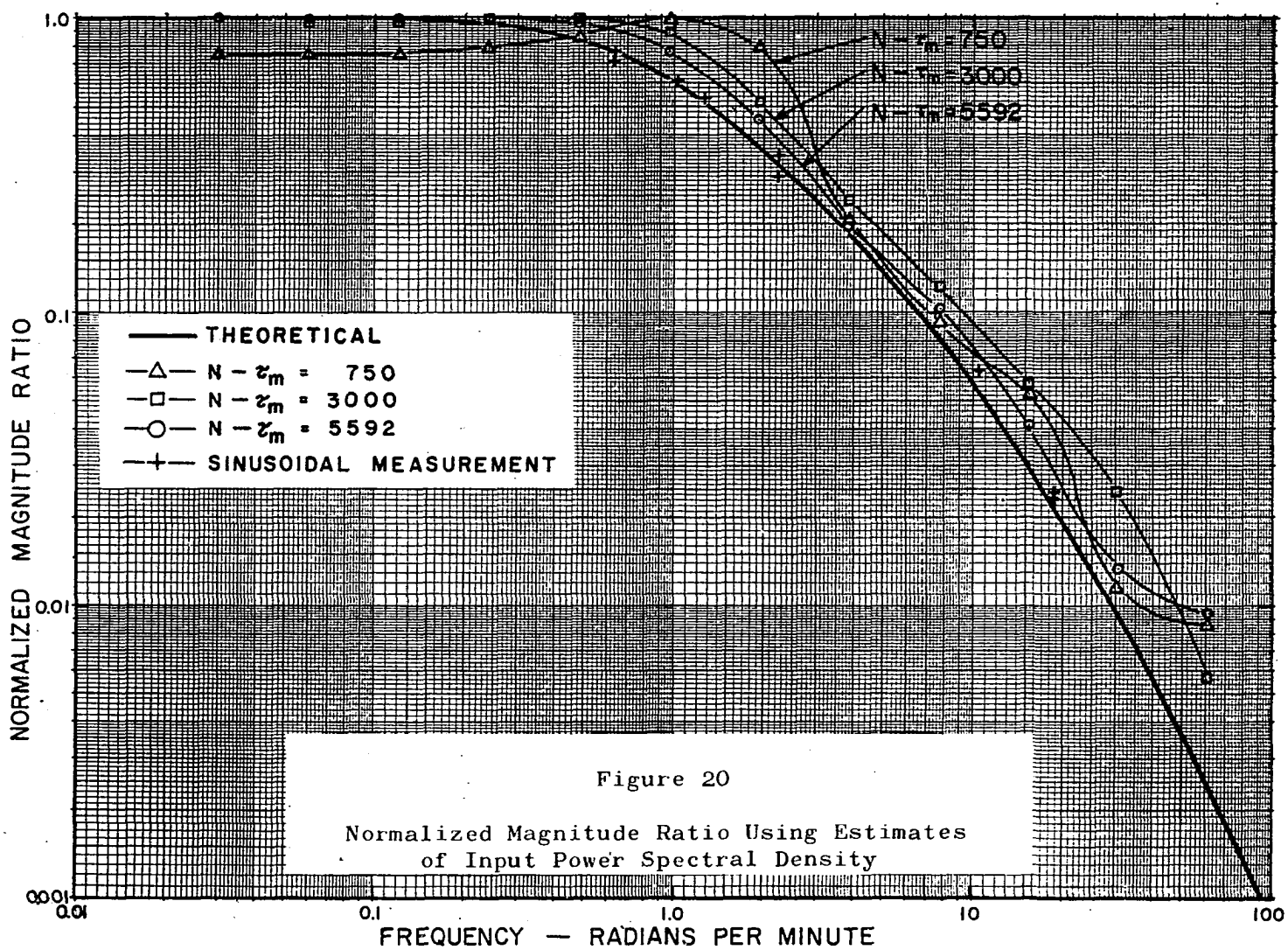

Figure 20

Normalized Magnitude Ratio Using Estimates of Input Power Spectral Density

the spectra which usually was at the lowest frequency calculation, so that the normalized magnitude ratio (estimate) was calculated as

$$\left|\overline{H(\omega)}^{*}\right| = \frac{\dfrac{\Phi_{rc}^{*}(\omega)}{\Phi_{rc}^{*}(\omega_{min})}}{\dfrac{\Phi_{rr}^{*}(\omega)}{\Phi_{rr}^{*}(\omega_{min})}} \tag{97}$$

The three record-length determinations, from 750, 3000, and 5592 products, are shown in Figure 20 in comparison with the derived and sinusoid frequency responses.

A better agreement is found when the normalized magnitude ratio is determined by the use of the theoretical, or expected value of the input power spectral density in Equation (97). Figure 21 shows these results. This agreement might have been expected, since it is, in effect, obtaining a ratio of an estimate and a known function rather than the ratio of two estimated functions.

Observations of the magnitude ratio estimates in Figure 21 and phase lag estimates in Figure 22 show clearly that the determinations improve as the record lengths increase. The estimates from the short record of 750 products have the largest excursion away from the sinusoidal and theoretical values. The determinations from the longest record, 5592 products, more nearly approach the expected response curves. These differences are believed to be due

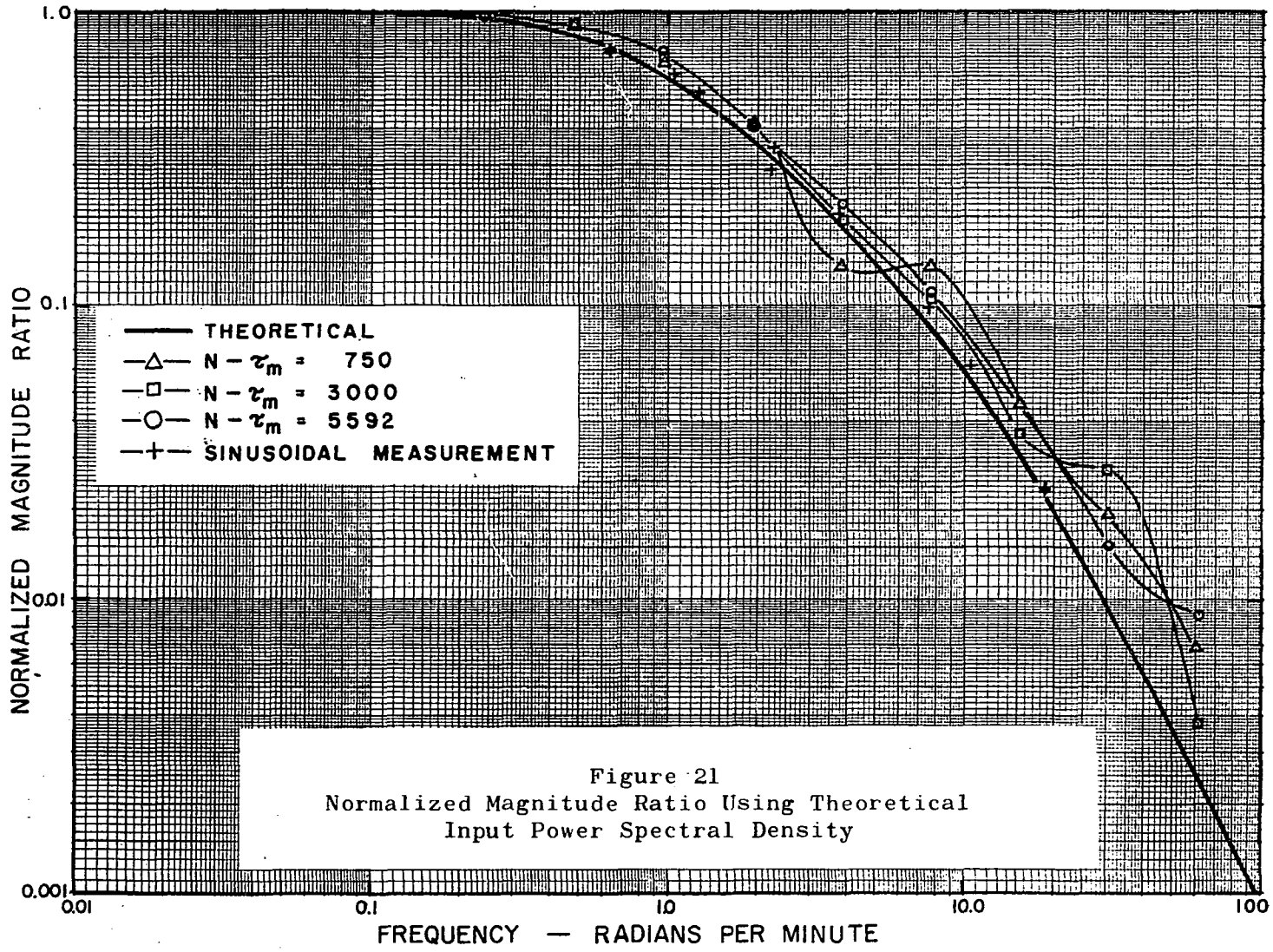

Figure 21
Normalized Magnitude Ratio Using Theoretical
Input Power Spectral Density

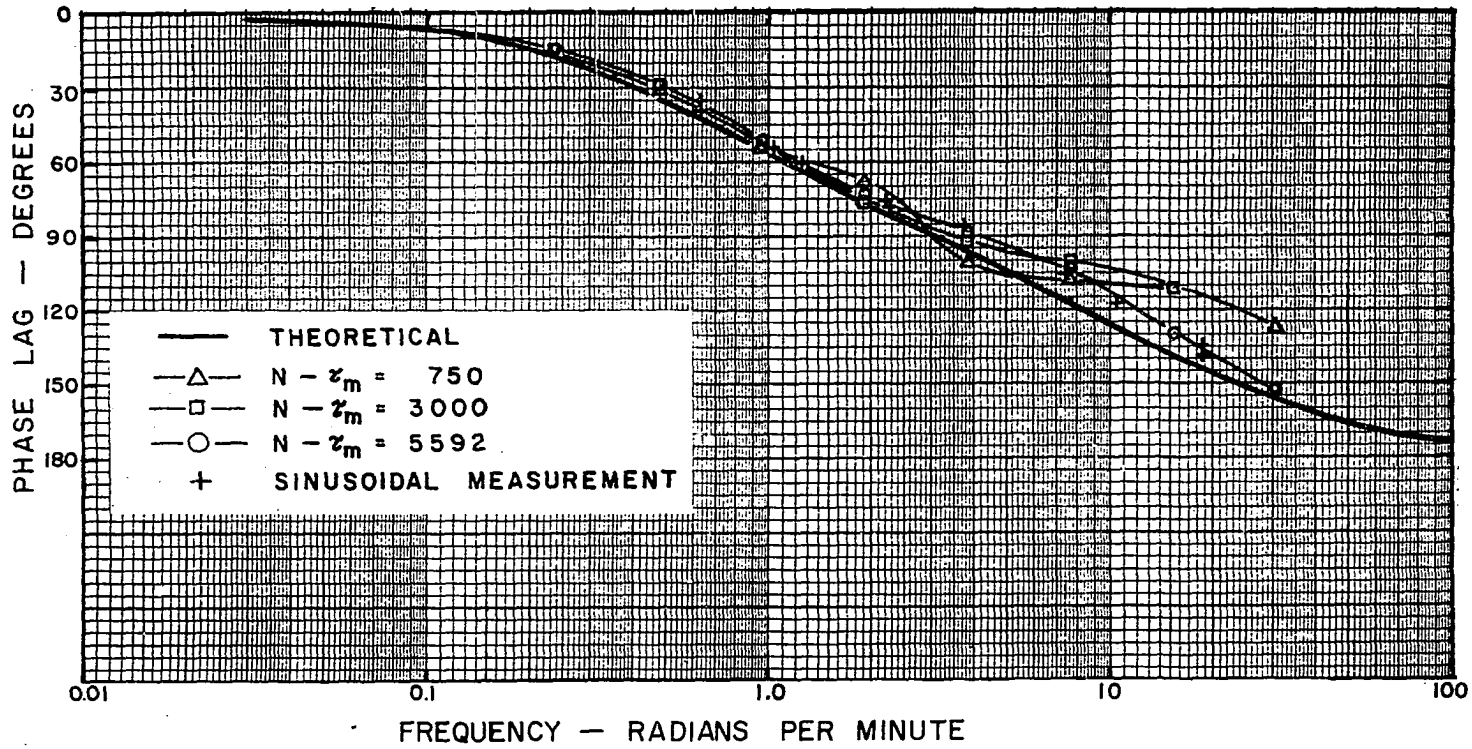

Figure 22

Process Phase Lag From Spectral Density Estimates

to the finite record length estimates calculated. A further explanation is believed to lie in the fact that some "noise" was generated within the process itself. Recorded data showed evidence of low amplitude, high frequency variations apparently associated with temperature eddies of the reactor fluid. The output temperature would then be related to the input as

$$c(t) = \int_o h(\lambda) \quad (t-\lambda)d\lambda \quad + \quad n(t) \tag{98}$$

where n(t) is the "noise" imposed upon the recordings. Under the assumption of having ergodic random variables above, a correlation relationship exists as

$$\phi_{rc}(\tau) = \int_o h(\lambda)\, \phi_{rr}(\tau-\lambda)d\lambda \quad + \quad \phi_{rn}(\tau) \tag{99}$$

and an equivalent spectral relationship exists as

$$\Phi_{rc}(\omega) = H(\omega)\, \Phi_{rr}(\omega) \quad + \quad \Phi_{rn}(\omega)$$

or

$$H(\omega) = \frac{\Phi_{rc}(\omega) - \Phi_{rn}(\omega)}{\Phi_{rr}(\omega)} \tag{100}$$

An actual calculation of $\phi^*_{rn}(\tau)$ could not be made since n(t) was not readily distinguishable in the output. However, under the condition that the value of $\phi_{rn}(\tau)$ was negative the magnitude curve of Figure 21 would appear high if the noise effect was not accounted for as in Equation (100).

Phase lag determinations show a remarkable agreement with sinusoidal measurements out to a frequency of 30 radians per minute. It is important to note that the correlation

results here agree with the sinusoidal, or experimental, results rather than the linear theoretical model. Above 30 radians per minute, the phase results were not reliable - as expected. Two reasons are that the input power spectrum is zero at both 37.7 and 75.4 radians per minute and the folding frequency was at 97.5 radians per minute.

Statistical Determinations for Two Inputs

The second part of the experimental work was the determination of the process frequency response while the process was under the influence of two input variables simultaneously. A typical portion of the experimental recording of these variables was shown in Figure 8. In the calculations the process variables were scaled for x(t) to represent coolant flow rate, y(t), the reactor inlet temperature and z(t) to represent the reactor outlet temperature, all as defined in Equations (89) to (91). Spectra of these variables have theoretical relationships similar to Equations (66) and (67) as

$$\Phi_{xz}(\omega) = H(\omega)\,\Phi_{xx}(\omega) + G(\omega)\,\Phi_{xy}(\omega) \qquad (101)$$

$$\Phi_{yz}(\omega) = H(\omega)\,\Phi_{yy}(\omega) + G(\omega)\,\Phi_{yy}(\omega) \qquad (102)$$

where $H(\omega)$ is the frequency response function between x(t) and z(t) and $G(\omega)$ is that between y(t) and z(t). It is the primary objective of the experimental work in this section to solve for $H(\omega)$.

Correlation Estimates. For the case of two input

variables the cross-correlation estimates, $\phi_{xz}^*(\tau)$ and autocorrelation estimates, $\phi_{xx}^*(\tau)$ were calculated from record lengths up to $N-\tau_m = 4800$ products at intervals of 600 each. In all these calculations the range of τ was $-21 \leq \tau \leq 201$ increments. Therefore the maximum delay was approximately 6.5 minutes, or a factor of approximately five times greater than the highest process time constant.

Figures 23, 24, and 25 show results of correlation estimates calculated from this experimental data. Values of $\phi_{xx}^*(\tau)$ and $\phi_{xz}^*(\tau)$ are shown for record lengths of $N-\tau_m =$ 1800, 3000, and 4800 products. The theoretical value for $\phi_{xy}^*(\tau)$ was zero since x(t) and y(t) were generated independently. Calculations of $\phi_{xy}^*(\tau)$ were therefore made for record lengths out to only $N-\tau_m = 3000$.

The correlation estimates $\phi_{xx}^*(\tau)$ and $\phi_{xz}^*(\tau)$ appeared similar to their counterparts in the case of one input. The autocorrelation function $\phi_{xx}^*(\tau)$ was identical in that it appeared as an isosceles triangle at the origin ($\tau = 0$) with some variance about a zero value for $\tau > 5.2$ increments due to its being a random estimate of the expected value. The cross-correlation estimates on the average showed maxima at a delay of approximately 9 sampling intervals, or 17.4 seconds, after the origin of the input pulse. The value of maximum cross-correlation was $\phi_{xz}^*(\tau) =$ 0.304 in dimensionless scale units of x(t) and z(t). This value compares with 0.588 for the one input case where the recording sensitivity was a factor of 5.9/3.2 greater.

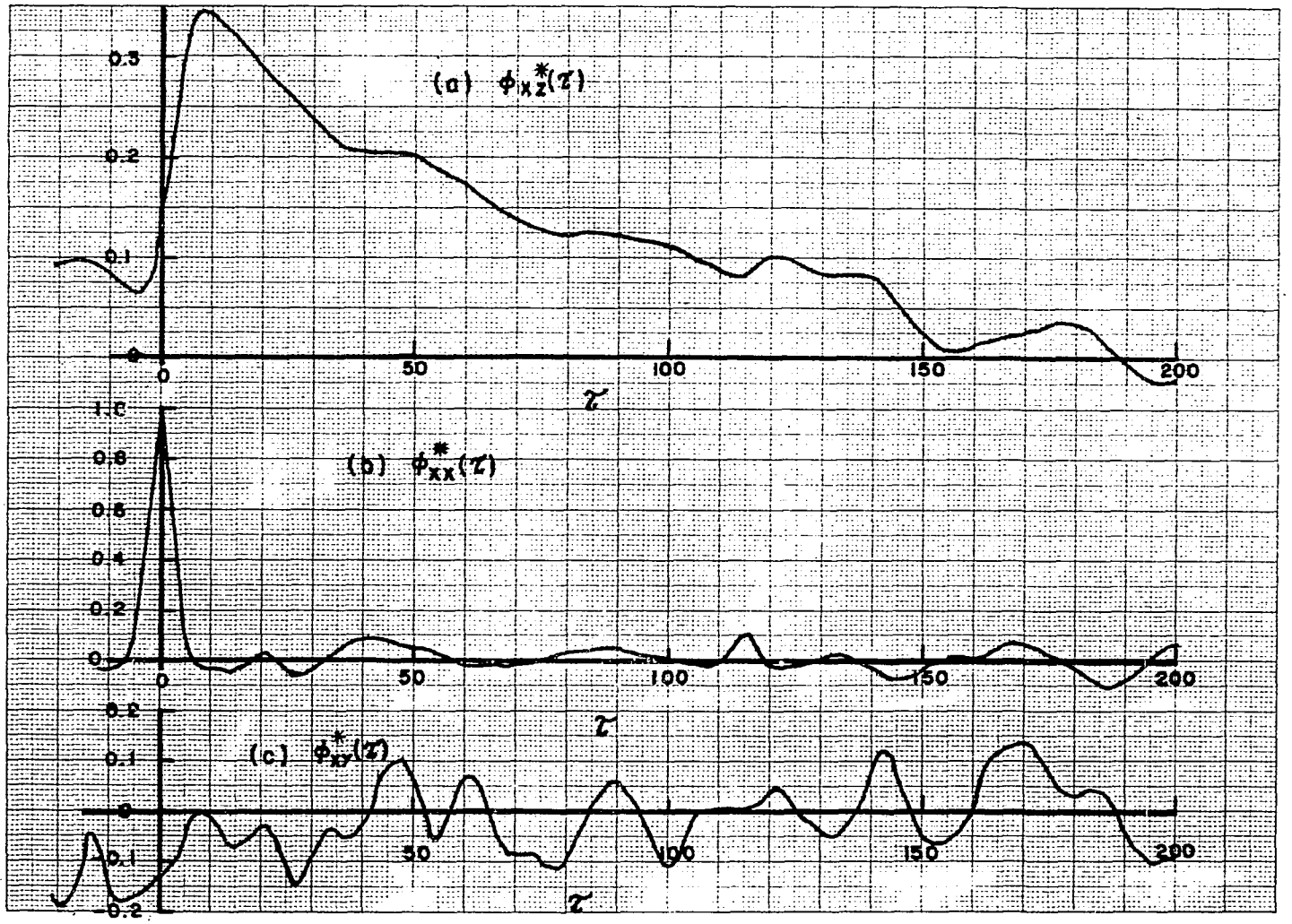

Figure 23

Correlation Estimates from a Record Length of $N-\tau_m \doteq 1200$

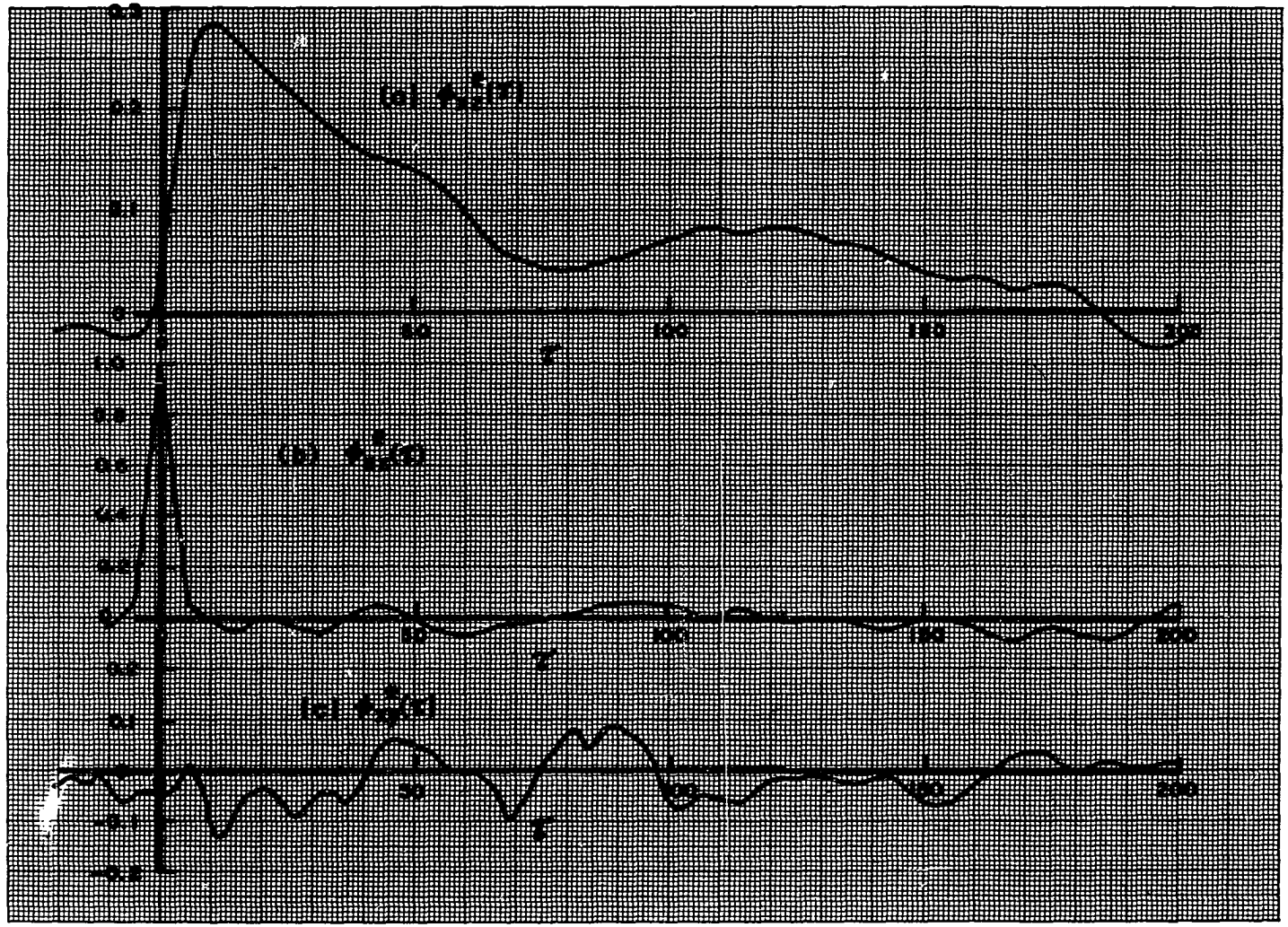

Figure 24

Correlation Estimates from a Record Length of $N-\tau_m = 3000$

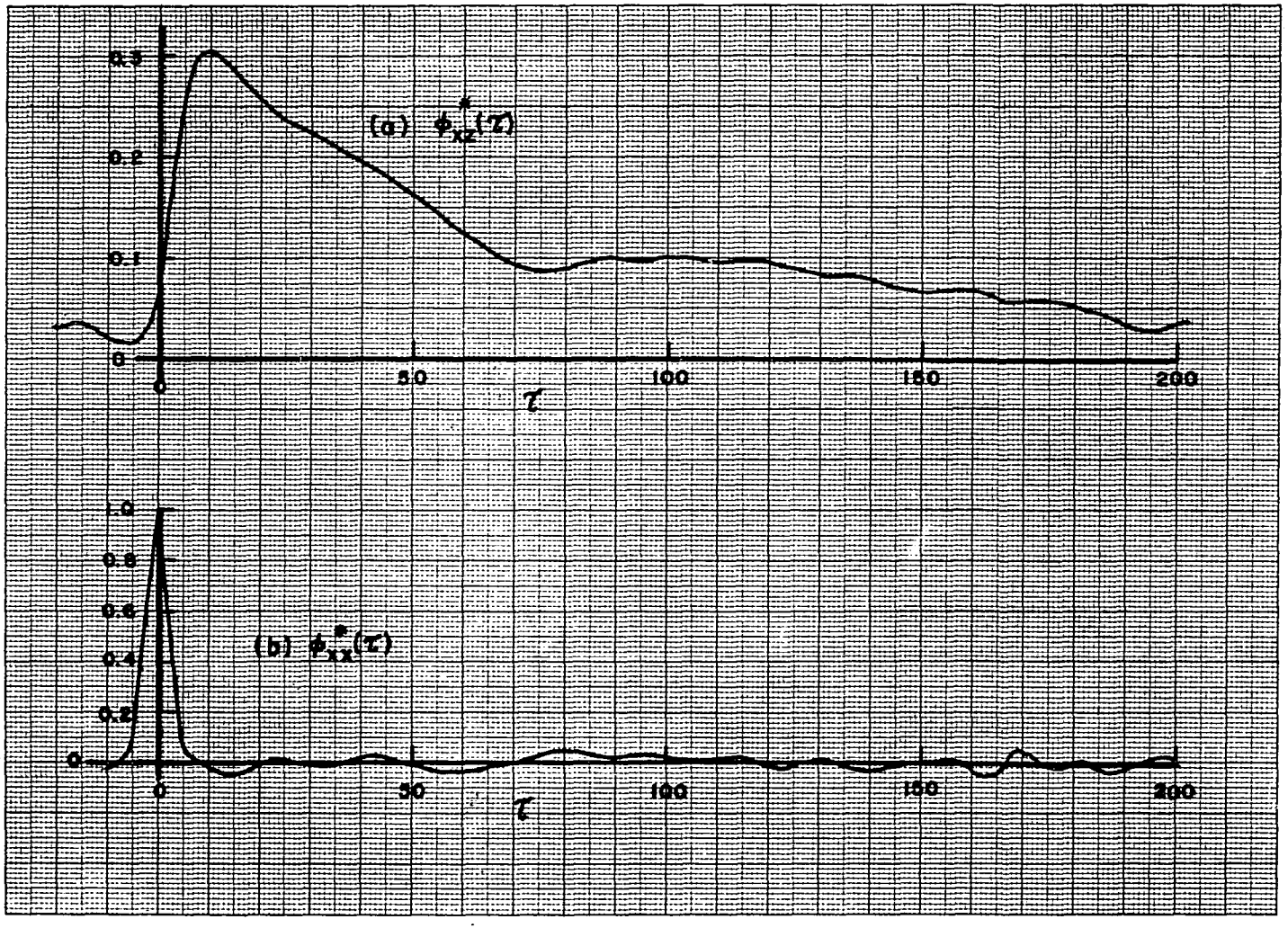

Figure 25

Correlation Estimates from a Record Length of $N-\tau_m = 4800$

By comparing the $\phi_{xz}^*(\tau)$ estimates in Figures 23, 24, and 25 it can be seen that each appears to have a bias value which is not zero. That is, the values of the estimates for large $|\tau|$ (negative and positive values) appear to settle to some value other than zero and which varies with record length. In spite of the fact that the product of average values of both variables over each record were subtracted as a bias as in Equation (92), there seems to be a slightly different bias value in effect. This difference again is probably due to the use of finite record lengths.

Ordinarily the frequency response $H(\omega)$ would be solved from Equations (101) and (102) by the relationship

$$H(\ ) = \frac{\Phi_{xz}(\omega)\ \Phi_{yy}(\omega) - \Phi_{yz}(\omega)\ \Phi_{xy}(\omega)}{\Phi_{xx}(\omega)\ \Phi_{yy}(\omega) - \Phi_{yx}(\omega)\ \Phi_{xy}(\omega)} \tag{103}$$

However, since x(t) and Y(t) were independent,

$$\Phi_{xy}(\omega) = \Phi_{yx}(\omega) = 0 \tag{104}$$

and the solution for $H(\omega)$ reduces to

$$H(\omega) = \frac{\Phi_{xz}(\omega)}{\Phi_{xy}(\omega)} \tag{105}$$

which is identical to the case when only one input and no noise signal exist. In view of this fact the correlation estimates of $\phi_{yy}(\tau)$ and $\phi_{yz}(\tau)$ were not computed. The correlation estimate $\phi_{xy}^*(\tau)$ was computed out to a record length of $N - \tau_m = 3000$ in order to detect any possible correlation. These estimates appeared merely as random

functions with variances that decreased with record length.

Spectral Estimates. Results of input power spectral density estimates, $\Phi_{xy}^*(\omega)$, are listed in Table 4. The input variable x(t) for the case of two inputs and the input r(t) for one input were generated identically and therefore the spectra of $\Phi_{xy}^*(\omega)$ were very similar to those of $\Phi_{rr}^*(\omega)$ shown in Figure 15. Both have the theoretical value

$$\Phi_{xx}(\omega) = \Phi_{rr}(\omega) = T_s \left(\frac{\sin \frac{\omega T_s}{2}}{\frac{\omega T_s}{2}} \right)^2 \qquad (106)$$

as determined in Appendix A, and appear to approach this function as sample length is increased. The Fourier transform calculations were made using the weighting function for k = 2.

The results of determining cross-power spectral density estimates $\Phi_{xz}^*(\omega)$ are listed in Table 5 for record lengths of $N - \tau_m$ = 3600, 4200, and 4800 products. These spectra are close in agreement with each other. The $\phi_{xz}^*(\tau)$ estimates, which were transformed to yield these spectra, all had apparent bias values close together but yet two slight adjustments were made on these functions as input data to the Fourier transform program. The first was that estimates for each record length were shifted in bias so that each had the same value at $\tau = 0$. This value of $\phi_{xz}^*(0)$ was selected as the value at which the estimate for $N - \tau_m = 4800$ crossed the $\tau = 0$ axis when it was shifted

TABLE 4

INPUT POWER SPECTRAL DENSITY ESTIMATES - TWO INPUTS

Frequency Radians Per Minute	N-τ_m= 1800	2400	3000	3600	4200	4800	Expected Value
0.03	12.31	11.35	9.05	11.77	10.81	11.39	10.0
0.06	12.15	10.87	8.90	11.37	10.79	11.29	10.0
0.12	12.05	10.77	9.00	11.09	10.74	11.26	10.0
0.24	11.83	10.47	8.86	10.75	10.37	10.89	10.0
0.48	10.95	9.39	8.26	9.56	9.19	9.65	10.0
0.96	7.80	6.83	6.87	7.24	6.99	7.65	9.99
1.92	7.73	8.70	14.38	13.89	12.86	12.02	9.92
3.84	12.43	13.96	11.93	10.57	9.80	8.91	9.66
7.68	7.37	7.89	8.69	9.47	9.93	10.50	8.70
15.36	6.07	6.20	5.36	5.22	5.80	5.69	5.60
30.72	0.439	0.370	0.381	0.398	0.417	0.493	0.460
61.44	0.154	0.203	---	0.210	0.213	0.204	0.321
122.88	0.054	0.045	---	0.038	0.035	0.036	0.0504

TABLE 5

CROSS-POWER SPECTRAL DENSITY ESTIMATES - TWO INPUTS
(WEIGHTING FUNCTION k = 2)

Frequency Radians Per Minute	N- τ_m = 3600		N- τ_m = 4200		N- τ_m = 4800	
	Magnitude	Degrees Lag	Magnitude	Degrees Lag	Magnitude	Degrees Lag
0.03	24.5	2.19	24.3	2.26	24.5	2.19
0.06	24.5	4.37	24.3	4.51	24.5	4.37
0.12	24.3	8.71	24.1	9.00	24.3	8.74
0.24	23.7	17.3	23.5	17.8	23.7	17.3
0.48	21.5	33.1	21.1	34.1	21.6	33.4
0.96	15.6	55.0	14.9	55.5	15.8	56.8
1.92	11.4	79.0	11.0	76.7	10.4	80.1
3.84	4.37	94.8	4.14	98.0	3.98	97.4
7.68	2.02	123.8	1.97	125.7	2.08	128.5
15.36	0.515	154.7	0.536	154.7	0.523	152.0
30.72	0.0235	125.2	0.0232	138.2	0.0243	133.4
122.88	0.00246	321.9	0.00227	329.4	0.00271	335.4

to have an apparently zero bias. In this manner all cross-correlation estimates were brought into close agreement. The second adjustment was that cross-correlation estimates were made to be zero for the negative values except for five discrete values near the origin where the function was allowed to approach zero smoothly.

Justifications of these adjustments are based on the following: (1.) Frequency information of interest is contained only in that part of the correlation function away from its bias level, (2.) The theoretical value of the cross-correlation function was zero for negative values except those near the origin which were part of the response to the autocorrelation pulse.

Table 6 lists results of cross-power spectral estimates determined for different weighting functions. Considerable smoothing of the magnitudes is achieved over the unweighted, truncated estimate. The low frequency portion of the magnitudes is affected somewhat due to the fact that the total area under the curve described by $\phi_{xz}(\tau) \cdot W_k(\tau)$ is decreased as the weighting is increased.

Process Frequency Response. Initial determinations of process frequency response were attempted by the use of Equation (101), which includes the effect of input cross-power spectral density as

$$\Phi_{xz}(\omega) = H(\omega)\,\Phi_{xx}(\omega) + G(\omega)\,\Phi_{xy}(\omega) \qquad (101)$$

The response, $G(\omega)$, was derived from the rather simple

TABLE 6

EFFECT OF WEIGHTING FUNCTION ON CROSS POWER SPECTRAL DENSITY ESTIMATE
($N-\tau_m = 4200$)

Frequency Radians Per Minute	Unweighted-Truncated		k = 1		k = 2	
	Magnitude	Phase Lag	Magnitude	Phase Lag	Magnitude	Phase Lag
0.03	31.7	3.21	27.2	2.64	24.3	2.26
0.06	31.7	6.42	27.1	5.26	24.3	4.51
0.12	31.3	12.8	26.8	10.5	24.1	9.00
0.24	29.8	25.4	25.8	20.7	23.5	17.8
0.48	24.1	48.2	22.3	39.3	21.1	34.1
0.96	11.5	61.9	13.9	58.9	14.9	55.5
1.92	11.9	81.9	11.4	77.8	11.0	76.7
3.84	4.63	97.8	4.18	97.3	4.14	98.0
7.68	1.86	116.5	1.97	124.6	1.97	125.7
15.36	0.672	158.4	0.559	154.5	0.536	154.7
30.72	0.00205	329.0	0.0217	138.0	0.0232	138.2
61.44	0.00477	115.7	0.0102	45.7	0.00977	46.3
122.88	0.00804	321.7	0.00244	328.9	0.00227	329.4

dynamic equations of the process, and estimates of each spectral density, $\Phi_{xz}(\omega)$, $\Phi_{xx}(\omega)$, and $\Phi_{xy}(\omega)$. The equation was then solved for $H(\omega)$.

Results from this determination were of no significant value, primarily due to the fact that variance of the $\Phi_{xy}(\omega)$ estimate was too large in magnitude. This variance indicates that this method would demand extremely long records for identifying multi-input systems where the input functions are correlated.

However, satisfactory results were obtained using the assumptions that the input cross power spectrum, $\Phi_{xy}(\omega)$, was zero. Results are shown in Figure 26 for the normalized magnitude ratio and in Figure 27 for phase lag. Both are determinations for record lengths of $N - \tau_m = 4800$. Table 7 lists results for three different record lengths. The normalized frequency responses were determined by the expression

$$H(\omega) = \frac{\dfrac{\Phi_{xz}^*(\omega)}{\Phi_{xz}(\omega_{min})}}{\dfrac{\Phi_{xx}(\omega)}{\Phi_{xy}(0)}} \quad \frac{1}{B(\omega)} \tag{107}$$

where $B(\omega)$ represents the normalized frequency response of the filter used to attenuate higher frequency noise and thus minimize aliasing of the noise. It should be noticed that the theoretical input spectra were used for the above determinations. The filter $B(\omega)$ had break frequencies at 82.2 and 541 radians per minute so that it was significant

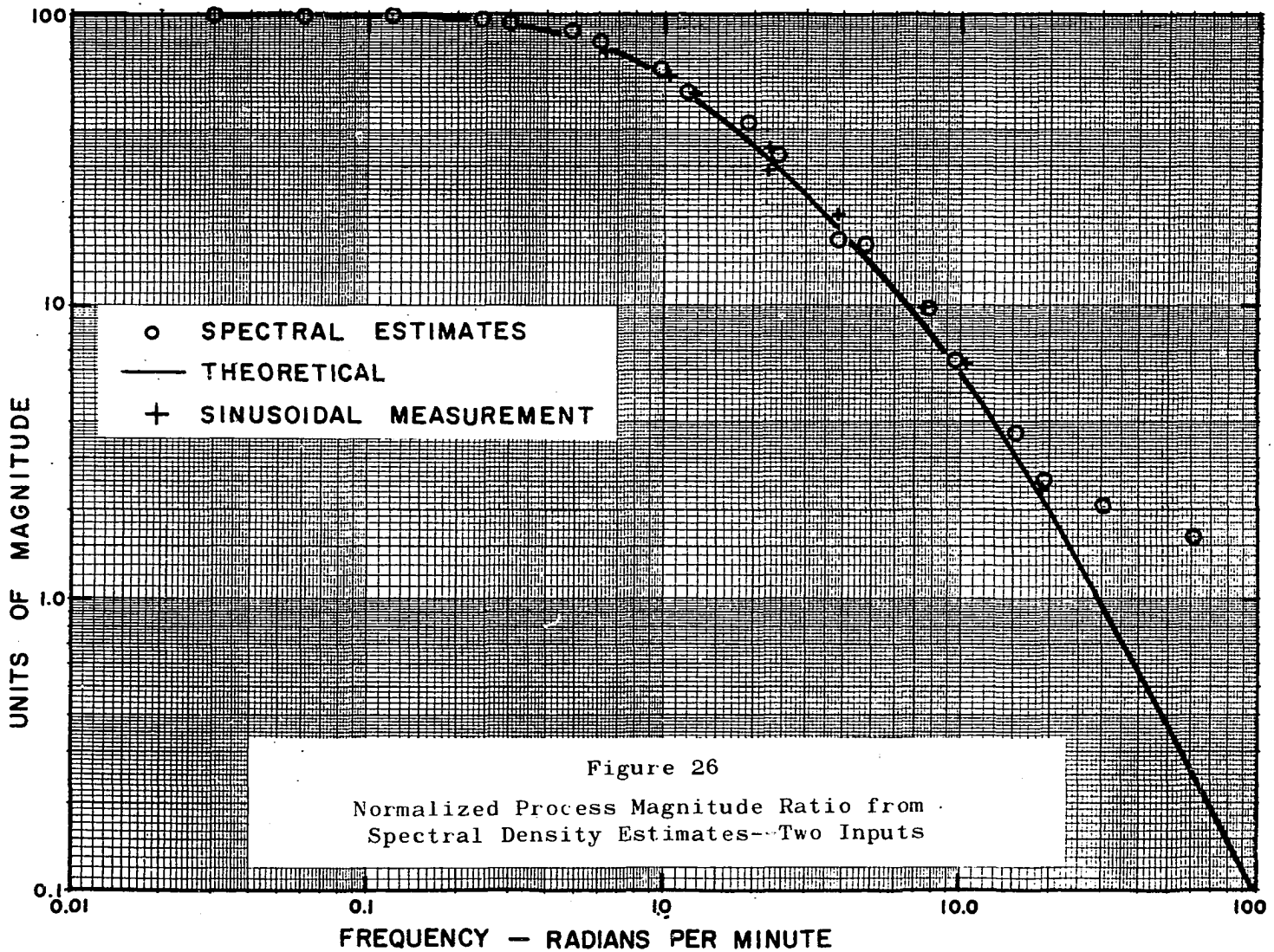

Figure 26

Normalized Process Magnitude Ratio from Spectral Density Estimates--Two Inputs

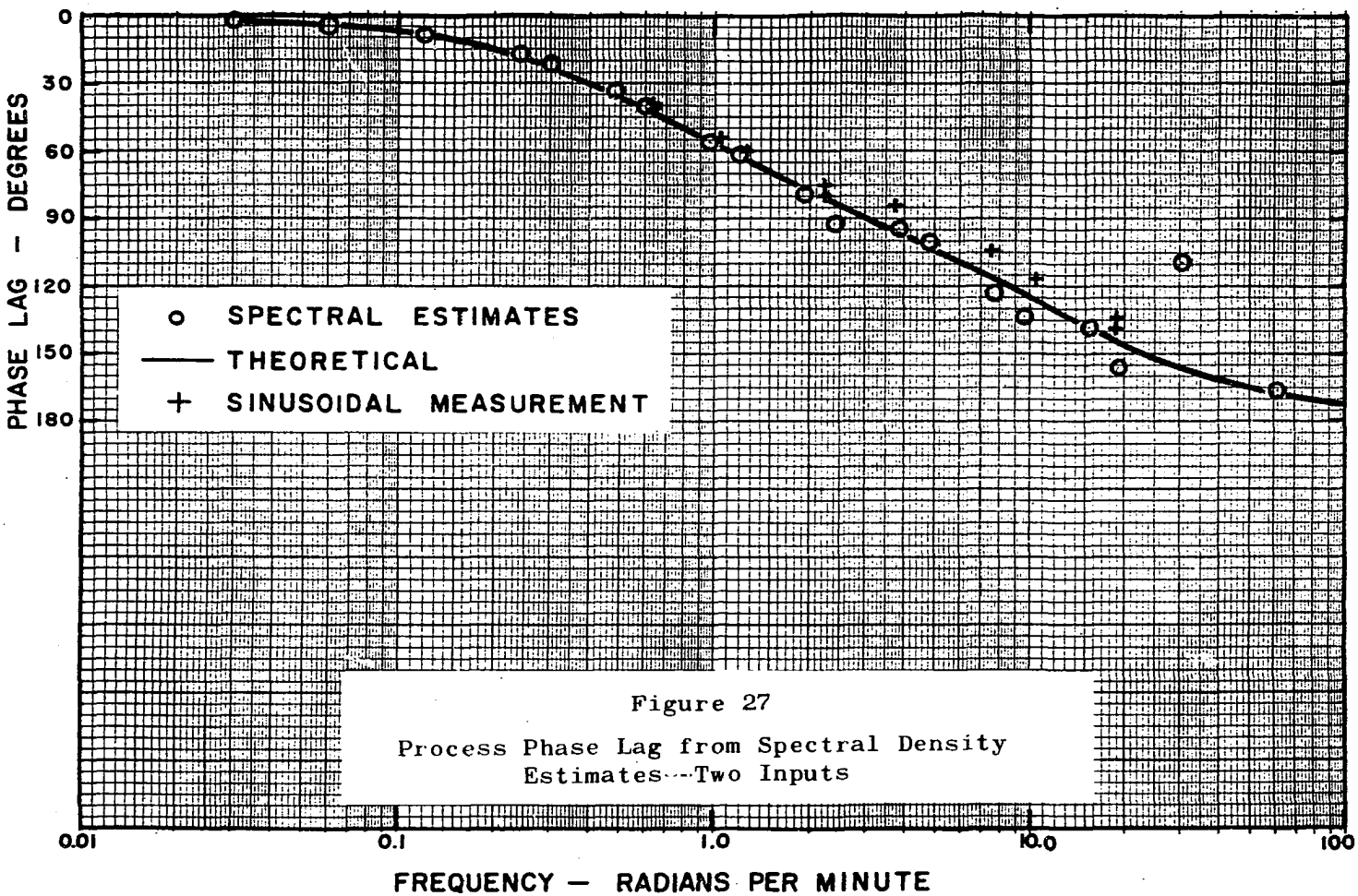

Figure 27

Process Phase Lag from Spectral Density Estimates---Two Inputs

TABLE 7

NORMALIZED PROCESS FREQUENCY RESPONSE RESULTS - FOR TWO INPUTS

Frequency Radians Per Minute	N- τ_m = 3600		N- τ_m = 4200		N- τ_m = 4800	
	Magnitude Ratio	Phase Lag Degree	Magnitude Ratio	Phase Lag Degree	Magnitude Ratio	Phase Lag Degree
0.03	1.0	2.19	1.0	2.26	1.0	2.19
0.06	0.998	4.37	1.0	4.51	1.0	4.37
0.12	0.991	8.71	0.992	9.00	0.991	8.74
0.24	0.966	17.25	0.965	17.8	0.968	17.32
0.48	0.876	33.14	0.868	34.1	0.882	33.41
0.96	0.635	55.7	0.613	56.2	0.645	56.0
1.92	0.467	77.4	0.453	75.2	0.426	78.5
3.84	0.183	91.7	0.175	95.0	0.168	94.3
7.68	0.0950	117.7	0.093	119.6	0.0980	122.4
15.36	0.0379	142.5	0.399	142.5	0.0363	139.7
30.72	0.0222	101.5	0.0222	114.5	0.0203	109.7
61.44	0.0151	-	0.0157	-	0.0161	166.4
122.88	0.0362	-	0.0342	-	0.0395	266.4

only in the high frequencies. The spectral estimates were calculated using the weighting function k = 2.

With reference to Figure 26, magnitude ratios appear to agree quite well with experimental, or sinusoidal, measurements out to approximately 20 radians per minute where the input is attenuated by a factor of approximately 0.03. It is interesting to note that above this frequency the conventional, sinusoidal measurements also could not be made with desirable accuracy due to low signal-to-noise ratios. Fluctuations in the recorded temperature, caused by eddys of fluid at varying temperatures, were of the same amplitudes as the sinusoidal response. While the sinusoidal measurements and the statistical results agree well in magnitude ratio, they both show less attenuation than the theoretical model predicts. This result is further verification of a slightly inaccurate mathematical model.

Phase lags determined by correlation as shown in Figure 27 agree closely with sinusoidal and theoretical results in the low frequencies out to approximately 20 radians per minute. However, the agreement at higher frequencies is not as good as for the case of one input function; the phase lags shown by correlation results are generally higher than expected.

Both magnitude and phase lag results determined by this statistical method appeared to be unreliable above

20 radians per minute for these particular tests. Several factors combine to give such errors and it is rather difficult to assign their contributions in a quantitative manner. Certainly no reliable determinations could be expected possible above the folding frequency, 97.5 radians per minute. It is believed that the factors responsible for these errors, listed in order of magnitude, are the following:

(1) The correlation functions, and therefore the spectral density functions, are estimates from finite length records.

(2) The relative power in the input power spectrum decreased rapidly above the frequency of 2 radians per minute. At frequencies of 37.7 and 75.4 radians per minute the input power was zero.

CHAPTER VIII

CONCLUSIONS

Summary of Experimental Program

The frequency response relation between coolant flow rate and reactor temperature of a laboratory, continuous, stirred-tank, chemical reactor was first determined by two direct approaches. These determinations, used as references of comparison for subsequent results were by direct sinusoidal measurements and by a theoretical approach of obtaining frequency response from the differential equations of an assumed model of the process.

Under the response to a single random input variable, the coolant flow rate, frequency response was then determined through the use of the relationship between auto- and cross-correlation functions and the impulse response of a linear system. Correlation estimates were calculated from recorded operating data for various record lengths. Fourier transforms of correlation estimates were calculated to yield estimates of the power spectral densities and the process frequency response.

Frequency response was determined similarly when the

process was forced by two statistically independent random variables -- coolant flow rate and reactor inlet temperature.

Comparison of Theoretical and Sinusoidally Measured Frequency Response

An interesting point was revealed upon comparing frequency response results between theoretical and sinusoidal measurements. Phase lag of sinusoidal measurements was generally less than that predicted by the results of the theoretical model. The discrepancy was thought to be due to the assumption of perfect mixing. It was more likely that mixing and heat transfer characteristics existed which were functions of the particular geometry of construction. One could conclude that optimum placement of sensing devices, such as thermocouples, in a reactor should be determined from the flow patterns and heat transfer geometries. Locations in streams of higher velocity, and which are affected more strongly by heat transfer surfaces, would appear to present slightly faster responses.

Single Input Frequency Response Determination

Time Parameters

For a determination of process frequency response by the "correlation" method a number of parameters are left to the choice of the experimenter. Such planning affects the quality of results and experience from this work is summarized in the following discussion.

Sampling Time, Δt. Choice of a sampling time is

determined quite well from the Nyquist folding frequency. The resulting spectrum will be folded at this frequency, $\omega = \frac{\pi}{t}$. It is recommended that this frequency be made to be approximately twice the highest frequency of interest in order to avoid this folding, or aliasing.

Maximum Correlation Argument, τ_m. The value of τ_m can be determined from an approximation of the highest process time constant. A τ_m equal to or greater than 4 (four) times the highest process time constant assures that approximately 98 per cent of the total response is recovered.

Record Length, T. It has been shown that variance of the correlation estimates decreases proportionately as $1/T^2$, or the standard deviation as $1/T$. With τ_m selected as above, the ratio T/τ_m is significant for qualifying record lengths. A minimum ratio of $T/\tau_m = 15$ is recommended to obtain significant information for design purposes. The experimental work for the highest value, $T/\tau_m = 32$, yielded good frequency response description.

Other Factors

Further considerations important to the correlation techniques are discussed below.

System Generated Noise. Frequently a system to be identified may generate noise within itself. If the noise has power in and above the range of frequency interest the use of a low-pass filter (preferably having a sharp cut-off at the upper frequency range) is quite helpful for minimizing

errors. If the system noise and input function are known to be uncorrelated, or $\phi_{rn}(\tau) = 0$, no trouble arises.

Input Power. Input power must be well distributed throughout the range of frequency interest. If only a narrow range, or ranges, of frequencies have power, accuracy is limited to these ranges. Frequently, normally operating processes may have to be given additional disturbances in order to cover all frequencies of interest. The experimental work has shown that accuracy could not be obtained in the region of zero input power.

Numerical Techniques. For the calculation of correlation functions, it is more desirable to use records having zero mean values, since frequency response is itself information about incremental changes. Also, it is desirable to subtract out mean values of the variables over the record length used, as in Equation (92).

The use of a weighting function, developed by Ross, has proved useful in yielding smoothed spectra upon transformation of truncated time functions.

Applications

Experimental work has shown that the method of auto-crosscorrelation and spectral analysis can yield frequency response information within the accuracy needed for designing most control systems. The fact that this technique identifies a nonlinear system in the form of a best linear system (in a least squares sense) has been

verified to some extent. Results compared to those of a linear model and actual sinusoid measurements have closely fitted the sinusoidal measurements.

Results herein are not limited merely to open loop, isolated systems; but the method can be applied to any dynamic system which is a component of a larger, more complex system just as long as the input and output variables can be measured.

Two Input-Single Output Frequency Response Determination

Results have shown that frequency response of a system having two inputs can be determined to a satisfactory degree when the two inputs are not correlated. Calculations in this case have to be made under the assumption that the cross-correlation between inputs is zero.

Attempts to solve for the frequency response functions for two inputs led to erroneous results due to the high magnitude of variance of the input cross-power spectral estimate. These results indicate that identification of multi-input frequency responses would require extremely long records for calculation of spectral estimates to the desired degree of accuracy.

BIBLIOGRAPHY

1. Aris, R., and Amundson, N. R., "Statistical Analysis of a Reactor," Chemical Eng. Science, Vol. 9, 1958, pp. 250-262.

2. Bellman, R., Adaptive Control Processes, New York: John Wiley and Sons, 1960.

3. Chang, C. M., "A New Technique of Determining System Characteristics from Normal Operating Records," Mech. Engineer's Thesis, M.I.T., 1955.

4. Cramer, Harald, Mathematical Methods of Statistics, Princeton: Princeton University Press, 1946.

5. Davenport, W. B., and Root, W. L., An Introduction to the Theory of Random Signals and Noise, New York: McGraw-Hill Book Company, Inc., 1958.

6. Fanning, R. J., "The Dynamic Heat Transfer Characteristics of a Continuous Agitated Tank Reactor," Ph.D. Thesis, University of Oklahoma, 1958.

7. Gardner, M. F., and Barnes, J. L., Transients in Linear Systems, Vol. 1, New York: John Wiley and Sons, Inc., 1942.

8. Goodman, T. P., "Experimental Determination of System Characteristics from Correlation Measurements," Sc. D. Thesis, Department of Mechanical Engineering, M. I. T., Cambridge, Mass., 1955.

9. Goodman, T. P., "Determination of the Characteristics of Multi Input and Nonlinear Systems from Normal Operating Records," Transactions of A.S.M.E., Vol. 79, (1957), pp. 567.

10. Goodman, T. P., and Reswick, J. B., "Determination of System Characteristics from Normal Operating Records," Transactions of A.S.M.E., Vol. 78, (1956), pp. 259.

11. Gore, F. E., "Dynamic Analysis of Systems Subject to Random Noise," M.S. Thesis, Saint Louis University, 1959.

12. Homan, C. J., and Tierney, J. W., "Determination of Dynamic Characteristics of Processes in the Presence of Random Disturbances," Chem. Eng. Science, Vol. 12, (1960), pp. 153.

13. Hougen, J. O., and Walsh, R. A., "Pulse Testing Method," Chem. Eng. Progr., Vol. 57, (1961), p. 69.

14. James, H. F., Nichols, N. B., and Phillips, R. S., Theory of Servomechanism, M.I.T. Radiation Laboratory Series, Vol. 25, New York: McGraw-Hill Book Co., 1947.

15. Kaiser, J. F., and Angell, R. K., "New Techniques and Equipment for Correlation Computation," Technical Memorandum, 7668-TM-2, Servomechanisms Laboratory, M. I. T., (Dec. 1957).

16. Kolmogorov, A. N., "Interpolyatsiya i ekstrapolyatsiya statsionarnykh sluchaynykh posledovatel'nostey" (Interpolation and extrapolation of stationary random sequences) Izvestiya AN SSSR, ser, matem., No. 5, 1941.

17. Kutin, B. N., "On the Calculation of the Correlation Function of a Stationary Random Process from Experimental Data," Automation and Remote Control, (English translation of Avtomatika i Telemekhanika), Vol. 8, (March 1957), pp. 221-246.

18. Laning, J. H., Jr., and Battin, R. H., Random Process in Automatic Control, New York: McGraw-Hill Book Co., 1956.

19. Lee, Y. W., Application of Statistical Methods to Communication Problems, Technical Report No. 181, Research Laboratory for Electronics, M.I.T., Cambridge 39, Massachusetts, (1950).

20. Lee, Y. W., Statistical Theory of Communication, New York: John Wiley and Sons, Inc., 1960.

21. Lee, Y. W., and Weisner, J. B., Electronics, Vol. 23, (1950), p. 86.

22. Margolis, S. G., "Application of Statistical Methods to the Measurements of Industrial Process Dynamics," S. M. Thesis, M.I.T., 1955.

23. The Rand Corporation, A Million Random Digits With 100,000 Normal Deviates, The Free Press, (1955).

24. Ross, D. T., "Improved Computational Techniques for Fourier Transformation," Report No. 7138-R-5, Servomechanism Laboratory, M.I.T., Cambridge, Massachusetts, (June 25, 1954).

25. Savant, C. J., Jr., Basic Feedback Control System Design, New York: McGraw-Hill Book Co., 1958.

26. Solodovnikov, V. V., Introduction to the Statistical Dynamics of Automatic Control Systems, Translation edited by J. B. Thomas and L. A. Zadeh, Dover Publication, 1960.

27. Stewart, W. S., "Dynamics of Heat Removal From a Jacketed, Agitated Vessel," Ph.D. Thesis, University of Oklahoma, 1960.

28. Truxal, J. G., Automatic Feedback Control System Sythesis. New York: McGraw-Hill Book Co., Inc., 1955.

29. Weiner, N., The Extrapolation, Interpolation, and Smoothing of Stationary Time Series with Engineering Applications, New York: John Wiley and Sons, (original work appeared as a report in 1942), 1949.

APPENDIX A

Autocorrelation of a Random Square Wave

Let us assume that a random square wave x(t) such as that shown in Figure 28 is a member of an ergodic random process.

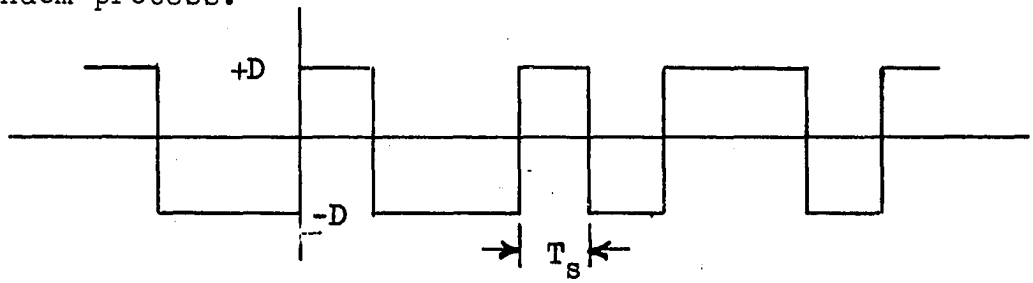

Figure 28

A Random Square Wave, x(t)

The function x(t) can be expressed as

$$x(t) = a_i \quad \text{for} \begin{cases} i & t\ (i + T_s) \\ i = 0, +T_s, +2T_s, \text{---} \end{cases} \qquad (108)$$

where the a_i's are independent random variables taking on the values -D and +D with equal probability.

Let us determine the autocorrelation function from a time averaging point of view. It is expressed as

$$\phi_{xx}(\tau) = \lim_{T \to \infty} \frac{1}{2T} \int_{-T}^{T} x(t)\, x(t + \tau)\, dt \qquad (109)$$

For values of $|\tau| > T_s$ the a_i's are independent and

have a zero mean so that the average value of the product $x(t)\ x(t+\tau)$ is zero or $\phi(\tau) = 0$.

When $\tau = 0$,

$$\phi_{xx}(0) = \overline{x(t)^2} = D^2 \tag{110}$$

For values of $0 \leq |\tau| \leq T_s$ the fraction of products $x(t)x(t+\tau)$ which are correlated is just $1 - \frac{|\tau|}{T_s}$.

The correlation function is then $D^2 \left[1 - \frac{|\tau|}{T_s}\right]$.

In summary,

$$\begin{aligned} \phi_{xx}(\tau) &= D \left[1 - \frac{|\tau|}{T_s}\right] && \text{for } 0 \leq |\tau| \leq T_s \\ &= 0 && \text{for } |\tau| > T_s \end{aligned} \tag{111}$$

Input Power Spectral Density

The input power spectral density can be determined as

$$\begin{aligned} \Phi_{xx}(\omega) &= \int_{-\infty}^{\infty} \phi_{xx}(\tau)\ e^{-i\omega\tau}\, d\tau \\ &= D^2 \int_{-T_s}^{T_s} \left[1 - \frac{|\tau|}{T_s}\right] e^{i\omega\tau}\, d\tau \\ &= 2D^2 \int_{0}^{T_s} \left[1 - \frac{t}{T_s}\right] \cos \tau\, d\tau \\ &= \frac{2D^2}{T_s\omega^2} \quad (1 - \cos \omega T_s) \\ &= D^2 T_s \left(\frac{\sin \frac{\omega T_s}{2}}{\frac{\omega T_s}{2}}\right)^2 \end{aligned} \tag{112}$$

APPENDIX B

Derivation of Theoretical System Frequency Response

Consider the equipment as shown in Figure 29 below

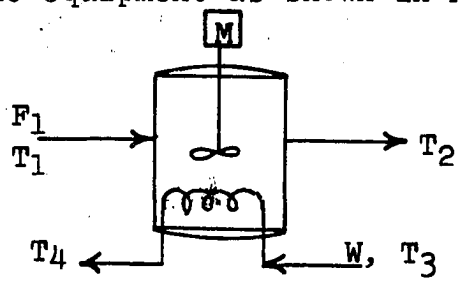

Figure 29

A Stirred Tank Reactor Model

For the derivations of dynamic equations concerning the reactor, let us make the following assumptions:

(1) The reactor fluid is perfectly stirred.

(2) Densities and heat capacities remain constant.

(3) The fluid in the cooling coil is uniform in temperature throughout the length of the coil and this temperature is the arithmetic average of inlet and outlet coolant temperature.

(4) The amount of energy imparted to the reactor fluid by the stirrer is negligible and heat transfer through reactor walls is negligible.

(5) The thermal capacitance of the cooling coil

wall is negligible.

An energy balance taken on the reactor fluid yields

$$\frac{dT_2}{dt} = \frac{F}{V\rho}(T_1-T_2) + \frac{UA}{V\rho c_p}(T_W-T_1) \qquad (113)$$

Likewise, an energy balance made on the cooling water inside the coil yields

$$\frac{dT_W}{dt} = \frac{W}{M}(T_3-T_4) + \frac{UA}{Mc_p}(T_2-T) \qquad (114)$$

According to assumption (3) above, $T_W = \frac{T_2 - T_4}{2}$. Each variable can be interpreted as the sum of a steady state value and a time varying part, such as

$$T_2 = \bar{T}_2 + T_2' \qquad (115)$$

$$T_4 = \bar{T}_4 + T_4' \qquad (116)$$

$$W = \bar{W} + W' \qquad (117)$$

At steady state conditions, Equation (113) and (114) become, respectively (using the definition of T_w)

$$0 = \left(\frac{F}{V\rho}\right)(T_1-\bar{T}_2) + \frac{UA}{V\rho c_p}\left(\frac{T_3}{2} + \frac{\bar{T}_4}{2} - \bar{T}_2\right) \qquad (118)$$

$$0 = \frac{\bar{W}}{M}(T_3 - \bar{T}_4) + \frac{UA}{Mcp}\left(\bar{T}_2 - \frac{T_3}{2} - \frac{\bar{T}_4}{2}\right) \qquad (119)$$

After combining Equation (113) through (119) and the definition of T_w the time varying parts of the variables can be related as

$$\frac{dT_2'}{dt} = -\left(\frac{F}{V\rho} + \frac{UA}{V\rho cp}\right)T_2' + \left(\frac{UA}{2V\rho c_p}\right)T_4' \qquad (120)$$

$$\frac{dT_4}{dt} = \left[\frac{2(T_3 - \bar{T}_4)}{M}\right] W' - \left(\frac{2\bar{W}}{M} + \frac{UA}{Mc_p}\right) T_4' - \left(\frac{2}{M}\right) T_4'W' + \left(\frac{2UA}{Mc_p}\right) T_2' \qquad (121)$$

Since this system is flow-forced, a non-linearity results in Equation (121) due to the product $T_4'W'$. This system of equations was programmed on an analog computer and the problem circuit is shown in Figure 30. The analog computer used was a Donner Scientific, Model 3100D, a part of the School of Chemical Engineering Graduate Research Process Control Laboratory at the University of Oklahoma. Normalized frequency response results obtained with this model showed no difference between using the $\frac{1}{M} T'W'$ term and omitting it. The model was therefore considered as being linear. The transfer function of the linear model was

$$\frac{T_2(s)}{W(s)} = \frac{4.215}{S^2 + 13.082s + 9.413} \qquad (122)$$

Units of temperature are in ^{o}F, flow is in pounds per minute, and time is in minutes. Constants for the coefficients of Equations (120) and (121) are listed in Table (8). The impulse response from the above model is

$$h(t) = .3646\ (e^{-.764t} - e^{-12.32t}) \qquad (123)$$

The time constants of the equipment were therefore approximately 1.31 minutes and 0.081 minutes.

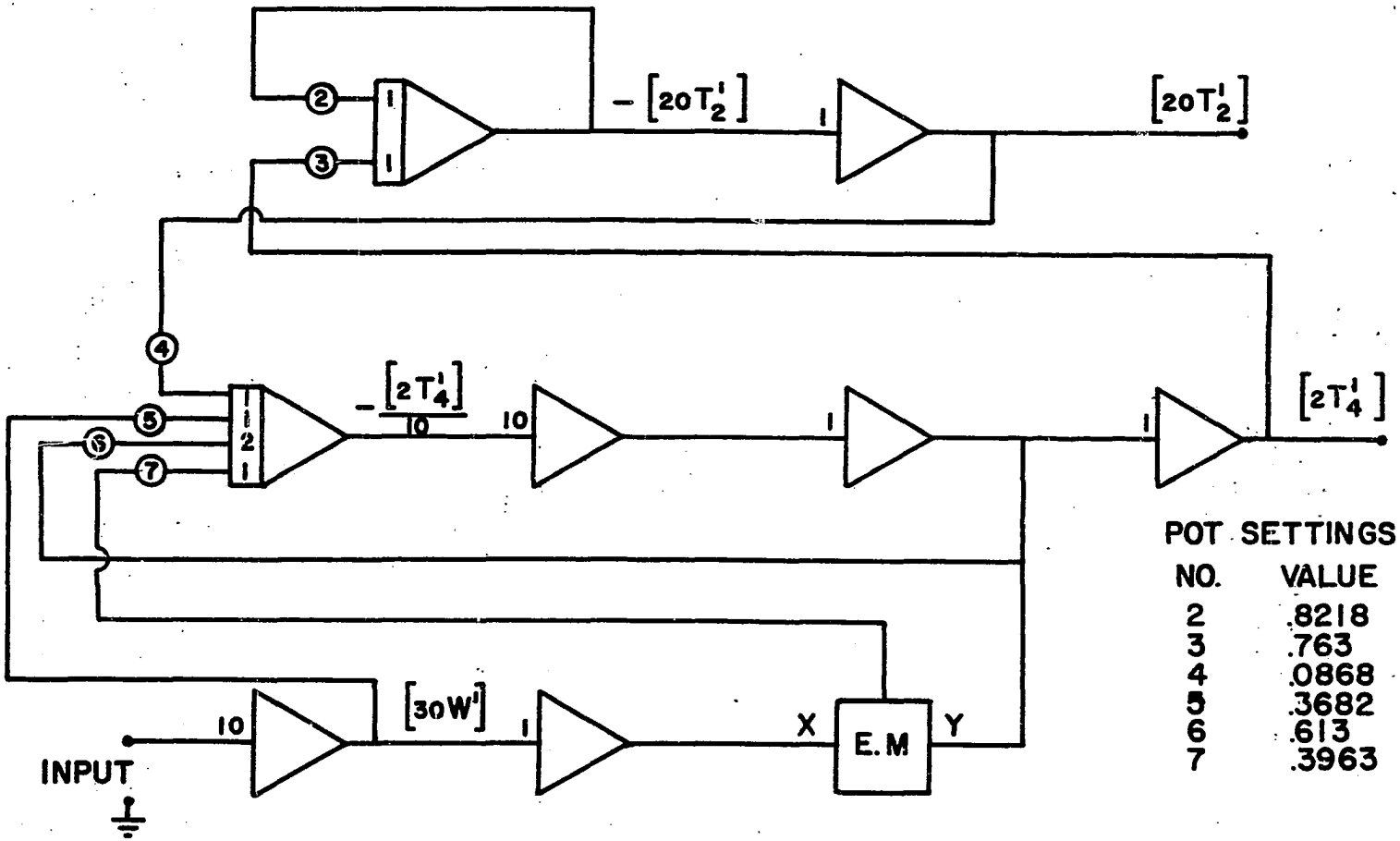

Figure 30

Analog Computer Circuit for Simulating Reactor Equations

TABLE 8

PARAMETER VALUES OF EXPERIMENTAL EQUIPMENT

$F = 32.0$ lbs./min.

$V = .7671$ ft^3.

$\rho = 62.4$

$U = 39.7$ B.T.U./min. ft^2. ^{o}F

$A = 1.84$ ft.^{2}

$c_p = 1.0$ B.T.U./lb. ^{o}F

$\overline{W} = 6.66$ lb./min.

$M = 1.682$ lb.

$T_1 = 140\ ^{o}F$

$T_3 = 70\ ^{o}F$

$\overline{T}_4 = 116.5$

APPENDIX C

Fourier Transformation

Computer Program

To compute the truncated Fourier transform,

$$F(\omega) = \int_{-T_m}^{T_m} f(t)e^{-i\omega t}\, dt \qquad (124)$$

by a digital computer the function, f(t) may be represented by straight line segments between discrete values as shown in Figure 31.

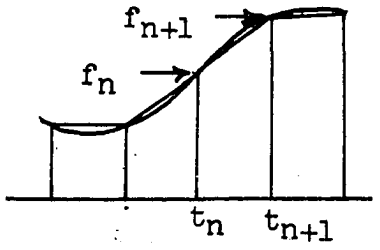

Figure 31

Straight Line Segment Representation of f(t)

Then between $t = t_n$ and $t = t_{n+1}$, we let

$$f(t) = \alpha_n + \beta_n(t-t_n) \qquad (125)$$

An approximation of Equation (124), signified by $F^*(\omega)$, can be made by

$$F^*(\omega) = \sum_{n=-N}^{N-1} \int_{n}^{n+1} \left[\alpha_n + \beta(t+t_n)\right] e^{-i\omega t}\, dt \qquad (126)$$

Because of the analytical integration between discrete

values, the accuracy of this expression depends upon the accuracy with which f(t) is represented and not upon the "scanning" frequency . Actually, the program used in this work incorporated the series of weighting functions developed by Ross (24) which are

$$W_k(t) = \left[1-\left(\frac{t}{T_m}\right)^2\right]^k \tag{127}$$

in order to smooth or compensate for the effect of truncating f(t) at $t = T_M = N\,t$. The transform calculation was therefore

$$F_k^*(\omega) = \sum_{n=-N}^{N-1} \int_n^{n+1} \left[W_k(t)\right]\left[\alpha_n+\beta_n(t-t_n)\right] e^{-i\Delta t}dt \tag{128}$$

After integration, this Equation (126) can be expressed in more suitable form for digital computation as the following:

$$F_k^*(\omega) = \frac{1}{W}\left\{f_N \sin\omega N\Delta t + \frac{1}{\omega\Delta t}\left[(f_n-f_{n-1})\cos\omega N\Delta t - (f_1-f_o) + \sum_{n=1}^{N-1}(2f_n-f_{n+1}-f_{n-1})\cos\omega n\Delta t\right]\right\}$$

$$+\frac{1}{\omega}\left\{f_{-N}\sin\omega N\Delta t + \frac{1}{\omega\Delta t}\left[f_{-N}-f_{-(N-1)})\cos\omega N\Delta t - (f_{-1}-f_0) + \sum_{n=-1}^{-(N-1)}(2f_n-f_{(n+1)}-f_{(n-1)})\cos\omega n\Delta t\right]\right\}$$

$$+\frac{i}{\omega}\left\{(f_N\cos\omega N\Delta t-f_o) - \frac{1}{\omega\Delta t}\left[(f_N-f_{N-1})\sin\omega N\Delta t + \sum_{n=1}^{N-1}(2f_n-f_{n+1}-f_{n-1})\sin\omega n\Delta t\right]\right\}$$

$$+ \underline{i} \left\{ -(\underline{f}_N \cos \omega N\Delta t - f_o) - \frac{1}{\omega t} \left[-(f_{-N} - f_{(N-1)}) \sin \omega N\Delta t - \sum_{n=1}^{N-1} (2f_n - f_{n+1} - f_{n-1}) \sin \omega n\Delta t \right] \right\} \quad (129)$$

where $f_n = W_k(n\Delta t) \cdot f(n\Delta t)$. The program was made to transform either an even function, an odd function, or an unsymmetrical function. Only the first line of terms is evaluated for an odd function. The values of sin $n\omega\Delta t$ and cos $n\omega\Delta t$ are determined by the identities

$$\sin n\omega\Delta t = \sin(n-1)\omega\Delta t \cos \omega\Delta t + \cos(n-1)\omega\Delta t \sin \omega\Delta t \quad (130)$$

$$\cos n\omega\Delta t = \cos (n-1)\omega\Delta t \cos \omega\Delta t - \sin(n-1)\omega\Delta t \sin \omega\Delta t \quad (131)$$

so that only the values of sin $\omega\Delta t$ and cos $\omega\Delta t$ are required to be found by their series expansion.

Results of Transform Program Accuracy

Accuracy of Straight Line Segment Fit. To test for the magnitude of error involved in representing a function by straight line segments, a simple function was transformed and the results compared with its theoretical transform. The function employed was $e^{-|t|}$ for $-5.91 \leq t \leq 5.91$ and was represented by 394 straight line segments over this interval. The theoretical, truncated, Fourier transform of this function is

$$F(\omega) \left\{ e^{-|t|} \right\} = 2 \int_0^{5.91} e^{-t} \cos \omega t \, dt =$$

$$= \frac{2}{1+\omega^2} \left[e^{-5.91} (\omega \sin 5.91\omega - \cos 5.91\omega) + 1 \right] \quad (132)$$

The comparison is listed in Table 9; the theoretical values are of slide rule accuracy. This comparison shows the program to give an unmeasurable error at the lower frequencies and an error of only 2% at 4 decades of attenuation.

Another test was made to determine the error possible from the combined truncation effect and straight line segment fit of f(t). The function transformed by the computer was the truncated theoretical impulse response h(t) of the experimental equipment or the desired expression was

$$F(\omega)\left\{h(t)\right\} = \int_0^{6.53} (e^{-.764t} - e^{-12.32t}) e^{-i\omega t}\, dt \qquad (133)$$

Amplitude factors have been omitted for simplicity. The impulse response was represented by 203 segments over the interval $0 \leq t \leq 6.53$ minutes. Results were compared with the frequency response function of Equation (122) normalized so that

$$\frac{F(\omega)\ \text{Theor.}}{F(0)} = \frac{9.413}{(9.413 - \omega^2) + j13.082\omega} \qquad (134)$$

Tables 10 and 11 show the comparison of results. The subscripts 0 to 1 designate the use of exponents 0 to 1 respectively for the program weighting function $W_k(t)$.

At the frequency of 122.8 radians per minute where the function is attenuated more than 3 decades, the magnitude error is approximately 5.5 per cent using no weighting function and approximately 7.5 per cent using the $W_1(t)$ as the weighting function. Error in phase lag is

TABLE 9

COMPARISON OF THEORETICAL AND PROGRAM FOURIER TRANSFORMS

Frequency (Radians Per Unit Time)	$F(\omega)$ (Theoretical) (Truncated)	$F(\omega)$ (Computer Program)
.032	2.0	2.0
.064	1.99	1.997
.128	1.97	1.9671
.256	1.878	1.879
.512	1.581	1.589
1.024	.976	.9732
2.048	.384	.3832
4.096	.1127	.1113
8.19	.0294	.02876
16.38	.00762	.007616
32.77	.00171	.001710
65.54	.000410	.000401
131.10	.0001562	.0001567
262.1	.00001662	.00001987
524.3	.00001410	.00001556
1048	.00000691	.00000614
2097	-.00000218	-.00000102

TABLE 10

COMPARISON OF COMPUTED AND THEORETICAL PROCESS MAGNITUED RATIOS

Frequency (Radians Per Minute)	$\frac{F(\omega)}{F(0)}$ (Theoretical)	$\frac{F_0(\omega)}{F_0(0)}$	$\frac{F_1(\omega)}{F_1(0)}$
.03	.9996	1.0	1.0
.06	.9969	.9912	.997
.12	.9878	.9812	.992
.24	.9539	.9526	.971
.48	.8465	.8512	.8939
.96	.6213	.6156	.6803
1.92	.3654	.3622	.4008
3.84	.1863	.1847	.2034
7.68	.08404	.08334	.09155
15.36	.03108	.03088	.03385
30.72	.009263	.009263	.01007
61.4	.002445	.002504	.002657
122.8	.0006197	.0006544	.000667
245.7	.0001558	.000144	.0001646
491.5	.00003896	.0000489	.00004186
983.0	.00000974	.000009829	.000004847

TABLE 11

COMPARISON OF COMPUTED AND THEORETICAL PHASE LAG

Frequency (Rad/Min)	$A(\omega)$ Theor. (Degrees Lag)	$A_o(\omega)$ (Degrees Lag)	$A_1(\omega)$ (Degrees Lag)
.03	2.39	2.30	2.04
.06	4.73	4.61	4.08
.12	7.09	7.20	8.12
.24	18.5	18.2	16.1
.48	34.4	34.4	31.1
.96	55.9	56.0	54.2
1.92	77.1	77.4	76.8
3.84	96.1	96.5	93.2
7.68	116.2	117.1	116.7
15.36	138.4	140.0	139.6
30.72	156.7	159.8	158.8
61.4	168.0	173.6	172.2
122.8	173.9	183.6	185.1
245.7	177.0	160.5	168.8
491.5	178.5	185.7	180.6
983.0	179.2	125.3	110.9

approximately 5.5 per cent for no weighting function and 6.4 per cent using $W_1(t)$. Since the function transformed was approximately the same as the cross-correlation function expected, these tests give a measure of best accuracy to be obtained by these numerical techniques.

Spectral Window of Weighting Functions

The weighting functions $w_k(t)$ have been used in this work to obtain better estimates of f(t) which may exist for all t but may be known only for $-T \leq t \leq T$. The effect of the $w_K(t)$ can alternatively be visualized by their "spectral windows." The product of the weighting function and the time function to be transformed has an equivalent expression in the frequency domain which is a convolution operation. The transform of the weighting function is sometimes called a "spectral window" because of this convolving window. The equivalence can be realized through the following derivation.

The product, $w_k(t)\ f(t)$ can be written as

$$W_k(t)\ f(t) = \int_{-\infty}^{\infty} W_k(\omega)\ e^{j\omega t}\ d\omega \int_{-\infty}^{\infty} F(\omega)\ e^{j\omega t}\ d\omega \qquad (135)$$

or, upon forming a double integral,

$$W_k(t)\ f(t) = \int_{-\infty}^{\infty} d\omega_2 \int_{-\infty}^{\infty} d\omega_1\ W_k(\omega_1)\ F(\omega_2)\ e^{j(\omega_1+\omega_2)t} \qquad (136)$$

For the inner integration a change of variable can be made such that $\omega_1 + \omega_2 = \omega$ and $d\omega_1 = d\omega$. Because the limits of

integration are infinite, they still remain infinite and we have

$$W_k(t)\ f(t) = \int_{-\infty}^{\infty} d\omega_2 \int_{-\infty}^{\infty} d\omega W_k(\omega-\omega_2)\ F(\omega_2)\ e^{j\omega t} \qquad (137)$$

By inverting the order of integration, we find,

$$W_k(t)\ f(t) = \int_{-\infty}^{\infty} d\omega \int_{-\infty}^{\infty} d\omega_2\ W_k(\omega-\omega_2)\ F(\omega_2)\ e^{j\omega t} \qquad (138)$$

or,

$$W_k(t)\ f(t) = \int_{-\infty}^{\infty} C(\omega)\ e^{j\omega t}\ d\omega \qquad (139)$$

where $C(\omega)$ is a spectrum resulting from the convolution in the inner integral of Equation (138).

If the spectrum $W_k(\omega)$ were an impulse at $\omega = 0$, a perfect recovery of $F(\omega)$ could be made. This situation is the desirable but physically impossible case for it requires that $w_k(t)$ be a constant for $-\infty < t < \infty$. In general, as the width of the $W_k(\omega)$ spectrum increases, so does its smoothing action because of this convolution operation on $F(\omega)$. Figure 32 shows some spectra of the weighting functions as calculated by the transform program described previously. As the amount of weighting (determined here by k) increases the spectrum shapes become wider and lower in amplitude at the origin.

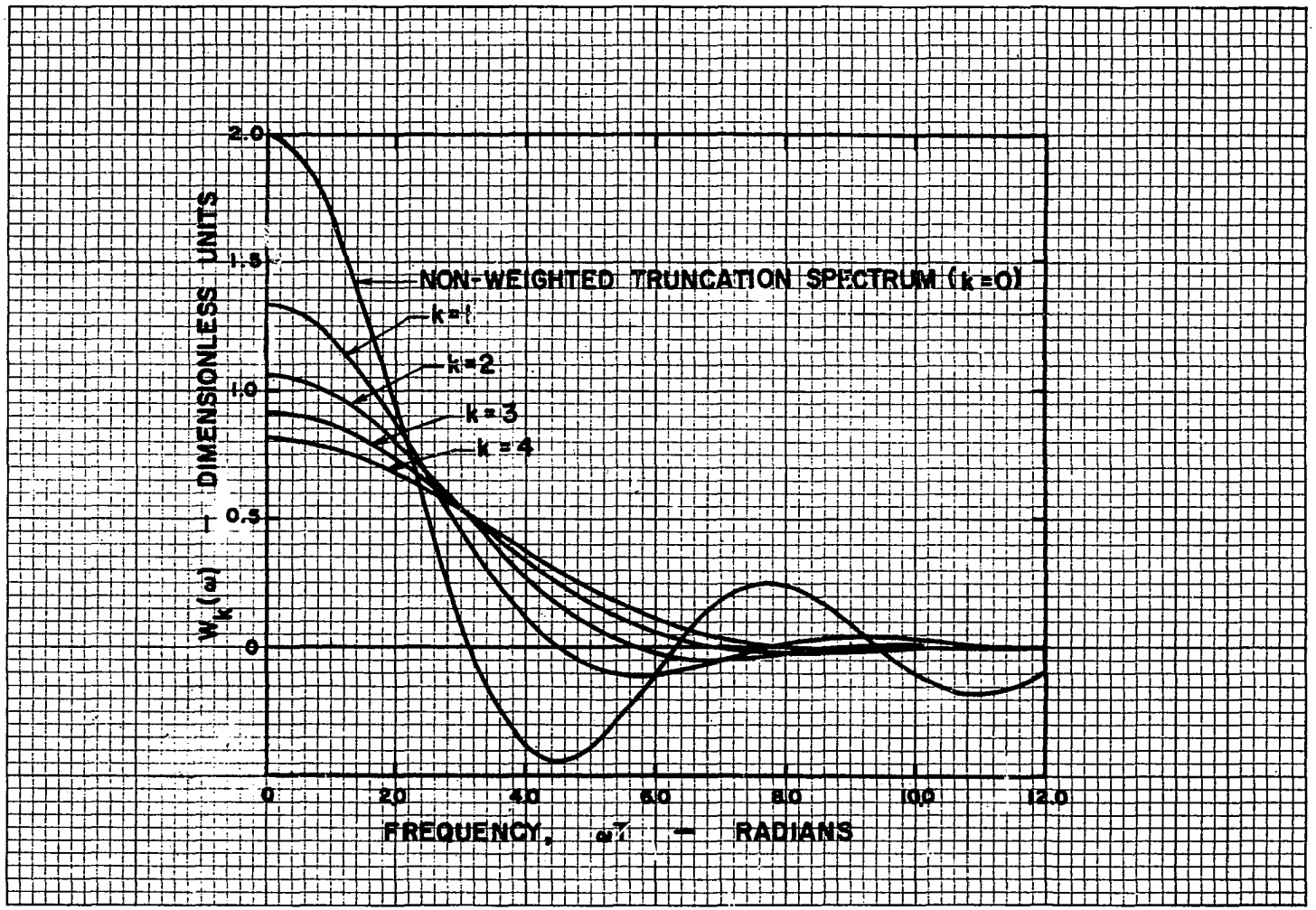

Figure 32

Spectra of Weighting Functions

APPENDIX D

Variance of Correlation Estimates

In measuring dynamics by the correlation method it is ordinarily desirable to know beforehand the necessary record length to use for any desired factor of accuracy. This section treats the variance between correlation estimates from a finite record length and the true correlation functions as the record length varies.

Variance of Autocorrelation Estimates

Consider the normalized autocorrelation estimate determined experimentally from a finite record length. This value may be calculated as

$$V^*(\tau) = \frac{\phi_{xx}^*(\tau) - \bar{x}_T^{\,2}}{\bar{x}^2_T - \bar{x}_T^{\,2}} \tag{140}$$

where the T subscript refers to the average over a time T. Assuming that x(t) is a member of an ergodic random process, the infinitely averaged value of the above is

$$V(\tau) = \frac{\phi_{xx}(\tau) - \bar{x}^{\,2}}{\bar{x}^2 - \bar{x}^2} \tag{141}$$

A variance expression between the two can be formed as

$$\sigma^2\left[V^*(\tau)\right] = E\left[\left(\frac{\phi^*_{xx}(\tau) - \bar{x}_T^2}{\bar{x}_T^2 - \bar{x}_T^2} - \frac{\phi_{xx}(\tau) - \bar{x}^2}{\bar{x}^2 - \bar{x}^2}\right)^2\right] \qquad (142)$$

For the experimental work herein, values of $x(t)$ were taken as plus or minus one so that $\bar{x}_T^2$ and $\overline{x_T^2}$ were both one and the mean value, $\bar{x}$, was zero. For this case Equation (142) then becomes

$$\sigma^2\left[V^*(\tau)\right] = E\left[\left(\frac{\phi_{xx}^*(\tau) - \bar{x}_T^2}{1 - \bar{x}_T^2} - \phi_{xx}(\tau)\right)^2\right]$$

$$= E\left[\left\{\frac{\phi_{xx}^*(\tau) - \bar{x}_T^2 - \phi_{xx}(\tau)(1-\bar{x}_T^2)}{1-\bar{x}_T^2}\right\}^2\right] \qquad (143)$$

For $\tau = 0$,

$$\sigma^2\left[V^*(0)\right] = E\left[\left\{\frac{(1-\bar{x}_T^2) - (1-\bar{x}_T^2)}{1-\bar{x}_T^2}\right\}\right] = 0 \qquad (144)$$

For $\tau > T_s$, Equation (143) shows,

$$\sigma^2\left[V^*(\tau)\right] = E\left[\left(\frac{\phi_{xx}^*(\tau) - \bar{x}_T^2}{1-\bar{x}_T^2}\right)^2\right] \qquad (145)$$

since the true autocorrelation becomes zero. In the experimental work $\bar{x}_T^2$ was found to be quite small so that the variance could be approximated as

$$\sigma^2\left[V^*(\tau)\right] \cong E\left[\phi_{xx}^*(\tau)^2\right] \qquad (146)$$

for $\tau > T_s$. The variance of the normalized estimate becomes approximately equal to the expected value of the correlation estimate squared. Upon taking the expected value inside the

equivalent double integration,

$$\sigma^2\left[V(\tau)\right] = \frac{1}{T^2}\int_0^T dt_1 \int_0^T dt_2\ E\left[x(t_1)x(t_1+\tau)x(t_2)x(t_2+\tau)\right] \tag{147}$$

When x(t) is a member of an ergodic random process which has a Gaussian probability distribution,

$$E\left[x(t_1)\ x(t_1+\tau)x(t_2)x(t_2+\tau)\right] = \phi_{xx}{}^2(t_2-t_1) + \phi_{xx}{}^2(\tau) + \phi_{xx}(t_2-t_1+\tau)\ \phi_{xx}(t_1-t_2+\tau) \tag{148}$$

The function of $\phi_{xx}(\tau)$ is zero in the region of $\tau > T_s$. Since we are interested in the region of $\tau > T_s$, the function is then zero in the range of interest. By a transformation and integration using Equation (148) in (147) the double integral can be reduced to

$$\sigma^2\left[V(\tau)\right] = \frac{2}{T^2}\int_0^T (T-t)\ \left[\phi_{xx}{}^2(t) + \phi_{xx}(t+\tau)\ \phi_{xx}(-t+\tau)\right] dt \tag{149}$$

In the experimental work the input autocorrelation function is known to be

$$\phi_{xx}(\tau) = 1 - \frac{|\tau|}{T_s} \quad \text{for } 0 \leq |\tau| \leq T_s$$

$$= 0 \quad \text{for } |\tau| > T_s \tag{150}$$

Substitution of this into Equation (149) and integration yields the result

$$\sigma^2\left[V(\tau)\right] = \frac{2T_s}{3T} - \frac{T_s^2}{6T^2} \tag{151}$$

This variance expression is independent of τ since the

autocorrelation is constant (zero) for $|\tau| > T_s$. The theoretical standard deviation of the autocorrelation was calculated from Equation (151) and shown in Figure (33) as a function of record length. In comparison, approximate values of standard deviation for the actual autocorrelation calculations are shown on this same figure. These latter values were obtained from autocorrelation calculations for $T_s < \tau < T_m$, or in this case, from 175 incremental values of $\phi_{xx}^*(\tau)$. The comparison shows a good verification of the theory even for such a relatively small number of experimental values used in estimating the standard deviations.

In conclusion, it can be seen that by the help of an expression such as Equation (149) a variance expression may be used to select a desirable record length. For the example herein a minimum of 3000 lagged products might be desirable for the correlation estimate, since the standard deviation changes rapidly up to that record length. These considerations assume that the true correlation function is known, which is most likely not the case. However, if the estimates are used in the expression such as Equation (149), the variance can, at least, be approximated. In this manner, the experimenter can approximate his accuracy and determine it better as he increases the record length used.

Variance of Crosscorrelation Estimates

The variance of crosscorrelation estimates may be

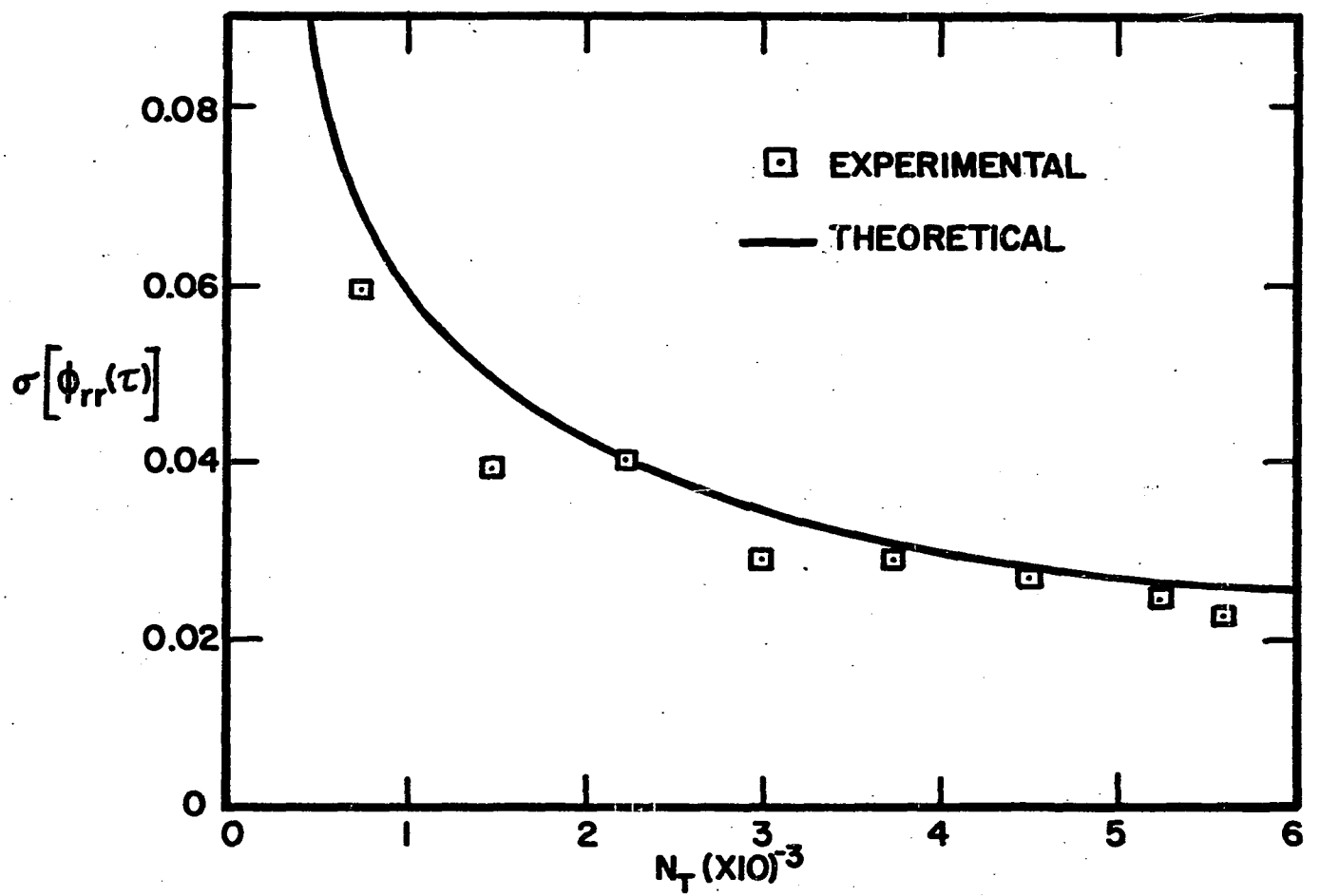

Figure 33

Theoretical Standard Deviation of the Autocorrelation Estimate

determined in a quite similar manner as the autocorrelation estimates. Consider the variance of such an estimate from a finite record length as

$$\sigma^2 \left[\phi_{rc}(\tau)\right] = E\left[\phi_{rc}^*(\tau) - \phi_{rc}(\tau)\right]^2 \qquad (152)$$
$$= E\left[\phi_{rc}^*(\tau)^2\right] - \phi_{rc}^2(\tau)$$

where $\phi_{rc}(\tau)$ is the expected value of the estimate $\phi_{rc}^*(\tau)$. Upon further evaluating the above we may write

$$^2\left[\phi_{rc}(\tau)\right] = \frac{1}{T}\int_0^T dt_1 \int_0^T dt_2 \; E\left[r(t_1)r(t_2)c(t_1\tau\right.$$

$$\left.c(t_2+\tau)\right] - \phi_{rc}^2(\tau) \qquad (153)$$

In similar manner to the previous section for members an ergodic random process and which have Gaussian probability distributions,

$$E\left[r(t_1)\, r(t_2)c(t_1+\tau)\, c(t_2+\tau)\right] = \phi_{rr}(t_2-t_1)\, \phi_{cc}(t_2-t_1)$$
$$+ \phi_{rc}^2(\tau) + \phi_{rc}(t_2+\tau-t_1)\, \phi_{rc}(t_1+\tau-t_2) \qquad (154)$$

Also use of this relationship in Equation (153) after a transformation and integration yields

$$\sigma^2\left[\phi_{rc}(\tau)\right] = \frac{2}{T^2}\int_0^T (T-t)\left[\phi_{rr}(t)\, \phi_{cc}(t) + \phi_{rc}(t+\tau)\right.$$
$$\left.\phi_{rc}(-t+\tau)\right] dt \qquad (155)$$

Unfortunately this relationship requires much more information than will ordinarily be known. In fact, it requires a knowledge of the system dynamics through the crosscorrelation function and also requires knowledge of autocorrelations of input and output. Similar to the

results of the previous section, the variance for a given τ and T may be approximated from the calculated results by the use of Equation (155).

Variance of Normalized Crosscorrelation. The variance of a normalized crosscorrelation estimate obtained from a finite record may be expressed as

$$\sigma^2\left[\phi_{rc}(\tau)\right] = E\left[\left(\frac{\phi_{rc}^*(\tau) - \bar{r}_T\bar{c}_T}{\overline{rc}_T - \bar{r}_T\bar{c}_T} - \frac{\phi_{rc} - \bar{r}\,\bar{c}}{\overline{rc} - \bar{r}\,\bar{c}}\right)^2\right] \tag{156}$$

It can be seen that at $\tau = 0$ this variance is zero. However the exact calculation for $\tau = 0$ is quite complicated and will not be considered here. Kutin (28) has considered approximations of some normalized correlation estimate variances.

APPENDIX E

LIST OF NOMENCLATURE

a	= an arbitrary constant
b	= an arbitrary constant
$c(t)$	= a variable of time
c_p	= heat capacity at constant pressure
d	= outside diameter of inner tube, except when used as a differential operator
e	= base of Naperian logarithms, 2.71812
$f(t)$	= function of time
$f_i(x,t)$	= i-th probability density function
$g(t)$	= an impulse response
$h(t)$	= an impulse response
j	= imaginary vector, $\sqrt{-1}$
k	= a constant
$n(t)$	= noise variable
r	= radial distance
$r(t)$	= function of time
s	= complex variable of Laplace transformation, a + j
t	= time variable
x	= longitudinal distance
$x(t)$	- function of time

$[x(t)]$ = a set of random variables

$x(t)^n$ = the n-th moment of x(t)

$y(t)$ = a function of time

$z(t)$ = a function of time

A = cross sectional area

$A_T(\omega)$ = Fourier transform of truncated function, f(t)

C = concentration of solute

D = diffusion coefficient

$F(\omega)$ = Fourier transform of f(t)

$G(\omega)$ = Fourier Transform of g(t)

$H(\omega)$ = Fourier Transform of h(t)

F = mass flow rate

$F_i(x,t)$ = i-th probability distribution function

M = mass of liquid inside heat transfer coils

N = total number of sampling intervals in a record

Q = a constant of time above which the impulse response is approximately zero

S = temperature of fluid in shell

$S(\omega,x)$ = power spectral density of the function x(t)

$S(\omega,x,y)$ = cross power spectral density between x(t) and y(t)

T = arbitrary constant of time; or temperature where locally defined in the text

U = overall heat transfer coefficient

V = reactor volume

$V(\tau)$ = a normalized correlation function

W = flow of coolant fluid

$w_k(t)$ = weighting function

$X(\omega)$ = Fourier transform of x(t)

$Y(\omega)$ = Fourier transform of y(t)

Greek Symbols:

α = the value of a discrete variable

α_{ik} = general moment of the order i x k

β = the slope between adjacent ordinates of a discrete variable

$\delta(t)$ = Dirac's delta function

η = a time variable

λ = a time variable

μ = a time variable

π = 3.1416

ρ = density

σ = a time variable

τ = a time variable

ϕ_{xx} = autocorrelation function of the variable x(t)

ϕ_{xy} = cross-correlation of the variables x(t) and y(t)

$\Phi_{xx}(\omega)$ = power spectral density of x(t)

$\Phi_{xy}(\omega)$ = cross power spectral density of x(t) and y(t)

Subscripts:

k = a positive discrete variable denoting the degree of weighting

n = a discrete variable denoting time abscissa

m = symbol denoting a maximum value

N = the maximum value taken by n

Superscripts:

$*$ = symbol denoting an estimate

Operator's:

∂ = operator of partial differentiation

d = operator of total differentiation

E = operator to indicate the expected value

Pr = operator to indicate the probability of an event

σ^2 = variance operator